ANALYSIS OF CORRUGATED SHELLS

by

SURENDRA TULSIDAS SHAH

S.B., Massachusetts Institute of Technology
(1955)

SUBMITTED IN PARTIAL FULFILLMENT OF

THE REQUIREMENTS FOR THE DEGREE OF

DOCTOR OF SCIENCE

at the

MASSACHUSETTS INSTITUTE OF TECHNOLOGY
February 1959

Signature of Author . . . .
          Department of Civil and Sanitary Engineering,
                    November 24, 1958

Certified by . . . .
                                        Thesis Supervisor

Accepted by . . . .
                Chairman, Departmental Committee
                    on Graduate Students

Abstract

ANALYSIS OF CORRUGATED SHELLS

by

SURENDRA TULSIDAS SHAH

Submitted to the Department of Civil and Sanitary Engineering on November 24, 1958, in partial fulfillment of the requirements for the degree of Doctor of Science in Civil Engineering.

A few years ago an unusual prefabricated Quonset-type structure known as the "Wonder Building" appeared in the building industry. The structure consists of corrugations with a depth of about 8 inches and a pitch of 2 feet running in the longitudinal direction. In addition to these corrugations, there are small secondary corrugations in the transverse direction which are introduced to facilitate the fabrication of the structure. The longitudinal edges are supported continuously so that each 2 feet wide transverse section behaves effectively as a two-hinged arch.

The secondary corrugations increase the flexibility in the transverse direction. In order to determine the effect of these corrugations, three types of corrugated pipes under axial and transverse forces were investigated. The results obtained were then applied to a structure having idealized major corrugations. The distortion of the major corrugations due to the effect of curvature in the transverse direction, similar to that which occurs in the bending of curved tubes, was also considered. The solution obtained for the idealized case was then used to arrive at an approximate solution of the actual structure.

The approximate solution is found to be in satisfactory agreement with the available test results.

Thesis Supervisor: Charles H. Norris

Title: Professor of Structural Engineering

ACKNOWLEDGEMENT

The author expresses his sincere appreciation to Professor Charles H. Norris, Professor of Structural Engineering, for his invaluable advice, encouragement, and guidance in the development of this thesis. For her assistance, the author expresses his debt of gratitude to his wife, Pallavi. Grateful acknowledgement is made for use of the facilities of the M.I.T. Computation Center. The contributions of the following are hereby acknowledged: Mr. Kirit Parikh, for assistance in programming for the IBM 704 Computer; Mr. Makarand Desai, Mr. Sukumar Parikh, and Mr. Jayant Shah for assisting in the final preparation; Mrs. Gladys D. Rand for the typing of the thesis; Miss Eva Bonis for preparing the illustrations; and Mrs. Anna Parks for the multilith reproduction.

TABLE OF CONTENTS

TABLE OF CONTENTS (Continued)

LIST OF FIGURES

CHAPTER 1

INTRODUCTION

A few years ago an unusual pre-fabricated Quonset-
type structure known as the "Wonder Building" appeared in
the building industry. The Wonder Building is built en-
tirely of 18-gauge galvanized shell metal. The sheet
metal is formed into a bath-tub shape as shown in Fig. 1.1,
and then given a secondary curved shape by forming second-
ary corrugations into the bottom portion of the shape (Fig.
1.2). The structural component so formed will be referred
to as a shell since its behaviour is very similar to that
of a long barrel shell.

These shells are then bolted together end-to-end to
form a complete arch, which is so supported at its ends
that it acts effectively as a two-hinged arch. This arch
then forms a two-foot long section of the building, and is
completely self-supporting. By bolting together successive
arches along the edges A a complete building is formed,
which may be as long as desired (Fig. 1.3).

The main advantage of this type of structure is the
great saving it makes in the cost of labour. Shells with
chord length of up to 9 feet are manufactured in the fac-
tory. These are then assembled in the field by bolting
them together to form the complete structure, and this pro-
cedure requires only unskilled labour. This type of

Section x-x
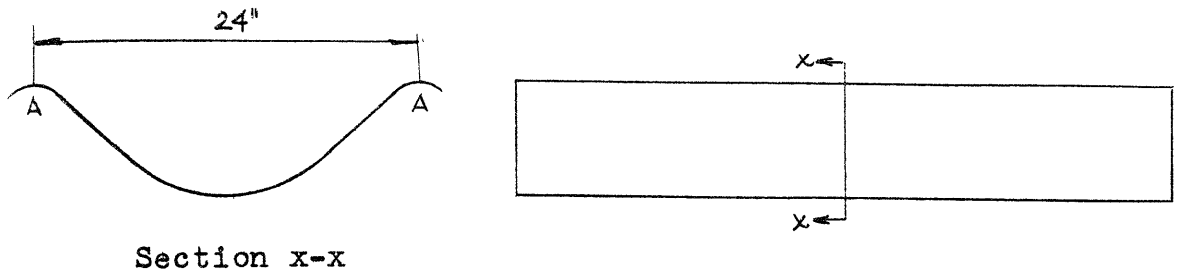
Fig. 1.1.   Straight Shell

Section x-x
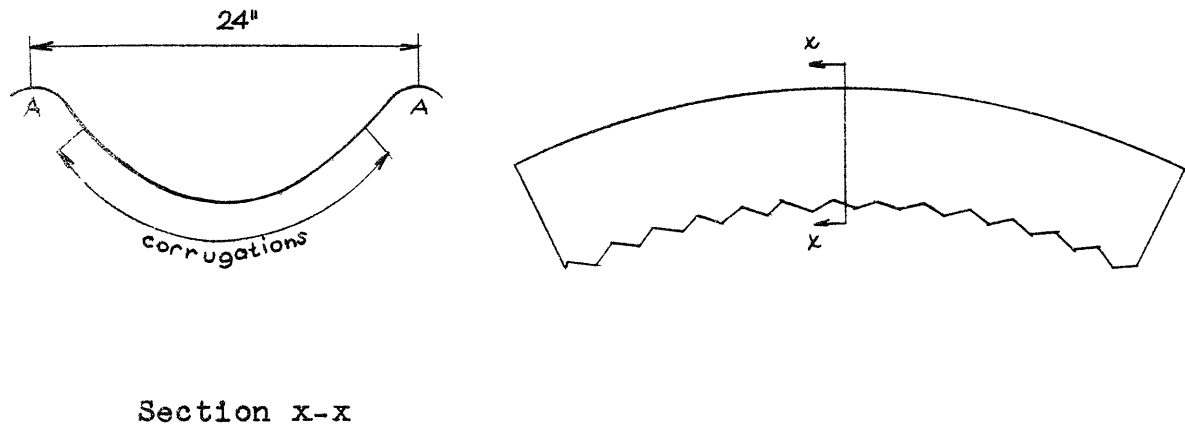
Fig. 1.2.   Curved Corrugated Shell

Section x-x
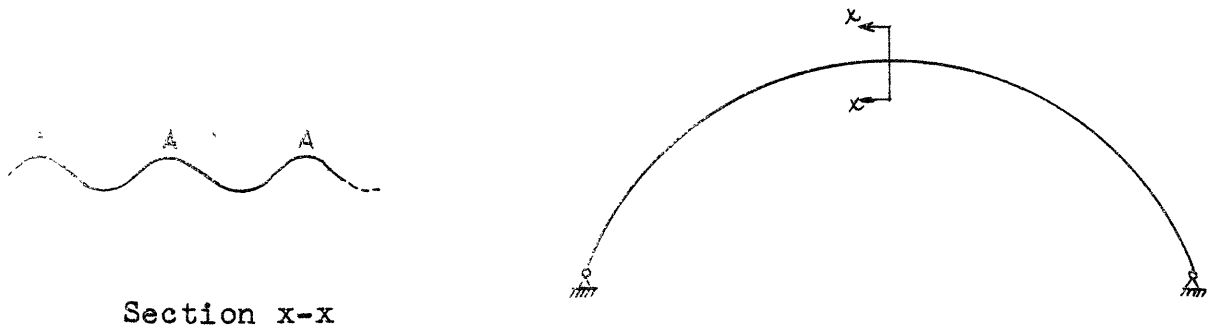
Fig. 1.3.   Corrugated Shell as Two-Hinged Arch

structure is ideal as a roof for warehouses, factories, and industrial buildings.

The presence of the secondary corrugations in the shell increases its flexibility in the span-wise direction. An axial force or a bending moment on it causes bending of these corrugations. This changes the radius of curvature of the cross section, which in turn produces circumferential stresses, much in the same way as in a corrugated pipe under an axial load or bending moment.

For this reason the case of a corrugated pipe is rigorously treated. Pipes having the types of corrugations shown in Fig. 3.1 are considered. It is seen that the corrugated pipes shown in this figure can be formed by combining several shells of revolution, either conical or ring shells. The general solutions for these types of shells are given in Chapter 2. By using appropriate boundary conditions, the stresses and flexibility of a corrugated pipe can be obtained as shown in Chapter 3. The increased flexibility of a corrugated pipe can be taken into account by using a "reduced modulus of elasticity," so that the deflections of corrugated pipes can be calculated by considering the pipe to be plain and using this reduced modulus as its modulus of elasticity.

The solution obtained for the pipe is next applied to a shell with a straight axis of an idealized cross section shown in Fig. 4.1(b), and having secondary corrugations

of the types considered for pipes. This procedure is strictly valid only when the shell is under pure bending so that the longitudinal forces are linearly distributed over any cross section. However, under the influence of snow and dead loads, transverse moments occur which distort the cross section, as in a multiple barrel shell, so that the assumption of linear distribution of the longitudinal forces is not strictly correct. But since the shell is stiffened transversely by the secondary corrugations and since the shell is long in comparison with the cross-sectional dimensions, the effect of the distortion of the cross section is very small on the longitudinal behaviour as explained in Chapter 4. Therefore, the longitudinal forces can be assumed to be linearly distributed and the solution for corrugated pipes can be used for these shells.

When these shells are curved and are subjected to a bending moment, distortion of the cross sections occurs similar to that which takes place in thin curved tubes. Not only does this distortion of the cross sections increase the flexibility of the shell but it also makes the distribution of the longitudinal forces nonlinear. It is shown in Chapter 5 that the secondary corrugations help to stiffen the transverse section, thereby considerably reducing the distortion of the cross sections. In nearly all cases the distortion is so small that it can safely be

neglected, and the longitudinal forces can be assumed to be linearly distributed over any cross section.

After this the analysis of the shell as a two-hinged arch can be performed very simply. In Chapter 6 the method of superposition is used to obtain the external moments and thrusts on any cross section. By neglecting the effect of distortion of the cross sections due to the curvature of the arch and the effect of shearing deformations, the analysis reduces to that for an ordinary arch. Having obtained the external moments and thrusts, the unit stresses can easily be found by using the solutions developed for corrugated pipes. The deflections can easily be obtained by considering the shell to be plain and using the reduced modulus as its modulus of elasticity, as in the case of corrugated pipes.

The cross section of the actual Wonder Building arch (Fig. 1.3) is much different than the idealized cross section of Fig. 4.1(b). The shape of the actual cross section is such that it cannot be represented by any simple geometrical figure. The problem is further complicated due to the fact that the shell has secondary corrugations in the bottom portion only. The corrugated portion consists of a circular arc and two tangents as shown in Fig. 7.1.

An approximate solution for this shell is given in Chapter 7. It is assumed that the circular corrugated arc

is a part of a complete pipe of radius 9.125 in., and that each of the two tangents is a part of a pipe whose radius is equal to infinity. The reduced moduli of elasticity for these portions are then equal to those for the corresponding pipes; the modulus for the portion which has no secondary corrugations is simply the modulus of elasticity of the material. The stresses and deflections are then found by a method very similar to the method of transformed sections used for beams of composite sections. The theoretical results were found to be in very good agreement with the available test results.

It is shown in Chapter 7 that for a given moment on any section of the shell, the maximum stress at this section depends primarily on the depth of the secondary corrugations; it increases as the depth increases. The shells are corrugated in the transverse direction mainly because it makes it easy to bend the shells into circular arcs. Therefore, the depth of the secondary corrugations increases with an increase in the curvature of the arc. But as the curvature increases, the span of the complete arch becomes shorter, so that the maximum moment in the arch due to a given loading decreases. Thus, an increase in depth of the secondary corrugations is accompanied by a reduction in the maximum moment in the arch, or vice versa, which enables one to use the same cross section over a wide range of span length.

Throughout the analysis it is assumed that the material follows Hooke's Law, is homogeneous, and isotropic.

CHAPTER 2

SHELLS HAVING THE FORM OF A SURFACE OF REVOLUTION

2.1. <u>General Case of Unsymmetrical Load</u>. Fig. 2.1 shows
an element, ABCD, cut from a shell of revolution by two
adjacent meridian planes and two parallel circles. The
position of the meridian plane is defined by the angle Θ,
measured from some datum meridian plane, and the position
of the parallel circle is defined by the angle ϕ, made by
the normal to the surface and the axis of rotation. The
meridian plane and the plane perpendicular to it are planes
of principal curvature at a point on the surface of revolu-
tion, and the corresponding radii of curvature are denoted
by r_1 and r_2, respectively. The radius of the parallel cir-
cle is denoted by r_0. Thus the length of the sides AD and
and BC is $r_1 d\phi$, that of AB is $r_0 d\Theta$, and that of CD is

$$(r_0 + \frac{dr_0}{d\phi} d\phi)\ d\Theta$$

The forces and moments per unit length acting on the
element ABCD are shown in Fig. 2.1 and are positive when
acting in the directions shown. In obtaining the equilib-
rium equations, it will be assumed that the shell surface
is free of any external load.

Equilibrium Equations: Let us consider the equilibrium of
the element ABCD by first projecting the forces in the di-
rection of the tangent to the meridian. The normal force
acting on the side AB is
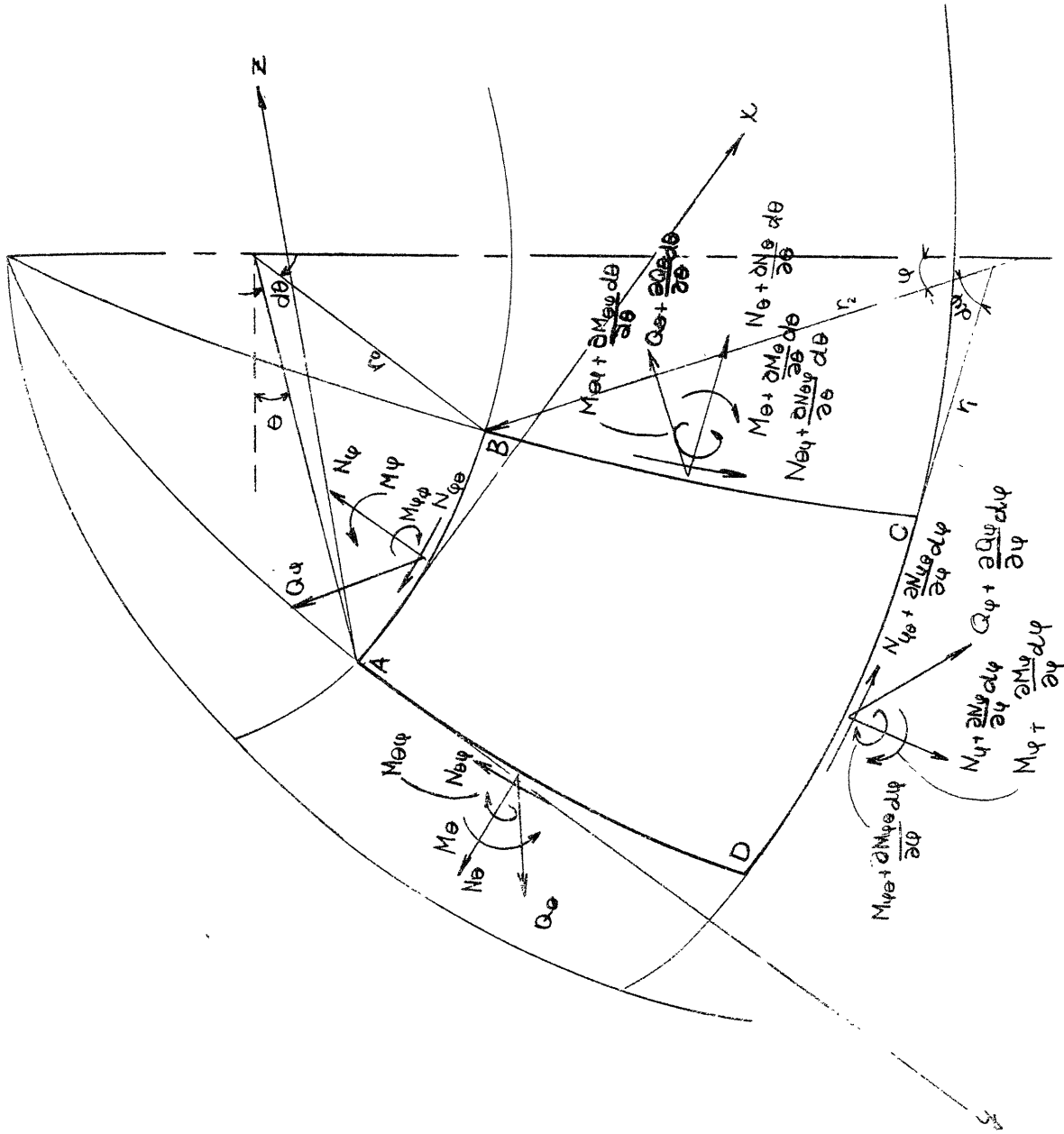
Fig. 2.1. Stresses Acting on an Element of the Shell

$$N_\phi r_o d\theta$$

The corresponding force on CD is

$$\left(N_\phi + \frac{\partial N_\phi}{\partial \phi} d\phi\right)\left(r_o + \frac{\partial r_o}{\partial \phi} d\phi\right) d\theta$$

By neglecting a small quantity of the second order, the resultant of these two forces in the y-direction is found to be equal to

$$N_\phi \frac{\partial r_o}{\partial \phi} d\phi d\theta + \frac{\partial N_\phi}{\partial \phi} r_o d\phi d\theta = \frac{\partial}{\partial \phi}(N_\phi r_o) d\phi d\theta \qquad (a)$$

The radial shear force, $Q_\phi r_o d\phi$, on the side AB has no component in the y-direction, while on the side CD the component of the radial shear force in the y-direction is

$$- \left(Q_\phi + \frac{\partial Q_\phi}{\partial \phi} d\phi\right)\left(r_o + \frac{\partial r_o}{\partial \phi} d\phi\right) d\theta d\phi$$

and this is equal to

$$- Q_\phi r_o d\phi d\theta \qquad (b)$$

if only the quantity of the first order is retained.

Now let us consider the forces acting on the other two sides, AD and BC. The normal forces on these two sides are $N_\theta r_1 d\phi$ and $\left(N_\theta + \frac{\partial N_\theta}{\partial \theta} d\theta\right) r_1 d\phi$, and have a resultant in the direction of the radius of the parallel circle equal to $N_\theta r_1 d\phi\, d\theta$. The component of this force in the y-direction is then

$$- N_\theta r_1 \cos\phi\, d\phi d\theta \qquad (c)$$

Finally, the lateral shear force on AD is $N_{\theta\phi} r_1 d\phi$ and on BC is

$$\left(N_{\theta\phi} + \frac{\partial N_{\theta\phi}}{\partial \theta} d\theta\right) r_1 d\phi$$

which give a resultant in the y-direction of

$$\frac{\partial N_{\theta\phi}}{\partial \theta} r_1 d\phi d\theta \qquad (d)$$

Summing up the forces (a) to (d), the equation of equilibrium of forces in the y-direction becomes

$$\frac{\partial}{\partial \phi}(N_\phi r_0) - N_\theta r_1 \cos\phi + \frac{\partial N_{\theta\phi}}{\partial \theta} r_1 - Q_\phi r_0 = 0$$

The other five equations of equilibrium could be obtained similarly, and they are stated below, together with the one obtained above:

$$\sum F_y = 0 : \frac{\partial}{\partial \phi}(N_\phi r_0) - N_\theta r_1 \cos\phi + \frac{\partial N_{\theta\phi}}{\partial \theta} r_1 - Q_\phi r_0 = 0$$

$$\sum F_x = 0 : \frac{\partial}{\partial \phi}(N_{\phi\theta} r_0) + \frac{\partial N_\theta}{\partial \theta} r_1 + N_{\theta\phi} r_1 \cos\phi - Q_\theta r_1 \sin\phi = 0$$

$$\sum F_z = 0 : N_\phi r_0 + N_\theta r_1 \sin\phi + \frac{\partial}{\partial \phi}(Q_\phi r_0) + \frac{\partial Q_\theta}{\partial \theta} r_1 = 0$$

$$\sum M_x = 0 : \frac{\partial}{\partial \phi}(M_\phi r_0) - M_\theta r_1 \cos\phi - \frac{\partial M_{\theta\phi}}{\partial \theta} r_1 - Q_\phi r_0 r_1 = 0$$

$$\sum M_y = 0 : \frac{\partial M_\theta}{\partial \theta} r_1 + \frac{\partial}{\partial \phi}(M_{\phi\theta} r_0) - M_{\theta\phi} r_1 \cos\phi - Q_\theta r_0 r_1 = 0$$

$$\sum M_z = 0 : M_{\phi\theta} r_0 + M_{\theta\phi} r_1 \sin\phi - N_{\phi\theta} r_0 r_1 + N_{\theta\phi} r_0 r_1 = 0$$

$$(2.1)$$

It can be shown that

$$N_{\phi\theta} = N_{\theta\phi}$$
$$M_{\phi\theta} = - M_{\theta\phi} \qquad (e)$$

if the thickness t of the shell is small in comparison with the radii of curvatures, r_1 and r_2.[1] However, an

[1] S. Timoshenko, "Theory of Plates and Shells," pp.352,353.

inconsistency results when these relationships are substituted in the last of the equilibrium Eqs. (2.1). This inconsistency is due to the fact that expressions (e) are only approximately true. If the exact expressions for $N_{\theta\phi}$, $N_{\phi\theta}$, $M_{\theta\phi}$, and $M_{\phi\theta}$ are used, then the last of Eqs. (2.1) is identically satisfied. In our further discussion, it will be assumed that the last of Eqs. (2.1) is always satisfied, and that the thickness of the shell is small in comparison with the radii of curvature, so that expressions (e) are valid.

Stress-Strain Relationships: With eight unknowns and only five equations provided by statics, additional equations, based upon the stress-strain relationships, must be introduced. If ξ_ϕ denotes the unit strain in the meridional direction, ξ_θ the corresponding strain in the direction perpendicular to the meridian, $\xi_{\phi\theta}$ the shearing strain, χ_ϕ and χ_θ the changes of curvature of the meridian and the plane perpendicular to the meridian, $\chi_{\phi\theta}$ the change of twist, E the Modulus of Elasticity and ν the Poisson's ratio, then, for thickness, t, small in comparison with r_2 and r_1, we have[2]

---

[2] Ibid, pp. 354,355.

$$N_\phi = \frac{Et}{1-\nu^2} (\epsilon_\phi + \nu\epsilon_\theta) \; ; \qquad N_\theta = \frac{Et}{1-\nu^2} (\epsilon_\theta + \nu\epsilon_\phi)$$

$$M = \frac{-Et^3}{12(1-\nu^2)} (\chi_\phi + \nu\chi_\theta); \quad M_\theta = \frac{-Et^3}{12(1-\nu^2)} (\chi_\theta + \nu\chi_\phi) \qquad \Big\} (f)$$

$$N_{\phi\theta} = N_{\theta\phi} = \frac{Et}{2(1+\nu)} \epsilon_{\phi\theta} \; ; \quad M_{\phi\theta} = -M_{\theta\phi} = \frac{Et^3}{12(1+\nu)} \chi_{\phi\theta}$$

Strain Displacement Relationships: The strains and the changes of curvature and twist can be related to the displacements u, v, and w, where u and v are the displacements in the directions of the tangents to the parallel circle and meridian, respectively, and considered plus when in the direction of increasing θ and ϕ , respectively; and w is the displacement in the direction normal to the shell surface, plus when directed inward. These relationships are[3]

$$\epsilon_\phi = \frac{1}{r_1} (\frac{\partial v}{\partial \phi} - w) \; ; \quad \epsilon_\theta = \frac{1}{r_2} (\frac{\partial u}{\partial \theta} \csc\phi + v \ctn\phi - w)$$

$$\epsilon_{\theta\phi} = \frac{1}{r_1} \frac{\partial u}{\partial \phi} + \frac{1}{r_2} \frac{\partial v}{\partial \theta} \csc\phi - \frac{u}{r_2} \ctn\phi$$

$$\chi_\phi = \frac{1}{r_1} \frac{\partial}{\partial \phi} (\frac{v}{r_1} + \frac{1}{r_1} \frac{\partial w}{\partial \phi}) \; ; \chi_\theta = \frac{1}{r_2} \ctn\phi (\frac{v}{r_1} + \frac{1}{r_1} \frac{\partial w}{\partial \phi})$$

$$+ \frac{\csc\phi}{r_2} \frac{\partial}{\partial \theta} (\frac{\csc\phi}{r_2} \frac{\partial w}{\partial \theta} + \frac{u}{r_2})$$

$$\chi_{\theta\phi} = \frac{1}{r_1} \frac{\partial}{\partial \phi} (\frac{\csc\phi}{r_2} \frac{\partial w}{\partial \theta} + \frac{u}{r_2}) - \frac{1}{r_1^2} \frac{\partial u}{\partial \phi}$$

(g)

[3] A. E. H. Love, "A Treatise on the Mathematical Theory of Elasticity," pp. 521, 524.

Stress Displacement Equations: Substituting the strain displacement equations (g) into the stress-strain relationships (f) gives

$$N_\phi = \frac{Et}{1-\gamma^2} \left[\frac{1}{r_1} \left(\frac{\partial v}{\partial \phi} - w \right) + \frac{\gamma}{r_2} \left(\frac{\partial u}{\partial \theta} \csc\phi + v \ctn\phi - w \right) \right]$$

$$N_\theta = \frac{Et}{1-\gamma^2} \left[\frac{1}{r_2} \left(\frac{\partial u}{\partial \theta} \csc\phi + v \ctn\phi - w \right) + \frac{\gamma}{r_1} \left(\frac{\partial v}{\partial \phi} - w \right) \right]$$

$$N_{\phi\theta} = N_{\theta\phi} = \frac{Et}{2(1+\gamma)} \left(\frac{1}{r_1} \frac{\partial u}{\partial \phi} + \frac{1}{r_2} \frac{\partial v}{\partial \theta} \csc\phi - \frac{u}{r_2} \ctn\phi \right)$$

$$M_\phi = -D \left\{ \frac{1}{r_1} \frac{\partial}{\partial \phi} \left(\frac{v}{r_1} + \frac{1}{r_1} \frac{\partial w}{\partial \phi} \right) \right.$$
$$\left. + \frac{\gamma}{r_2} \left[\frac{1}{r_1} \left(v + \frac{\partial w}{\partial \phi} \right) + \sec\phi \frac{\partial}{\partial \theta} \left(\frac{1}{r_2} \frac{\partial w}{\partial \theta} \csc\phi + \frac{u}{r_2} \right) \right] \ctn\phi \right\}$$

$$M_\theta = -D \left\{ \frac{1}{r_2} \left[\frac{1}{r_1} \left(v + \frac{\partial w}{\partial \phi} \right) + \sec\phi \frac{\partial}{\partial \theta} \left(\frac{1}{r_2} \frac{\partial w}{\partial \theta} \csc\phi + \frac{u}{r_2} \right) \right] \ctn\phi \right.$$
$$\left. + \frac{\gamma}{r_1} \frac{\partial}{\partial \phi} \left(\frac{v}{r_1} + \frac{1}{r_1} \frac{\partial w}{\partial \phi} \right) \right\}$$

$$M_{\phi\theta} = -M_{\theta\phi} = \frac{D(1-\gamma)}{r_1} \left[\frac{\partial}{\partial \phi} \left(\frac{1}{r_2} \frac{\partial w}{\partial \theta} \csc\phi + \frac{u}{r_2} \right) - \frac{1}{r_1} \frac{\partial u}{\partial \phi} \right]$$

$$(2.2)$$

where $D = \dfrac{Et^3}{12(1-\gamma^2)}$ $\qquad\qquad (2.3)$

Substituting expressions (2.2) in Eqs. (2.1) will then yield five equations in terms of the five unknown quantities u, v, w, Q_ϕ, and Q_θ.

2.2. Shells of Revolution Under Axially Symmetrical Load

Distribution. It can be concluded from the condition of symmetry that only normal stresses will act on the sides of the element ABCD (see Fig. 2.1) lying in the meridian plane. Hence

$$Q_\Theta = N_{\phi\Theta} = N_{\Theta\phi} = M_{\Theta\phi} = M_{\phi\Theta} = 0$$

Also due to symmetry the circumferential displacement u must be zero. The remaining stresses and displacements will all be independent of Θ. With these conditions the equilibrium Eqs. (2.1) reduce to

$$\frac{d}{d\phi}(N_\phi r_o) - N_\Theta r_1 \cos\phi - Q_\phi r_o = 0$$

$$N_\phi r_o + N_\Theta r_1 \sin\phi + \frac{d}{d\phi}(Q_\phi r_o) = 0 \qquad (2.4)$$

$$\frac{d}{d\phi}(M_\phi r_o) - M_\Theta r_1 \cos\phi - Q_\phi r_o r_1 = 0$$

and the stress displacement Eqs. (2.2) become

$$N_\phi = \frac{Et}{1-y^2}\left[\frac{1}{r_1}\left(\frac{dv}{d\phi} - w\right) + \frac{y}{r_2}(v\ ctn\phi - w)\right]$$

$$N_\Theta = \frac{Et}{1-y^2}\left[\frac{1}{r_2}(v\ ctn\phi - w) + \frac{y}{r_1}\left(\frac{dv}{d\phi} - w\right)\right]$$

$$M_\phi = -D\left[\frac{1}{r_1}\frac{d}{d\phi}\left(\frac{v}{r_1} + \frac{1}{r_1}\frac{dw}{d\phi}\right) + \frac{y}{r_2}\left(\frac{v}{r_1} + \frac{1}{r_1}\frac{dw}{d\phi}\right)ctn\phi\right] \qquad (2.5)$$

$$M_\Theta = -D\left[\frac{1}{r_2}\left(\frac{v}{r_1} + \frac{1}{r_1}\frac{dw}{d\phi}\right)ctn\phi + \frac{y}{r_1}\frac{d}{d\phi}\left(\frac{v}{r_1} + \frac{1}{r_1}\frac{dw}{d\phi}\right)\right]$$

Substitution of expressions (2.5) into the equilibrium Eqs. (2.4) yields three equations with the three

unknowns v, w, and Q_ϕ. But considerable simplification of the equations can be obtained by the introduction of two new variables, U and V, where

$$
\left.
\begin{aligned}
U &= r_2\, Q_\phi \\
V &= \frac{1}{r_1}\left(v + \frac{dw}{d\phi}\right)
\end{aligned}
\right\}
\qquad (2.6)
$$

It should be noted V is the expression for the rotation of the tangent to the meridian.[4]

To simplify the transformation, we replace the first of the equilibrium Eqs. (2.4) by one obtained by considering the equilibrium of the portion of the shell above the parallel circle defined by the angle ϕ (Fig. 2.2). If the resultant edge load on the edge AB of a shell of revolution is $2\pi r F$, then the equation of equilibrium is

$$
2\pi r_o N_\phi \sin\phi + 2\pi r_o Q_\phi \cos\phi = 2\pi r F
$$

from which

$$
N_\phi = \frac{rF}{r_o}\csc\phi - Q_\phi \ctn\phi = \frac{r}{r_2}F\csc^2\phi - \frac{1}{r_2}U\ctn\phi \qquad (2.7)
$$

From the second of Eqs. (2.5) we have

---

[4] This method of analysing stresses in shells was developed for the case of a spherical shell by H. Reissner, "Muller-Breslau-Festschrift," p. 181, Leipzig, 1912; it was generalized and applied to particular cases by E. Meissner, David W. Taylor Model Basin Translation 238, and by H. Wissler, "Festigkeitsberechnung von Ringflachenschalen," doctoral thesis, Zurich, 1916.
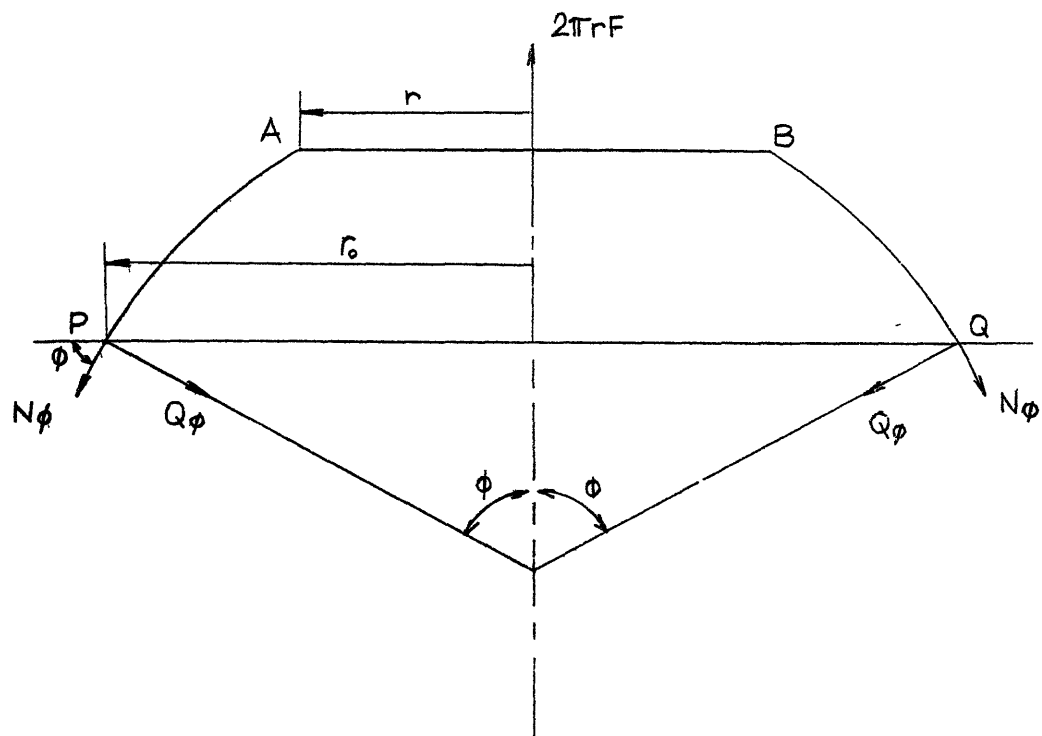
Fig. 2.2.   Equillbrium of a Portion of Shell
Above a Parallel Circle
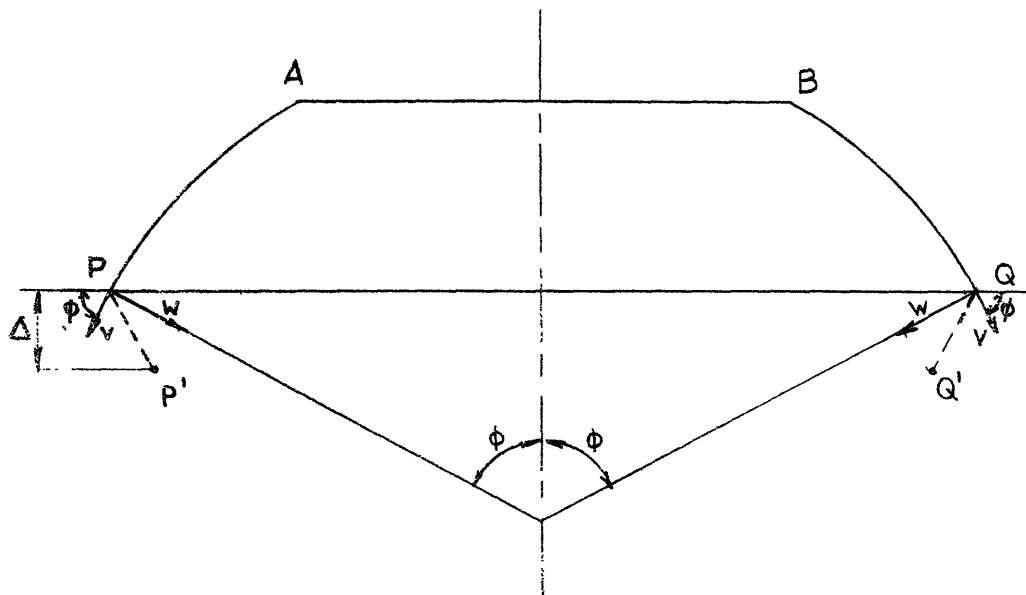
Fig. 2.3.   Displacements in a Shell

$$N_\Theta r_1 \sin\phi = -N_\phi r_o - \frac{d}{d\phi}(Q_\phi r_o)$$

Substitution of Eq. (a) in this and noting that $r_o = r_2 \sin\phi$ gives

$$N_\Theta = -\frac{1}{r_1}\left(rF \csc^2\phi + \frac{dU}{d\phi}\right) \tag{2.8}$$

From the first two of Eqs. (2.5) we readily obtain

$$\frac{dv}{d\phi} - w = \frac{r_1}{Et}(N_\phi - \gamma N_\Theta)$$

$$v \operatorname{ctn}\phi - w = \frac{r_2}{Et}(N_\Theta - \gamma N_\phi) \tag{a}$$

Elimination of w from these two equations leads to

$$\frac{dv}{d\phi} - v \operatorname{ctn}\phi = \frac{1}{Et}\left[(r_1 + \gamma r_2)N_\phi - (r_2 + \gamma r_1)N_\Theta\right] \tag{b}$$

Differentiation of Eq. (a) gives (if t is assumed to be constant)

$$\frac{dv}{d\phi}\operatorname{ctn}\phi - v \csc^2\phi - \frac{dw}{d\phi} = \frac{1}{Et}\frac{d}{d\phi}\left[r_2(N_\Theta - \gamma N_\phi)\right]$$

The derivate $\frac{dv}{d\phi}$ can now be eliminated from the last two equations, to yield

$$v + \frac{dw}{d\phi} = r_1 V = \frac{\operatorname{ctn}\phi}{Et}\left[(r_1 + \gamma r_2)N_\phi - (r_2 + \gamma r_1)N_\Theta\right]$$

$$- \frac{1}{Et}\frac{d}{d\phi}\left[r_2(N_\Theta - \gamma N_\phi)\right]$$

Substituting expressions (a) and (b) for N_ϕ and N_Θ, we finally obtain the first of the two equations relating to U and V

$$\frac{r_2}{r_1^2} \frac{d^2U}{d\phi^2} + \frac{1}{r_1}\left[\frac{d}{d\phi}\left(\frac{r_2}{r_1}\right) + \frac{r_2}{r_1}\,ctn\phi\right]\frac{dU}{d\phi} - \frac{1}{r_1}\left[\frac{r_1}{r_2}\,ctn^2\phi - \gamma\right]U$$

$$= Et\ V + Z \qquad\qquad (c)$$

where $\quad Z = -\ rF\ csc^2\phi\ ctn\phi\left[\frac{1}{r_2} - \frac{r_2}{r_1^2} + \frac{tan\phi}{r_1}\frac{d}{d\phi}\left(\frac{r_2}{r_1}\right)\right] \qquad (2.9)$

The second equation relating U and V is obtained by sub-stituting the last two of Eqs. (2.5) in the last of Eqs. (2.4) and using the notations (2.6). In this way

$$\frac{r_2}{r_1^2}\frac{d^2V}{d\phi^2} + \frac{1}{r_1}\left[\frac{d}{d\phi}\left(\frac{r_2}{r_1}\right) + \frac{r_2}{r_1}\,ctn\phi\right]\frac{dV}{d\phi} - \frac{1}{r_1}\left[\frac{r_1}{r_2}\,ctn^2\phi - \gamma\right]U$$

$$= -\ \frac{U}{D} \qquad\qquad (d)$$

By introducing the notation

$$L(\dots) = \frac{r_2}{r_1^2}\frac{d^2}{d\phi^2}(\dots) + \frac{1}{r_1}\left[\frac{d}{d\phi}\left(\frac{r_2}{r_1}\right) + \frac{r_2}{r_1}\,ctn\phi\right]\frac{d}{d\phi}(\dots)$$

$$-\ \frac{1}{r_2}\,ctn^2\phi\ (\dots) \qquad\qquad (2.10)$$

Eqs. (c) and (d) can be written in the following forms:

$$\left.\begin{array}{l} L\ (U) + \dfrac{\gamma U}{r_1} = EtV + Z \\[3mm] L\ (V) - \dfrac{\gamma V}{r_1} = -\ \dfrac{U}{D} \end{array}\right\} \qquad (2.11)$$

This system of two simultaneous differential equa-tions of the second order can be reduced to a single equa-tion of the fourth order. Operating on the first of Eqs. (2.11) by L(.....) gives

$$LL(U) + \nu L(\frac{U}{r_1}) = Et\, L(V) + L(Z)$$

Substituting the second of Eqs. (2.11) in this gives

$$L(V) = \frac{\nu V}{r_1} - \frac{U}{D} = \frac{\nu}{Etr_1}\left[L(U) + \frac{\nu U}{r_1} - Z\right] - \frac{U}{D}$$

Using this, we obtain

$$LL(U) + \nu L(\frac{U}{r_1}) - \frac{\nu}{r_1}L(U) - \frac{\nu^2}{r_1^2}U = -\frac{Et}{D}U + L(Z) - \frac{\nu}{r_1}Z$$

If r_1 is constant, as is the case for spherical, conical, and ring shells, then

$$L(\frac{U}{r_1}) = \frac{1}{r_1}L(U)$$

Using the notation

$$\mu^4 = \frac{Et}{D} - \frac{\nu^2}{r_1^2} \tag{2.12}$$

$$LL(U) + \mu^4(U) = L(Z) - \frac{\nu Z}{r_1} \tag{2.13}$$

Similarly

$$LL(V) + \mu^4(V) = -\frac{Z}{D} \tag{2.14}$$

The application of Eqs. (2.13) and (2.14) to partic-ular cases of a truncated conical shell and a ring shell will be discussed in the next two articles. However, the expression for the relative displacement between two parallel circles will first be found.

The deflection Δ_P of any point P on the shell sur-face in the direction of the shell axis can be found in

terms of the stresses N_ϕ and N_Θ. In Fig. 2.3 P' represents

the displaced position of P_1. From the figure, it is seen

that Δ_P is given in terms of the displacements v and w by

the expression

$$\Delta_P = v \sin\phi + w \cos\phi$$

Integration of the differential eq. (b) gives

$$v = \frac{\sin\phi}{Et}\left\{\int\frac{1}{\sin\phi}\left[N_\phi(r_1 + \gamma r_2) - N_\Theta(r_2 + \gamma r_1)\right]d\phi + C\right\} \quad (e)$$

in which C is a constant of integration.

From Eq. (a)

$$w = v\, ctn\phi - \frac{r_2}{Et}(N_\Theta - \gamma N_\phi) \quad (f)$$

Substitution of these two expressions for v and w in the

expression for Δ_P yields

$$\Delta_P = \frac{1}{Et}\left\{\int\left[N_\phi(r_1 + \gamma r_2) - N_\Theta(r_2 + \gamma r_1)\right]d\phi - r_2(N_\Theta - \gamma N_\phi) + C_1\right\}$$

The relative deflection between two parallel circles

whose positions are defined by the angles ϕ_1 and ϕ_2 can be

found by solving the above expression for Δ_P between the

limits ϕ_1 and ϕ_2. Denoting this deflection by Δ, we have

$$\Delta = \frac{1}{Et}\left\{\int_{\phi_1}^{\phi_2}\left[N_\phi(r_1 + \gamma r_2) - N_\Theta(r_2 + \gamma r_1)\right]d\phi - \left[r_2(N_\Theta - \gamma N_\phi)\right]_{\phi_1}^{\phi_2}\right\} (2.15)$$

2.3. <u>Truncated Conical Shell Under Axially Symmetrical</u>

<u>Load</u>. A truncated conical shell, ABCD, is shown in Fig. 2.4.

The dimensions b, c, h, and r are defined in this figure.
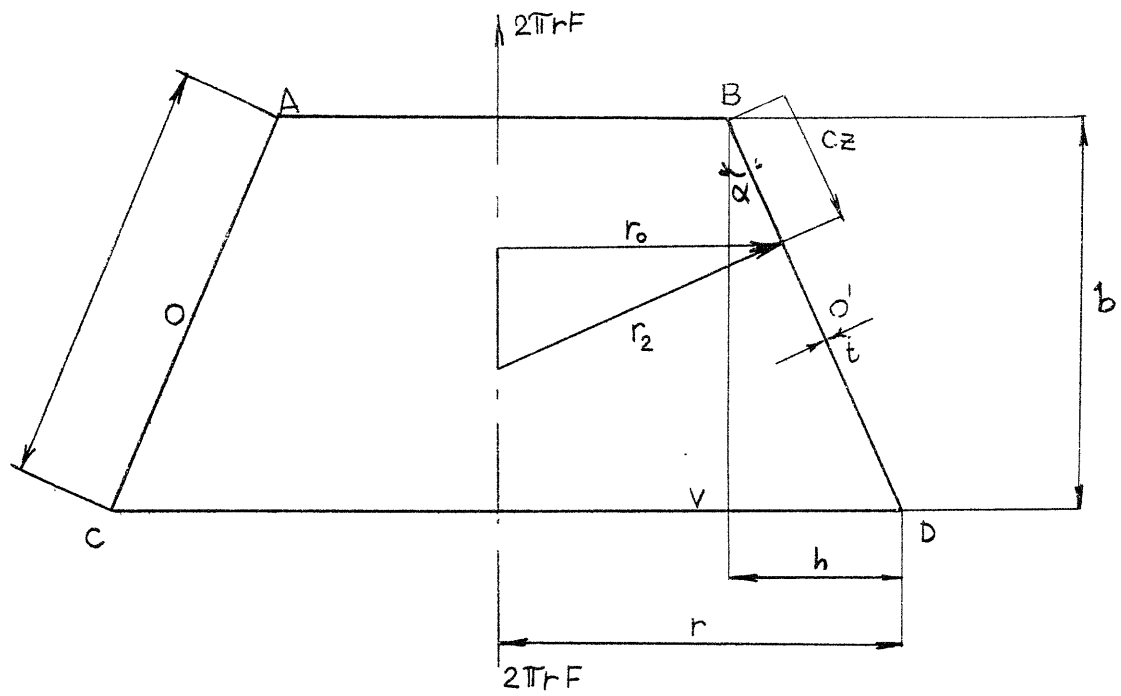
Fig. 2.4.   Truncated Conical Shell

To apply the general equations developed above to this case, we introduce in place of ϕ a new variable z which is the product of c and the distance along the meridian from the edge AB (see Fig. 2.4). The length of an infinitesimal element of a meridian is now cdz, instead of $r_1 d\phi$. As a result,

$$\frac{d}{d\phi} = \frac{r_1}{c} \frac{d}{dz} \quad ; \quad \frac{d^2}{d\phi^2} = \frac{d}{d\phi}(\frac{r_1}{c} \frac{d}{dz}) = \frac{r_1^2}{c^2} \frac{d^2}{dz^2} + \frac{1}{c} \frac{dr_1}{d\phi} \frac{d}{dz}$$

Using these transformations, and noting that r_1 is constant for a conical shell, the operator $L(\ldots)$ of Eq. (2.10) becomes

$$L(\ldots) = \left[\frac{r_2}{c^2} \frac{d^2}{dz^2}(\ldots) + (\frac{1}{c} \frac{dr_2}{dz} + \frac{r_2}{r_1} ctn\phi) \frac{1}{c} \frac{d}{dz}(\ldots) \right.$$
$$\left. - \frac{1}{r_2} ctn^2\phi (\ldots) \right] \tag{a}$$

Observing that ϕ is constant, and using the notation α for $\pi/2 - \phi$, we obtain (see Fig. 2.4)

$$r_2 = \frac{r}{cos\alpha} (1 - \frac{h}{r} + \frac{h}{r} z) \quad ; \quad \frac{dr_2}{dz} = \frac{h}{cos\alpha} \tag{b}$$

Substituting these expressions into (a) and putting $r_1 = \infty$, the symbol $L(\ldots)$ becomes

$$L(\ldots) = \left[\frac{r_2}{c^2} \frac{d^2}{dz^2}(\ldots) + \frac{h}{c^2 cos\alpha} \frac{d}{dz}(\ldots) - \frac{tan^2\alpha}{r_2}(\ldots) \right] \tag{c}$$

For the special case of a conical shell, Eqs. (2.9) and (2.13) reduce to

$$Z = - \frac{r}{r_2} F \sec^2\alpha \ \tan\alpha \qquad\qquad (d)$$

and $\quad LL(U) + \mu^4 U = L(Z) \qquad\qquad (e)$

The expression for Z when operated by L gives

$$L(Z) = 0$$

Eq. (e) then becomes

$$LL(U) + \mu^4 U = 0 \qquad\qquad (2.16)$$

which can be written in one of the following two forms:

$$L\left[L(U) \pm i\mu^2 U\right] \mp i\mu^2 \left[L(U) \pm i\mu^2 U\right] = 0$$

where $\quad i = \sqrt{-1}$

These equations indicate that the solutions of the second order equations

$$L(U) \pm i\mu^2 U = 0 \qquad\qquad (2.17)$$

are also the solutions of Eq. (2.16).

Using the expressions (b) and (c) in the first of Eqs. (2.17) gives

$$\frac{1}{c^2} \frac{r}{\cos\alpha}(1 - \frac{h}{r} + \frac{h}{r} z) \frac{d^2 U_1}{dz^2} + \frac{h}{c^2\cos\alpha} \frac{dU}{dz}$$

$$- \frac{\tan^2\alpha \ \cos\alpha}{r} \frac{U_1}{(1-h/r+h/r \ z)} + i\mu^2 \ U_1 = 0$$

Multiplying by $\frac{c^2\cos\alpha}{r} (1 - \frac{h}{r} + \frac{h}{r} z)$, and introducing the notations

$$\rho = \frac{h}{r}$$

$$a = \frac{\mu^2 c^2 \cos\alpha}{r} = \sqrt{12(1-\gamma^2)}\ \frac{bc}{rt}$$

(f)

finally yields the equation

$$(1 - \rho + \rho z)^2 \frac{d^2 U_1}{dz^2} + \rho(1 - \rho + \rho z)\frac{dU_1}{dz}$$

$$- \left[\rho^2 - ia\ (1 - \rho + \rho z)\right] U_1 = 0 \qquad (2.18)$$

The solution of Eq. (h) can be found in the form of power series in z multiplied by a power of z,

$$U_1 = z^s \sum_{k=0}^{\infty} A_k z^k \qquad (g)$$

The method of Frobenius was used for the determination of s and the recurrence formulae for the coefficients.[5] It was found that $s = 0$ and 1.

For $s = 0$, the recurrence formula is

$$k(k-1)(1-\rho)^2 A_k = -\left\{ \rho(1-\rho)(k-1)(2k-3)\ A_{k-1} \right.$$

$$\left. + \left[\rho^2(k-1)(k-3) + ia(1-\rho)\ A_{k-2}\right] + ia\rho\ A_{k-3} \right\} \qquad k \geqslant 1$$

When $k = 1$, the recurrence formula is identically satisfied, leaving A_1 as well as A_0 arbitrary.

When $s = 1$, the solution obtained is the same as that corresponding to the coefficient A_1 for the case

[5] F. B. Hildebrand, "Advanced Calculus for Engineers," pp. 132-139.

$s = 0$. Hence the complete solution of (2.18) can be expressed as

$$U_1 = \sum_{k=0}^{\infty} A_k \, z^k \qquad \text{(h)}$$

where

$$A_k = - \frac{1}{k(k-1)(1-\rho)^2} \left\{ \rho(1-\rho)(k-1)(2k-3)\, A_{k-1} \right.$$
$$\left. + \left[\rho^2(k-1)(k-3) + ia(1-\rho) \right] A_{k-2} + ia\rho\, A_{k-3} \right\} \qquad k \geqslant 2 \quad \text{(i)}$$

Separating the series (i) into its real and imaginary parts, we obtain

$$U_1 = A_0(I_1 + i\, I_2) + A_1 z(I_3 + i\, I_4)$$

where $I_1, \ldots, I_4$ are power series which are convergent when $(1-\rho + \rho z) \neq 0$.

By inspection, the solution of the second of Eqs. (e) is

$$U_2 = A_0(I_1 - i\, I_2) + A_1 z(I_3 - i\, I_4)$$

Solutions U_1 and U_2 together represent the complete system of independent solutions of Eq. (2.16). By using the sums and differences of solutions U_1 and U_2, the general solution of Eq. (2.16) can be written in the form:

$$U = AI_1 + BI_2 + CI_3 + DI_4 \qquad \text{(2.19)}$$

where A, B, C, and D are arbitrary constants.

Substituting (2.19) in the first of Eqs. (2.11) gives

$$V = \frac{\sin \alpha}{Etb(1-\varrho+\varrho z)} \left[\frac{1}{\varrho}(1-\varrho+\varrho z)^2(AI_1'' + BI_2'' + CI_3'' + DI_4'') \right.$$

$$+ (1-\varrho+\varrho z)(AI_1' + BI_2' + CI_3' + DI_4') - \varrho(AI_1 + BI_2 + CI_3 + DI_4)$$

$$\left. + Fh \sec\alpha \csc\alpha \right] \tag{2.20}$$

where $I' \equiv \dfrac{dI}{dz}$, $I'' \equiv \dfrac{d^2 I}{dz^2}$

2.4. <u>Ring Shell</u>. A ring shell is shown in Fig. 2.5. The radius r is as defined in Fig. 2.5. The angle ϕ varies from ϕ_0 to $\pi - \phi_0$. For this case it is convenient to solve Eq. (2.14) for V. Since this is a linear nonhomogeneous differential equation, its solution can be separated into V_H, the solution of (2.14) with Z = 0 (homogeneous solution), and V_P a particular solution of Eq. (2.14).

Homogeneous Solution: Setting Z = 0 in Eq. (2.14) gives

$$LL(V_H) + \mu^4 V_H = 0 \tag{a}$$

Eq. (a) is similar to Eq. (2.16) and hence it can be concluded that the solution of the second order equations

$$L(V_H) \pm i\mu^2 V_H = 0 \tag{b}$$

are also solutions of Eq. (a)

From Fig. 2.5 we see that

$$\left. \begin{array}{l} r_1 = \text{constant} \\[4pt] r_2 = (r-r_1)\csc\phi + r_1 \\[4pt] \dfrac{dr_2}{d\phi} = -(r-r_1)\csc\phi \; \text{ctn}\,\phi \end{array} \right\} \tag{c}$$
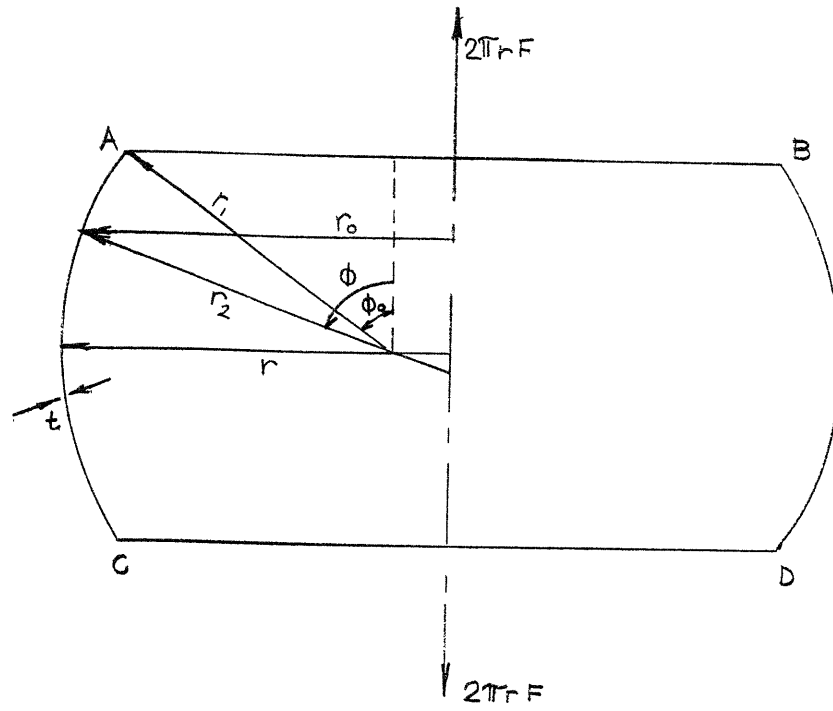
Fig. 2.5. Ring Shell

With these relationships, the symbol L(...) of Eq. (2.10)

becomes

$$L(...) = \frac{r_2}{r_1^2} \frac{d^2}{d\phi^2}(...) + \frac{ctn\phi}{r_1} \frac{d}{d\phi}(...) - \frac{1}{r_2} ctn^2\phi \ (...) \qquad (d)$$

Using this in the first of Eqs. (b) gives

$$\frac{r_2}{r_1^2} \frac{d^2 V_{H1}}{d\phi^2} + \frac{ctn\phi}{r_1} \frac{dV_{H1}}{d\phi} - \frac{1}{r_2} ctn^2\phi \ V_{H1} + i\mu^2 \ V_{H1} = 0 \qquad (e)$$

A further simplification is obtained by introducing the

new variable

$$x = 1 - sin\phi . \qquad (f)$$

With this change

$$\frac{d}{d\phi} = - cos\phi \frac{d}{dx} \quad , \quad \frac{d^2}{d\phi^2} = cos^2\phi \frac{d^2}{dx^2} + sin\phi \frac{d}{dx} \qquad (g)$$

Using these relationships, Eq. (e) becomes

$$\frac{r_2}{r_1^2} cos^2\phi \ \frac{d^2 V_{H1}}{dx^2} + \frac{1}{r_1}(\frac{r_2}{r_1} sin\phi - \frac{cos^2\phi}{sin\phi}) \frac{dV_{H1}}{dx}$$

$$- (\frac{1}{r_2} ctn^2\phi - i\mu^2) \ V_{H1} = 0$$

By noting that

$$cos^2\phi = 1 - sin^2\phi = x(2-x)$$

$$ctn^2\phi = \frac{cos^2\phi}{sin^2\phi} = \frac{x(2-x)}{(1-x)^2}$$

and $$r_2 = (r-r_1)csc\phi + r_1 = \frac{r-r_1 x}{1-x}$$

we have

$$\frac{x(r-r_1 x)}{r_1^2 (1-x)} (2-x) \frac{d^2 V_{H1}}{dx^2} + \frac{1}{r_1} \left[\frac{r-r_1 x}{r_1} - \frac{x(2-x)}{1-x} \right] \frac{dV_{H1}}{dx}$$

$$- \left[\frac{x(2-x)}{(1-x)(r-r_1 x)} - i\mu^2 \right] V_{H1} = 0$$

Multiplying by $\dfrac{r_1^2 (1-x)(r-r_1 x)}{xr^2}$, and introducing the notations

$$\left. \begin{array}{l} \lambda = \dfrac{r_1}{r} \\[2mm] a_1 = \dfrac{\mu^2 r_1^2}{r} = \dfrac{r_1}{r} \sqrt{\dfrac{12(1-\gamma^2) r_1^2}{t^2} - \gamma^2} \end{array} \right\} \qquad\qquad (h)$$

finally yields the equation

$$(2-x)(1-\lambda x)^2 \frac{d^2 V_{H1}}{dx^2} + \frac{1}{x} \left[(1-x)(1-\lambda x)^2 - \lambda x(2-x)(1-\lambda x) \right] \frac{dV_{H1}}{dx}$$

$$- \frac{1}{x^2} \left[\lambda^2 x^2(2-x) - i\, a_1 x(1-x)(1-\lambda x) \right] V_{H1} = 0 \qquad\qquad (i)$$

Here again the solution can be found in the form of power series in x multiplied by a power of x

$$V_{H1} = x^s \sum_{k=0}^{\infty} A_k x^k$$

The method of Frobenius was again used for the determination of s and the recurrence formulae for the coefficients. It was found that s = 0 and 1/2 for this case. For s = 1/2 the recurrence formula is

$$A_k = \frac{1}{k(2k+1)} \left\{ \left[\frac{1}{4}(2k-1)^2(1+4\lambda) - ia_1 \right] A_{k-1} \right.$$

$$- \left[\rho(k-1)(2k-3)(1+\lambda) - 2\lambda^2 - ia_1(1+\lambda) \right] A_{k-2}$$

$$\left. + \left[\frac{\lambda^2}{4}(2k-3)(2k-5) - \lambda^2 - ia_1\lambda \right] \right\} \qquad k \geqslant 1 \qquad (j)$$

A second solution corresponding to s = 0 is of the form

$$V_{H1} = \sum_{k=0}^{\infty} A_k x^k$$

Because of symmetry, $\left[V \right]_\phi = -\left[V \right]_{\pi-\phi}$ for all values of ϕ.

Since the series corresponding to s = 0 cannot satisfy this condition, the second solution should not be considered. Hence the complete solution of Eq. (i) can be expressed as

$$V_{H1} = x^{1/2} \sum_{k=0}^{\infty} A_k x^k \qquad (k)$$

where A_k is given by the recurrence formula (j).

Separating the series (k) into real and imaginary parts, we obtain

$$V_{H1} = A_0(J_1 + i J_2) \qquad (1)$$

where J_1 and J_2 are power series multiplied by $x^{1/2}$, the series being convergent when $(2-x)(1-\lambda x)^2 \neq 0$.

As was shown for the case of the truncated cone, the complete solution of Eq. (a) can be represented in the

following form

$$V_H = C_1 J_1 + C_2 J_2 \qquad\qquad (m)$$

where C_1 and C_2 are arbitrary constants.

Substituting (1) in the first of Eqs. (b) gives

$$L(J_1 + i\, J_2) + i\, \mu^2(J_1 + i\, J_2) = 0$$

$$\therefore \left[L(J_1) - \mu^2 J_2\right] + i\left[L(J_2) + \mu^2 J_1\right] = 0$$

For this to be an identity,

$$L(J_1) = \mu^2 J_2$$

$$L(J_2) = -\mu^2 J_1$$

Substituting Eq. (m) in the second of Eq. (2.11) and using the above relationships gives

$$U_H = D\left(C_2 \mu^2 + C_1 \frac{\nu}{r_1}\right) J_1 - \left(C_1 \mu^2 - C_2 \frac{\nu}{r_1}\right) J_2 \qquad (n)$$

Having obtained the homogeneous solution of Eq. (2.11), we shall next attempt to find its particular solution system.

Particular Solution: If

$$S = S_1 + i\, S_2 \qquad\qquad (o)$$

is a particular solution of the inhomogeneous equation

$$L(S) - i\, \mu^2 S = Z \qquad\qquad (p)$$

then it can be shown by direct substitution that

$$\left.\begin{aligned}V_P &= -\frac{1}{\mu^2 D}\, S_2 \\[6pt] U_P &= S_1 - \frac{\nu}{\mu^2 r_1}\, S_2\end{aligned}\right\} \qquad (q)$$

is the particular solution system of Eqs. (2.11). The solution of the differential equation (p) will also be obtained in terms of power series.

Using the relationships (c), (f), and the first of the expressions (h) in Eq. (2.9) gives

$$Z = \frac{F(1-\lambda) \cos\phi}{\lambda^2(1-\lambda x)(1-x)^4} (2 + \lambda - 3\lambda x)$$

Let $\quad S = S_1 + i S_2 = Fr(1-\lambda) W \ ctn \phi$ $\qquad$ (r)

The differential equation (p) then becomes

$$L(W \ ctn\phi) - i \mu^2 W \ ctn\phi = \frac{\cos\phi}{\lambda r_1(1-\lambda x)(1-x)^4} (2+\lambda- 3\lambda x)$$

The symbol $L(...)$ is defined by (d), and ϕ is related to x by the expression (f). Using this in the above differential equation gives

$$(1-\lambda x)(2-x)(1-x)^2 \frac{d^2W}{dx^2}$$

$$+ \frac{(1-\lambda x)(1-x)}{x} \left[(1-\lambda x)(1-x)^2 + 2(1-\lambda x) - \lambda x(1-x)(2-x) \right] \frac{dW}{dx}$$

$$+ \frac{1}{x^2} \left[2x(1-\lambda x)^2 - \lambda x(1-\lambda x)(1-x) - \lambda^2 x^2(1-x)^2(2-x) \right.$$

$$\left. - i \ a_1 x(1-\lambda x)(1-x)^3 \right] W = \frac{1}{x^2} (2+\lambda) \ x-3\lambda x^2 \qquad (s)$$

A solution of the above equation can be taken in the form

$$W = \sum_{k=0}^{\infty} B_k \ x^k \qquad (t)$$

Substituting the series (t) in Eq. (s) and equating the coefficients for each power of x to zero, we obtain the following recurrence formula for B_k:

$$B_k = \frac{1}{k(2k+1)} \left\{ N_k - \sum_{s=0}^{4} \left[(k-s-1)(k-s-2)R_{s+1} \right. \right.$$
$$\left. \left. + (k-s-1)P_{s+1} + Q_{s+1} \right] B_{k-s-1} \right\}$$
$$(B_o = 0 \ , \ k \geqslant 1) \qquad\qquad (u)$$

where

$$N_1 = (2+\lambda) \quad ; \quad N_2 = -3\lambda \quad ; \quad N_3 = N_4 = N_5 = \ldots\ldots = 0$$

$$R_1 = -(5+4\lambda) \ ; \ R_2 = (4+10\lambda+2\lambda^2) \ ; \ R_3 = -(1+8\lambda+5\lambda^2) \ ;$$
$$R_4 = 2\lambda(1+2\lambda) \ ; \ R_5 = -\lambda^2$$

$$P_1 = -(5+8\lambda) \ ; \ P_2 = (3+15\lambda+5\lambda^2) \ ; \ P_3 = -(1+10\lambda+10\lambda^2) \ ;$$
$$P_4 = \lambda(3+7\lambda) \ ; \ P_5 = -2\lambda^2$$

$$Q_1 = (2-\lambda-ia_1) \ ; \ Q_2 = -(3\lambda+\lambda^2-3ia_1-ia_1\lambda);$$
$$Q_3 = (6\lambda^2-3ia_1-3ia_1\lambda) \ ; \ Q_4 \quad -(4\lambda^2-ia_1-3ia_1) \ ; \ Q_5=(\lambda^2-ia_1\lambda)$$

Separating the series into real and imaginary parts, we obtain

$$W = J_3 + i J_4$$

where J_3 and J_4 are converging power series when $(1-\lambda x)(2-x)(1-x) \neq 0$.

S_1 and S_2 can then be related to J_3 and J_4 by the expression (r) giving

$$S_1 = F\ r\ (1-\lambda)\ \text{ctn}\,\phi\ J_3 = F\ r(1-\lambda)\ \sqrt{\frac{x(2-x)}{1-x}}\ J_3$$

$$S_2 = F\ r\ (1-\lambda)\text{ctn}\,\phi\ J_4 = F\ r(1-\lambda)\ \sqrt{\frac{x(2-x)}{1-x}}\ J_4$$

Substitution of these relationships in (q) yields

$$V_P = -\frac{Fr(1-\lambda)}{\mu^2 D}\ \sqrt{\frac{x(2-x)}{1-x}}\ J_4$$

$$U_P = Fr(1-\lambda)\ \sqrt{\frac{x(2-x)}{1-x}}\ \left(J_3 - \frac{\gamma}{\mu^2 r_1}\ J_4\right)$$

as the particular solution system of the differential equations (2.11). Since these are linear equations, it is permissible to add the homogeneous and the particular solutions to obtain the complete solution.

Thus $\quad U = U_H + U_P$

$$V = V_H + V_P$$

or

$$U = D\left[(C_2\mu^2 + C_1\frac{\gamma}{r_1})\ J_1 - (C_1\mu^2 - C_2\frac{\gamma}{r_1})\ J_2\right]$$

$$+ Fr(1-\lambda)\ \sqrt{\frac{x(2-x)}{1-x}}\ \left(J_3 - \frac{\gamma}{\mu^2 r_1}\ J_4\right) \qquad (2.21)$$

$$V = C_1 J_1 + C_2 J_2 - \frac{Fr(1-\lambda)}{\mu^2 D}\ \sqrt{\frac{x(2-x)}{1-x}}\ J_4 \qquad (2.22)$$

2.5. <u>Equations for Forces, Moments, and Displacements in Terms of U and V</u>. Having the expressions for U and V, we

can obtain all the forces, moments, and displacements in terms of these two quantities. The forces N_ϕ and N_θ are found from Eqs. (2.7) and (2.8). The bending moments M_ϕ and M_θ are obtained from the last two of Eqs. (2.5) by setting $\frac{1}{r_1}(v + \frac{dw}{d\phi})$ equal to V. The only displacement that will be of interest is the relative deflection between two parallel circles defined by the angles ϕ_1 and ϕ_2. This is obtained by substituting Eqs. (2.7) and (2.8) into Eq. (2.15). The equations resulting from these substitutions are

$$Q_\phi = \frac{1}{r_2} U$$

$$N_\phi = \frac{1}{r_2} (Fr \csc^2\phi - U \ctn\phi)$$

$$N_\theta = -\frac{1}{r_1}(r F \csc^2\phi + \frac{dU}{d\phi})$$

$$M_\phi = -D (\frac{1}{r_1}\frac{dV}{d\phi} + \frac{\nu V \ctn\phi}{r_2})$$

$$M = -D (\frac{\nu}{r_1}\frac{dV}{d} + \frac{V \ctn\phi}{r_2})$$

$$\Delta = \frac{1}{Et}\left\{\int_{\phi_1}^{\phi_2}\left[r(\frac{r_1}{r_2} + \frac{r_2}{r_1}) F \csc^2\phi + (\frac{r_2}{r_1} + \nu) \frac{dU}{d\phi}\right.\right.$$
$$\left. - (\frac{r_1}{r_2} + \nu) U \ctn\phi\right]d\phi + \left[r(\frac{r_2}{r_1} + \nu) F \csc^2\phi\right.$$
$$\left.\left. + \frac{r_2}{r_1} \cdot \frac{dU}{d\phi} - \nu U \ctn\phi\right]_{\phi_1}^{\phi_2}\right\}$$

$$(2.23)$$

CHAPTER 3

CORRUGATED PIPES

3.1. <u>Corrugated Pipe Under Axial Load</u>. Pipes with three
different types of corrugation are shown in Fig. 3.1, each
subjected to an axial load of $2\pi rF$. The first one has
V-shaped corrugations; the corrugations of the second one
consists of concave circular arcs, while those of the pipe
in (c) consist of a series of alternating concave and con-
vex circular arcs. These three types of corrugations will
be referred to as V-shaped corrugations, cusped corruga-
tions, and undulating corrugations, respectively.

The dimensions of the corrugation will be defined
by the symbols b, c, and h. (See Fig. 3.1.) In our fur-
ther discussion we shall refer to b as the width of a
corrugation, c as the length, and h as the depth of a
corrugation. The thickness t of the pipe wall will be
assumed to be constant over the entire pipe length. The
radius r of the pipe will be considered to mean the aver-
age radius of the pipe. It will be seen that all the
quantities defined above have the same meaning for all
three types of corrugations.

Each of the three corrugated pipes shown in Fig.
3.1 can be considered as being formed by combining several
shells of revolution such as ABCD, CDEF, ... If the
pipe is sufficiently long, any one such shell can be ana-
lysed and considered to be typical for the entire pipe.

$2\pi r F$

$2\pi r F$

$2\pi r F$

$2\pi r F$

$2\pi r F$

$2\pi r F$

A C E

B D F

A C E

B D F

A C E

B D F

r

r

r
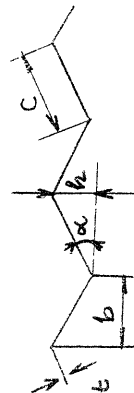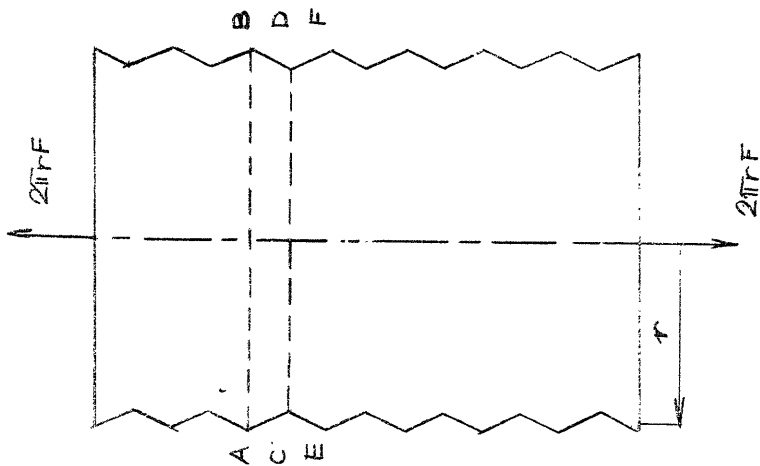
(a) V-Shaped Corrugations
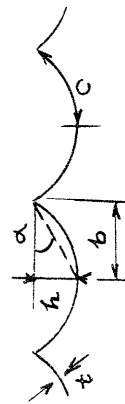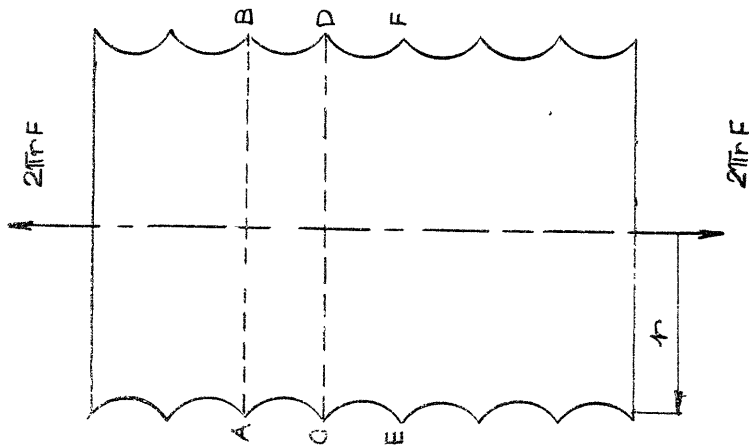
(b) Cusped Corrugations
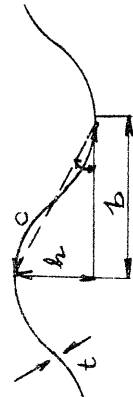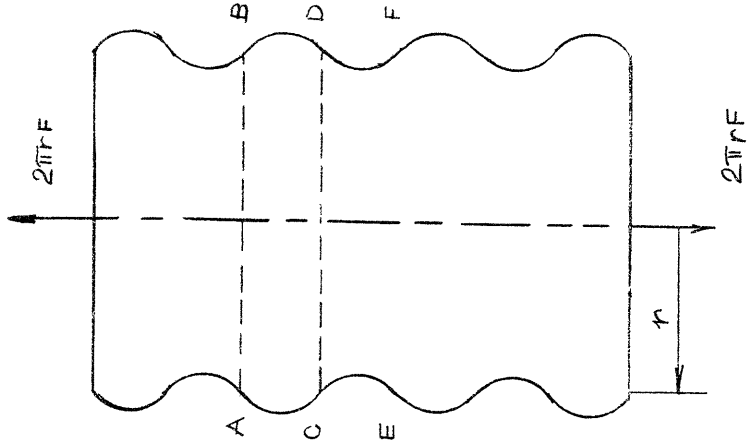
(c) Undulating Corrugations

Fig. 3.1. Corrugated Pipes

The shells ABCD, CDEF, ... for the pipe in (a) are truncated conical shells, whereas those for (b) and (c) are ring shells. Each one of these shells is subject to an axially symmetrical load of $2\pi rF$. This load acts along the edges AB, CD, EF, ... only, so that the shell surface can be considered to be free of any external load (the weight of the shell being neglected).

In Chapter 2, we have obtained solutions for truncated conical shells and convex ring shells, such as ABCD of Fig. 3.1(a) and (c), respectively, subjected to the type of loading mentioned above. The solution for the concave ring shell, such as CDEF of Fig. 3.1(b) and (c), can be directly obtained from that for a convex ring shell, if the parameter

$$\rho = \frac{h}{r} \tag{2.1}$$

is small and if the edge conditions are the same. For if ρ is small, the radius of curvature r_2 is approximately the same for corresponding points of the two shells (see Fig. 3.2). However, the curvature of the meridian for the convex and concave shells is of the opposite kind. Hence, the force N_θ and moments M_ϕ and M_θ for the two shells which arise due to this curvature will be of the same magnitude, but opposite in sign, for these two shells, whereas the force N_ϕ will be of the same sign and magnitude. Also since the forces and moments are of the same magnitude
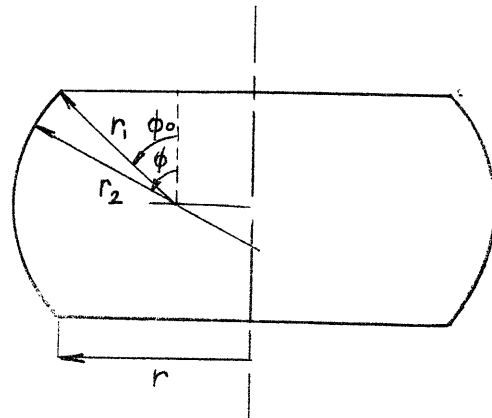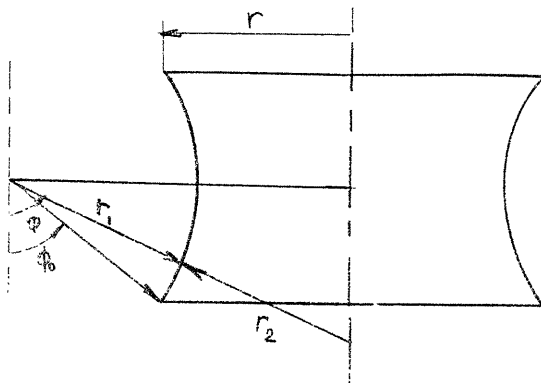
$$r_2 = \csc\phi\left[r + r_1\,(\sin\phi - \sin\phi_0)\right]$$
$$= r\csc\phi\left[1 + \rho\,\frac{(\sin\phi - \sin\phi_0)}{(1 - \sin\phi_0)}\right]$$
$$\approx r\csc\phi$$

(a) Convex Ring Shell

$$r_2 = \csc\phi\left[r - r_1\,(\sin\phi - \sin\phi_0)\right]$$
$$= r\csc\phi\left[1 - \rho\,\frac{(\sin\phi - \sin\phi_0)}{(1 - \sin\phi_0)}\right]$$
$$\approx r\csc\phi$$

(b) Concave Ring Shell

Fig. 3.2. Ring Shells

for the convex and concave ring shells, the strain energy
due to the axial force of $2\pi rF$ must be the same for the
two. By equating the strain energy to the external work,
it follows that the expansion of the shells in the direc-
tion of their axes of revolution must also be the same.
Thus, if ρ is small the solution of a convex ring shell
can be directly used for a concave shell by only changing
the signs of N_Θ, M_ϕ, and M_Θ. Unless otherwise stated, ρ
will be assumed to be small in our further discussion.

In each of the three cases, it is only necessary to
analyse the shell ABCD and consider it to be typical for
the entire pipe length. The stresses and deflection for
the conical shell can be obtained by using the general so-
lutions (2.19) and (2.20), while those for the ring shell
can be obtained from (2.21) and (2.22). The constants ap-
pearing in these solutions can be determined from the
boundary conditions at the edges AB and CD.

Because of the restraint from adjacent shells, the
rotation of the meridian at the edges AB and CD of Fig.
3.1(a) and (b) must be zero. Furthermore, there can be no
component of force normal to the axis of revolution at
these edges. The expression for the rotation of a tangent
to the meridian is given by the second of Eqs. (2.6), while
the component of force normal to the axis of revolution is
equal to $Q_\phi \sin\phi - N_\phi \cos\phi$ (see Fig. 2.2). The forces Q_ϕ and
N_ϕ are related to the parameter U by the first two of Eqs.

(2.23). Thus, the boundary conditions at the edges AB and
CD can be written as

$$V = 0 \quad \Bigg\} \qquad \text{(a)}$$
$$Q_\phi \sin\phi - N_\phi \cos\phi = \frac{\csc\phi}{r_2}(U - Fr\cot n\phi) = 0 \quad \Bigg\}$$

For the pipe with the undulating corrugations it
can be concluded from the antisymmetry of the deformations
that there would be inflection points at the edges AB and
CD and that the circumferential force N_Θ, given by the
third of Eqs. (2.23), must be zero. In equation form the
boundary conditions at the edges AB and CD are

$$\frac{1}{r_1} \frac{dV}{d\phi} = 0 \quad \Bigg\} \qquad \text{(b)}$$
$$N_\Theta = -\frac{1}{r_1}\left(rF\csc^2\phi + \frac{dU}{d\phi}\right) = 0 \quad \Bigg\}$$

where V is the rotation of a tangent to the meridian.

With these boundary conditions the constants appear-
ing in the solutions (2.19) through (2.22) can be deter-
mined, thereby obtaining expressions for U and V for all
the three cases. Substitution of these expressions into
Eqs. (2.23) will finally give the forces and moments in the
shell and the relative deflection Δ between the edges AB
and CD can be found. It should be noted that Δ represents
the deflection of an axially loaded corrugated pipe of
length equal to the perpendicular distance between AB and
CD. The unit stresses in the circumferential direction and
in the meridian direction (i.e. perpendicular to the

circumferential direction) can easily be obtained from the values of the forces and moments.

In the meridional direction, the unit stress in the extreme fibre is given by

$$\sigma_\phi = \frac{N_\phi}{t} \pm \frac{6M_\phi}{t^2} \qquad (c)$$

In order to obtain a dimensionless quantity, we shall divide σ_ϕ by

$$\sigma = \frac{F}{t} \qquad (d)$$

which is the stress in a plain pipe having the same thickness and mean radius as the corrugated one. The ratio σ_ϕ/σ will be called the meridional stress factor and will be denoted by the symbol K_ϕ

$$K_\phi = \frac{N_\phi}{F} \pm \frac{6M_\phi}{Ft}$$

Similarly, for the circumferential direction we have

$$K_\theta = \frac{N_\theta}{F} \pm \frac{6M_\theta}{Ft}$$

in which K_θ is the circumferential stress factor.

For all practical purposes it is only necessary to know the absolute maximum value of the stresses. So in our further discussion we will take K_ϕ and K_θ to mean the absolute maximum values of these two factors, i.e.

$$K_\phi \equiv \left[\left| \frac{N_\phi}{F} \right| + \left| \frac{6M_\phi}{Ft} \right| \right]_{max} \qquad (e)$$

$$K_\Theta = \left[\left| \frac{N_\Theta}{F} \right| + \left| \frac{6M_\Theta}{Ft} \right| \right]_{max} \tag{f}$$

Then in order to obtain the maximum value of the stresses in the meridional and circumferential directions in a corrugated pipe, one merely multiplies the stress in a corresponding plain pipe by the stress factors K_ϕ and K_Θ, respectively.

In place of calculating the relative deflection Δ between the edges AB and CD, it is convenient to obtain a "reduced modulus of elasticity" for a corrugated pipe, so that deflection calculations for a corrugated pipe can be made by considering the pipe to be plain but having this reduced modulus as its modulus of elasticity. The ratio of the modulus of elasticity of the pipe material to this reduced modulus will be called the modular ratio and will be denoted by the symbol N. It is evident that N is equal to the ratio of Δ for a corrugated pipe to the corresponding Δ for a plain pipe of the same major dimensions.

Use was made of the IBM 704 Computer at the M.I.T. Computation Center to obtain values of K_ϕ, K_Θ, and N for all three types of corrugations. It was found that these factors could be put in the following forms

$$K_\phi = 1 + \frac{h}{t} k_\phi \tag{3.1}$$

$$K_\Theta = \frac{h}{t} k_\Theta \tag{3.2}$$

$$N = \cos\alpha + \frac{ch^2}{bt^2} n \tag{3.3}$$

in which

$$\alpha = \tan^{-1} \frac{h}{b} \tag{3.4}$$

and k_ϕ, k_Θ, and n are, in general, functions of α and another parameter β, where

$$\beta = \sqrt{\frac{bc}{rt}} \tag{3.5}$$

The quantities k_ϕ, k_Θ, and n were calculated for values of β ranging from 0 to 5, with α varying from 0.1 to 1.5 radians for V-shaped corrugations and from 0.05 to 0.75 radians for the circular corrugations. The value of Poisson's ratio, γ, was taken to be 0.3 in these calculations. The results of these calculations are shown in Figs. A.1 through A.9 in Appendix A.

Comparison of Eqs. (e) and (3.1) shows that the value of $\left|\frac{N_\phi}{F}\right|$ is unity. However, this is not correct. For the V-shaped and cusped corrugations its value was $\cos\alpha$ and $\cos 2\alpha$, respectively, whereas for the undulating corrugations its value ranged from 1 to 2.25 depending upon the value of α and β. But in comparison with the value of $\frac{h}{t} k_\phi$ this term is small, except for very shallow corrugations, i.e. for small α, and its value then approaches that given. Hence, its value can be taken equal to unity without introducing any appreciable error in K_ϕ.

The term $\cos\alpha$ in Eq. (3.3) is also not correct for the circular corrugations. This term represents the effect of the meridional direct stresses N_ϕ. The correct value of this term is given by the expression

$$\frac{\alpha}{\sin 2\alpha} + \frac{\cos 2\alpha}{2} \tag{g}$$

However, this expression differs from $\cos\alpha$ only for large values of α, and the difference is maximum for semi-circular corrugations (i.e. for $\alpha = \pi/4$) when the error is less than 10%. But for large values of α, the second term of Eq. (3.3) is so large that the resulting error in N is negligible if expression (g) is approximated by $\cos\alpha$. Hence, it is permissible to make this approximation. This also makes it possible to have the expression for N of the same form for all three types of corrugations.

The parameter β given by expression (3.5) has the same significance as the parameter $1/\lambda$ used in connection with beams on elastic foundation.[1] λ is known as the characteristic length since it has the dimension of length, whereas β is a dimensionless quantity obtained by multiplying $\frac{1}{\lambda}$ by a quantity which has a dimension of length. In our case this quantity is $\sqrt{bc}$. In further discussion we will refer to β as the pipe characteristic, as it is the parameter which primarily influences the factors K_ϕ, K_θ, and N.

---

[1] M. Hetenyi, "Beams on Elastic Foundation."

It should be mentioned that the charts shown in Appendix A are valid only when the thickness of the pipe is small in comparison with the two principal radii of curvature of the corrugations. This is so because the solutions for conical and ring shells presented in Chapter 2, on which the results of the charts are based, were obtained under these assumptions. The radius of curvature r_1 of the meridian is infinite for V-shaped corrugations; hence, t/r_1 is zero. For the circular corrugations

$$r_1 \sim \frac{h}{1-\cos 2\alpha}$$

and so $t(1-\cos 2\alpha)/h$ must be small. The other radius of curvature r_2 is proportional to the radius of the pipe r, so that t/r must also be small.

The only other assumption made is that the ratio $\rho = h/r$ is small. In order to study the effect of ρ, the modular ratio N was calculated for V-shaped corrugations, for $\rho = 0.05$, 0.10, and 0.15 and $\alpha = 0.7$. The results of these calculations are shown in Fig. A.3, so that they could be compared with the curve for small values of ρ. It is seen that there is considerable difference between the curves when β is small. But when β is small, ρ must also be small in order that the ratio t/r be small; for

$$\beta^2 = \frac{bc}{rt} = \frac{h^2}{rt}\, \text{ctn}\,\alpha\, \csc\alpha = \rho^2\, \frac{r}{t}\, \text{ctn}\,\alpha\, \csc\alpha$$

For $\alpha = 0.7$, we have

$$\frac{t}{r} = 1.843 \frac{\rho^2}{\beta^2}$$

from which it is seen that ρ must be small when β is so, in order that the ratio t/r be small. When β is larger, the variation between the values of N for the various values of ρ is small. The same general trend was found for the stress factors, K_ϕ and K_Θ.

A similar investigation was carried out for the cusped corrugation which revealed the same results as for the V-shaped corrugations. For the undulating corrugations, however, the effect of ρ on the results could not be studied as the boundary conditions (b) are correct only when ρ is small. Since these types of corrugations behave similar to the V-shaped and cusped corrugations, it would be reasonable to assume that the factors K_ϕ, K_Θ, and N would also be insensitive to ρ as long as the ratio t/r is small.

Donnell[2] has studied the flexibility of pipes having V-shaped and undulating semi-circular corrugations. He considered a longitudinal strip of the pipe as being supported on an elastic foundation and by using the method of internal energy he obtained expressions for the modular ratio for the two types of corrugations. In terms of the notation of this chapter, his results are

---

[2] L. H. Donnell, "The Flexibility of Corrugated Pipes Under Longitudinal Forces and Bending," Trans. Am.Soc.Mech. Eng., APM-54-7-69, 1932.

V-shaped Corrugations:

$$N = 1 + \frac{ch^2}{bt^2} \left[1 + 0.125\beta^4 - 0.00219\beta^6\right]^{-1}$$

Semi-Circular Corrugations:

$$N = 1 + 1.5\frac{ch^2}{bt^2}\left[1 + 0.0625\beta^4 - 0.00435\beta^{5.2}\right]^{-1}$$

(h)

In obtaining these expressions, Donnell also assumed that the depth of the corrugations is small compared with the radius of the pipe, and that the wall thickness is fairly small compared with the radius of curvature of the corrugations. It is seen that these two expressions are of the same form as the expression (3.3). The first term in the expressions (h) represents the effect of meridional axial stresses. As was shown earlier, it is approximately equal to $\cos\alpha$, though the resulting error in N is negligible if the effect of axial stresses is approximated by unity. In deriving the expressions (h) Donnell used $Et^3/12$ as the flexural rigidity of the strip. Since any change in the shape of the cross section of the strip is prevented by the adjacent strips in a manner similar to that in plates, $Et^3/12(1-\gamma^2)$ should be used for its flexural rigidity. With these two changes, the above expressions for N become

V-shaped Corrugations:

$$N = \cos\alpha + \frac{ch^2}{bt^2}\left[(1-\gamma^2)\left\{1 + 0.125(1-\gamma^2)\beta^4 - 0.00219(1-\gamma^2)^{1.5}\beta^6\right\}^{-1}\right]$$

(3.6)

Semi-Circular Corrugations:

$$N = \cos\alpha + \frac{ch^2}{bt^2}\left[1.5(1-\nu^2)\left\{1 + 0.0625(1-\nu^2)\beta^4 - 0.00435(1-\nu^2)^{1.3}\beta^{5.2}\right\}^{-1}\right]$$

(3.7)

N was calculated from these two expressions for $\nu = 0.3$ and for values of β ranging from 0 to 5. The results of these calculations are shown in Figs. A.3 and A.9, so that they could be compared with the results obtained by using the solution for conical and ring shells. It is seen that the agreement between the results of the two methods is very good.

3.2. **Explicit Solution for an Axially Loaded Pipe with V-shaped Corrugations.** In order to show that the factors K_ϕ, K_θ, and N can also be used for the case of a corrugated pipe under bending, an explicit solution for a pipe with V-shaped corrugations will be developed. This solution will be expressed very simply in terms of trigonometric and hyperbolic functions instead of in terms of power series.

In the previous article it was shown that the solution obtained for small values of ρ gives good results also when ρ is relatively large, as long as the wall thickness is small compared to the radius of the pipe. This would make it reasonable to assume ρ is zero. Under this assumption Eq. (2.18) becomes

$$\frac{d^2U_1}{dz^2} + ia\ U_1 = 0 \qquad\qquad (a)$$

This represents the first of Eqs. (2.17). It is convenient to shift the origin of z from the edge AB (see Fig. 2.4) to the edge OO' midway between the edges AB and CD. For this purpose we shall introduce a new variable y, where

$$y = z - \frac{1}{2} \qquad\qquad (3.8)$$

With this change, Eq. (a) becomes

$$\frac{d^2U_1}{dy^2} + ia\ U_1 = 0 \qquad\qquad (3.9)$$

This is an ordinary linear differential equation the solution of which is

$$U_1 = C_1 e^{\eta}(\cos\eta + i\ \sin\eta) + C_3 e^{-\eta}(\cos\eta - i\ \sin\eta) \qquad (b)$$

where

$$\eta = y\sqrt{\frac{a}{2}} = y\gamma \qquad\qquad (3.10)$$

As before, the complete solution of Eq. (2.17) is then

$$U = (C_1 e^{\eta} + C_3 e^{-\eta})\ \sin\eta + (C_2 e^{\eta} + C_4 e^{-\eta})\cos\eta \qquad (c)$$

If the depth of the corrugation is small relative to the radius of the pipe, then the point O will be a point of inflection, so that the shear forces Q_ϕ at $\pm\eta$ will be equal. If we use this condition and observe that

$$Q_\phi \equiv \frac{1}{r_2}\ U = \frac{\cos\alpha}{r_0}\ U \approx \frac{\cos\alpha}{r}\ U$$

we have, from (c), that

$$(C_1 e^{\eta} + C_3 e^{-\eta}) \sin\eta + (C_2 e^{\eta} + C_4 e^{-\eta}) \cos\eta = (C_1 e^{-\eta} + C_3 e^{\eta})(-\sin\eta)$$
$$+ (C_2 e^{-\eta} + C_4 e^{\eta}) \cos\eta$$

Transposing and collecting like terms gives

$$(C_1 + C_3)(e^{\eta} + e^{-\eta}) \sin\eta + (C_2 - C_4)(e^{\eta} - e^{-\eta}) \cos\eta = 0$$

This can be satisfied for all values of η only if

$C_1 = - C_3$ and $C_2 = C_4$.

Then solution (c) becomes

$$U = C_1(e^{\eta} - e^{-\eta}) \sin\eta + C_3(e^{\eta} + e^{-\eta}) \cos\eta$$

Using the relationships

$$\frac{e^{\eta} - e^{-\eta}}{2} = \sinh\eta \quad ; \quad \frac{e^{\eta} + e^{-\eta}}{2} = \cosh\eta$$

and introducing the notations

$$f_1 = \sin\eta \sinh\eta \quad , \quad f_2 = \cos\eta \cosh\eta$$

finally gives

$$U = C_1 f_1 + C_2 f_2 \qquad\qquad (3.11)$$

For future reference, we shall tabulate f_1 and f_2 and their first and second derivatives with respect to η.

$$f_1 = \sin\eta \, \sinh\eta \qquad\qquad ; \quad f_2 = \cos\eta \, \cosh\eta$$

$$f_1' \equiv \frac{df_1}{d\eta} = \sin\eta \, \cosh\eta + \cos\eta \, \sinh\eta \; ;$$

$$f_2' \equiv \frac{df_2}{d\eta} = \cos\eta \, \sinh\eta - \sin\eta \, \cosh\eta$$

$$f_1'' \equiv \frac{d^2 f_1}{d\eta^2} = 2 \, f_2 \qquad\qquad ; \quad f_2'' \equiv \frac{d^2 f_2}{d\eta^2} = -2 \, f_1$$

$$(3.12)$$

Using expressions (c) and (d) of Chapter 2 in the first of Eqs. (2.11) we obtain for V, the expression

$$V = \frac{1}{Et}\left[\frac{ar\sec\alpha}{c^2}(C_1 f_2 - C_2 f_1) + \sqrt{\frac{a}{2}} \; \frac{h}{c^2 \cos\alpha}(C_1 f_1' + C_2 f_2')\right.$$

$$\left. - \frac{\sin\alpha \, \tan\alpha}{r}(C_1 f_1 + C_2 f_2) + F \tan\alpha \, \sec\alpha\right]$$

This can also be written as

$$V = \frac{ar}{Etbc}\left[(C_1 f_2 - C_2 f_1) + \frac{\varrho}{\sqrt{2a}}(C_1 f_1' + C_2 f_2')\right.$$

$$\left. - \frac{\varrho^2}{a}(C_1 f_1 + C_2 f_2) + \frac{\varrho c^2}{ab} F\right]$$

If ϱ is small, the last three terms in the above expression are small compared with the first term, and could thus be neglected. This then gives for V

$$V = \frac{ar}{Etbc}(C_1 f_2 - C_2 f_1)$$

The constants C_1 and C_2 can be determined from the boundary conditions (a) of Art. 3.1 at the edges $(y = \pm \frac{1}{2})$:

$$V = 0$$

$$\frac{1}{r} (U - Fr \tan\alpha) = 0$$

$$\left. \right\} \qquad at \ y = \pm \frac{1}{2}$$

which gives for C_1 and C_2 the expressions:

$$C_1 = Fr \tan\alpha \ \frac{f_1(\sqrt{a/\delta})}{f_1^2(\sqrt{a/\delta}) + f_2^2(\sqrt{a/\delta})}$$

$$C_2 = Fr \tan\alpha \ \frac{f_2(\sqrt{a/\delta})}{f_1^2(\sqrt{a/\delta}) + f_2^2(\sqrt{a/\delta})}$$

From Eqs. (2.23) the expressions for the forces, moments, and displacements can easily be found. If ρ is neglected, these expressions are

$$Q_\phi = F \sin\alpha \ (Af_1 + Bf_2)$$

$$N_\phi = F \sec\alpha \left[1 - \sin^2\alpha \ (Af_1 + Bf_2)\right]$$

$$N_\theta = - \frac{\sqrt{3(1-\gamma^2)}}{\gamma} \ \frac{Fh}{t} \ (Af_1' + Bf_2')$$

$$M_\phi = - \frac{Fh}{2\gamma} \ (Af_2' - Bf_1')$$

$$M_\theta = \gamma M_\phi = - \frac{\gamma Fh}{2\gamma} \ (Af_2' - Bf_1')$$

$$\left. \right\} \qquad (3.13)$$

$$\Delta = \frac{Fb}{Et} \left[\cos\alpha + \frac{6(1-\gamma^2)}{\gamma^3} \ \frac{ch^3}{bt^2} \ (\frac{\sinh\gamma - \sin\gamma}{\cosh\gamma + \cos\gamma})\right] \qquad (3.14)$$

where

$$\gamma = \sqrt{\frac{a}{2}} = \beta \sqrt[4]{3(1-\gamma^2)} = \sqrt[4]{3(1-\gamma^2) \ \frac{b^2 c^2}{r^2 t^2}} \qquad (d)$$

and

$$A = \frac{\sqrt{(\cosh\gamma - 1)(1-\cos\gamma)}}{\cosh\gamma + \cos\gamma} \quad ; \quad B = \frac{\sqrt{(\cosh\gamma +1)(\cos\gamma + 1)}}{\cosh\gamma + \cos\gamma}$$

(e)

The expressions for the displacements v and w will be needed in the next article. They can be obtained very simply by substituting the above expressions for N_ϕ and N_θ in Eqs. (e) and (f) of Art. 2.2. These expressions, for small values of ρ, are

$$v = \frac{Fb}{Et} y$$

$$w = \frac{3(1-\gamma^2)}{\gamma^3} \frac{Fc^2h}{Et^3} (Af_1' + Bf_2')$$

(3.15)

The constant of integration appearing in (e) was taken to be zero so that the displacement v would be zero at y = 0.

The stress factors K_ϕ and K_θ and the modular ratio N can readily be calculated from Eqs. (3.13) and (3.14). Calculations show that for values of β ranging from 0 to 5, the absolute maximum values of N_θ, M_ϕ, and M_θ occur at the crests of the corrugations, that is, at the edges AB and CD. Hence, in calculating expressions for K_ϕ and K_θ, the stresses should be calculated at these edges, i.e. at $y = \pm \frac{1}{2}$. The expressions for K_ϕ, K_θ, and N are

$$K_\phi = 1 + \frac{3h}{\gamma t} \frac{\sinh\gamma + \sin\gamma}{\cosh\gamma + \cos\gamma}$$

(3.16)

$$K_\theta = \frac{h}{t} \left[\frac{\sqrt{3(1-\gamma^2)} \, (\sinh\gamma - \sin\gamma) + 3\gamma(\sinh\gamma + \sin\gamma)}{\gamma(\cosh\gamma + \cos\gamma)} \right]$$

(3.17)

$$N = \cos\alpha + \frac{6(1-\gamma^2)}{\gamma^3} \frac{ch^2}{bt^2} \left(\frac{\sinh\gamma - \sin\gamma}{\cosh\gamma + \cos\gamma}\right) \qquad (3.18)$$

These expressions were calculated for various values of γ ranging from 0 to 6.5 with $\nu = 0.3$. When the results of these calculations were plotted it was found that the curves coincided almost exactly with the corresponding curves shown in Figs. A.1 to A.3. It should be noted that γ is related to the pipe characteristic β by expression (d).

3.3. <u>Corrugated Pipe Under Pure Bending</u>. The stress distribution in a corrugated pipe bent by couples acting at its ends is not symmetrical about the pipe axis as was the case for an axial load. The circumferential displacement u, the lateral shear forces $N_{\phi\theta} = N_{\theta\phi}$, the torsional moments $M_{\phi\theta} = -M_{\theta\phi}$, and the radial shear force Q_θ will no longer be zero. Hence, the equilibrium equations (2.1) and the stress-displacement relationships given by Eqs. (2.2) must be used instead of the Eqs. (2.4) and (2.5).

When expressions (2.2) are substituted into Eqs. (2.1), a system of five simultaneous partial differential equations results, two of which are of the third order. The solution of this system of equations can be obtained, if at all, with only the greatest of difficulty. However, it is possible to obtain the solution for the case of V-shaped corrugations by making use of the solution (3.13)

obtained in the previous article for an axially loaded pipe.

Before doing this, it is helpful to rewrite Eqs. (2.1) and (2.2) for the special case of a conical shell such as ABCD of Fig. 3.1(a). With the notation of Art. 3.2, the equilibrium equations (2.1) become

$$
\frac{1}{c}\frac{\partial}{\partial y}(N_\phi r_o) - N_\theta \sin\alpha + \frac{\partial N_{\theta\phi}}{\partial\theta} = 0
$$

$$
\frac{1}{c}\frac{\partial}{\partial y}(N_{\phi\theta} r_o) + N_{\theta\phi}\sin\alpha + \frac{\partial N_\theta}{\partial\theta} - Q_\theta\cos\alpha = 0
$$

$$
\frac{1}{c}\frac{\partial}{\partial y}(Q_\phi r_o) + N_\theta\cos\alpha + \frac{\partial Q_\theta}{\partial\theta} = 0
$$

$$
\frac{1}{c}\frac{\partial}{\partial y}(M_\phi r_o) - M_\theta\sin\alpha - \frac{\partial M_{\theta\phi}}{\partial\theta} - Q_\phi r_o = 0
$$

$$
\frac{1}{c}\frac{\partial}{\partial y}(M_{\phi\theta} r_o) - M_{\theta\phi}\sin\alpha + \frac{\partial M_\theta}{\partial\theta} - Q_\theta r_o = 0
$$

$$(3.19)$$

The stress-displacement relationships (2.2) for a conical shell become

$$
N_\phi = \frac{Et}{1-\nu^2}\left[\frac{1}{c}\frac{\partial v}{\partial y} + \frac{1}{r_o}\left(\frac{\partial u}{\partial\theta} + v\sin\alpha - w\cos\alpha\right)\right]
$$

$$
N_\theta = \frac{Et}{1-\nu^2}\left[\frac{1}{r_o}\left(\frac{\partial u}{\partial\theta} + v\sin\alpha - w\cos\alpha\right) + \frac{\nu}{c}\frac{\partial v}{\partial y}\right]
$$

$$
N_{\phi\theta} = N_{\theta\phi} = \frac{Et}{2(1+\nu)}\left(\frac{1}{c}\frac{\partial u}{\partial y} + \frac{1}{r_o}\frac{\partial v}{\partial\theta} - \frac{u}{r_o}\sin\alpha\right)
$$

$$
M_\phi = -D\left[\frac{1}{c^2}\frac{\partial^2 w}{\partial y^2} + \frac{\nu}{r_o}\left(\frac{1}{c}\frac{\partial w}{\partial y}\sin\alpha + \frac{1}{r_o}\frac{\partial^2 w}{\partial\theta^2} + \frac{1}{r_o}\frac{\partial u}{\partial\theta}\cos\alpha\right)\right]
$$

$$
M_\theta = -D\left[\frac{1}{r_o}\left(\frac{1}{c}\frac{\partial w}{\partial y}\sin\alpha + \frac{1}{r_o}\frac{\partial^2 w}{\partial\theta^2} + \frac{1}{r_o}\frac{\partial u}{\partial\theta}\cos\alpha\right) + \frac{\nu}{c^2}\frac{\partial^2 w}{\partial y^2}\right]
$$

$$
M_{\phi\theta} = -M_{\theta\phi} = D(1-\nu)\left[\frac{1}{c}\frac{\partial}{\partial y}\left(\frac{1}{r_o}\frac{\partial w}{\partial\theta} + \frac{u}{r_o}\cos\alpha\right)\right]
$$

$$(3.20)$$

A pipe with couples $\pi r^2 F_1$ acting at its ends is shown in Fig. 3.3. Again here it is necessary to consider only the element ABCD. The boundary conditions at the edges are the same as those for a corrugated pipe under an axial load, namely, that the rotation of the tangent to the meridian at the edges must be zero and that there can be no component of force parallel to the edges.

From equilibrium, the resultant of the forces parallel to the pipe axis must be equal to the applied couple $\pi r^2 F_1$. An assumption as to the distribution of these forces must be made in order to find their values. In a plain pipe, these forces vary linearly across any cross section. It seems reasonable to assume that the same is true for a corrugated pipe too. Under this assumption, the longitudinal force at any point is equal to $F_1 \sin\theta$, where θ is the angle measured in the anti-clockwise direction from the neutral axis of the pipe. The corresponding force for a pipe under axial load of $2\pi r F$ is constant and equal to F. This suggests that the forces Q_ϕ, N_ϕ, and N_θ, the moments M_ϕ and M_θ, and the displacements v and w for the case of bending can be taken to be given also by Eqs. (3.13) and (3.15), if F is taken to be equal to $F_1 \sin\theta$. If this is assumed, then the expression for the above stresses and displacements for the case of bending are
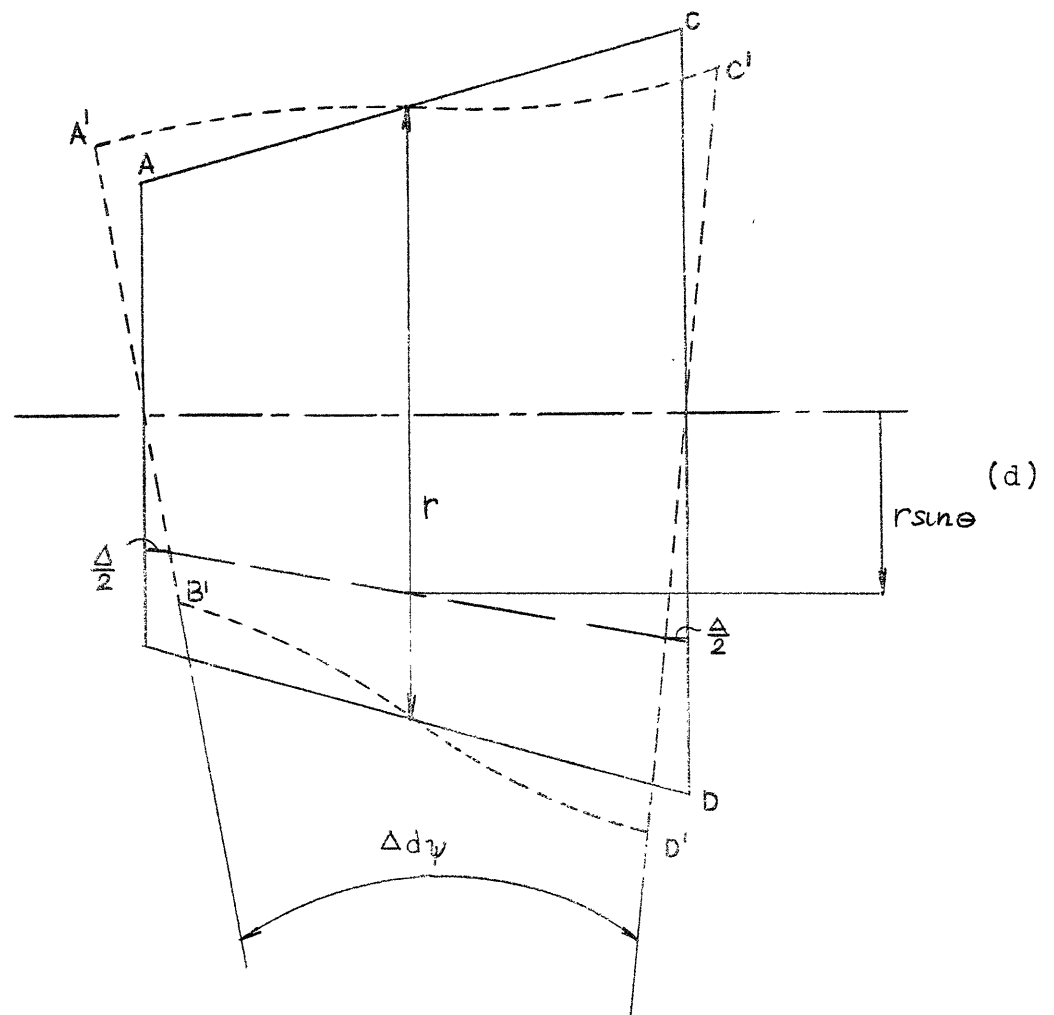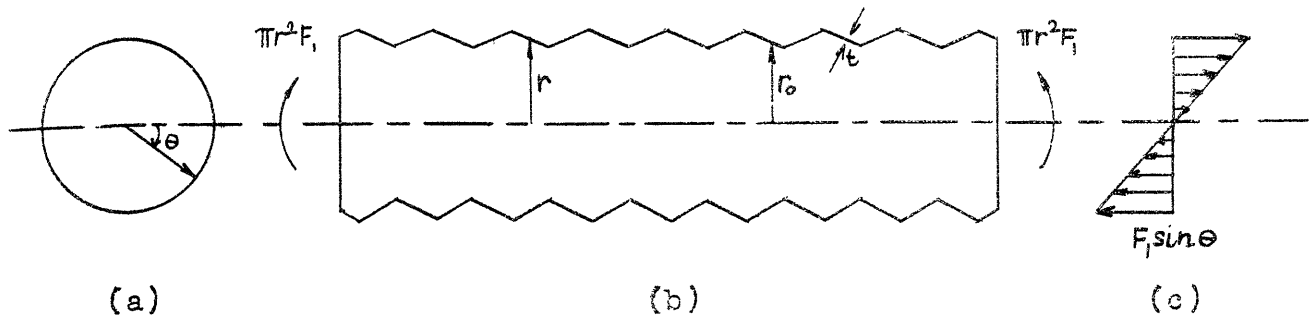
Fig. 3.3. Bending of a Corrugated Pipe

$$Q_\phi = \sin\alpha \ (Af_1 + Bf_2) \ F_1 \sin\Theta$$

$$N_\phi = \sec\alpha \left[1 - \sin^2\alpha \ (Af_1 + Bf_2)\right] \ F_1 \ \sin\Theta$$

$$N_\Theta = - \ \frac{\sqrt{3(1-\nu^2)}}{\gamma} \ \frac{h}{t} \ (Af_1' + Bf_2') \ F_1 \ \sin\Theta$$

$$M_\phi = - \ \frac{h}{2\gamma} \ (Af_2' - Bf_1') \ F_1 \ \sin\Theta$$

$$M_\Theta = - \ \frac{\nu h}{2\gamma} \ (Af_2' - Bf_1') \ F_1 \ \sin\Theta$$

$$(3.21)$$

$$v = \frac{b\gamma}{Et} \ F_1 \ \sin\Theta$$

$$w = \frac{3(1-\nu^2)}{\gamma^3} \ \frac{c^2 h}{Et^3} \ (Af_1' + Bf_2') \ F_1 \ \sin\Theta$$

$$(3.22)$$

where all the quantities appearing on the right hand side
of these equations are defined in Art. 3.3.

In addition to these stresses and displacements,
there would also be lateral shear forces, $N_{\phi\Theta} = N_{\Theta\phi}$, tor-
sional moments $M_{\phi\Theta} = - M_{\Theta\phi}$, radial shear force Q_Θ and the
circumferential displacement u. We shall first attempt to
obtain the torsional moments. For this purpose, the dis-
placement u will be assumed to be small relative to the
partial derivative of the displacement w with respect to
Θ. It will be shown later that this assumption is actually
correct. Then by substituting the expression for w given
above into the last of Eqs. (3.20), we obtain

$$M_{\phi\Theta} = - M_{\Theta\phi} = \frac{(1-\nu)}{4} \ \frac{ch}{\gamma^3} \ \frac{\partial}{\partial\gamma} \left[\frac{1}{r_0} \ (Af_1' + Bf_2')\right] \ F_1 \ \cos\Theta \qquad (a)$$

From Eq. (3.10)

$$\frac{\partial}{\partial y} = \frac{\partial}{\partial \eta} \frac{\partial \eta}{\partial y} = \gamma \frac{\partial}{\partial \eta} \qquad \text{(b)}$$

The radius r_o of the parallel circle is

$$r_o = r \, (1 + \rho y)$$

When ρ is small,

$$r_o \approx r \qquad \text{(c)}$$

Using (b) and (c) in (a) and noting that the functions f_1 and f_2 and their derivatives are given by Eq. (3.12), we get

$$M_{\phi \Theta} = - \, M_{\Theta \phi} = \frac{(1-\gamma)}{2} \frac{ch}{\gamma^2} \frac{1}{r} (Af_2 - Bf_1) \, F_1 \cos \Theta$$

Using expression (d) of the previous article for γ, we finally obtain the expression

$$M_{\phi \Theta} = - \, M_{\Theta \phi} = \frac{(1-\gamma)t \, \tan\alpha}{2\sqrt{3(1-\gamma^2)}} (Af_2 - Bf_1) \, F_1 \cos \Theta \qquad \text{(d)}$$

The expression for Q_Θ can be found by substituting expressions for M_Θ and $M_{\phi\Theta}$ given by Eqs. (3.21) and (d) in the last of the equilibrium equations (3.19). In the latter equation, the term $M_{\Theta\phi}\sin\alpha$ is small in comparison with the other terms for small values of ρ, and can thus be neglected. Also, r_o is approximately equal to r. This gives the expression

$$Q_\theta = \left[\frac{(1-\nu)}{2\sqrt{3(1-\nu^2)}} \frac{\gamma t \tan\alpha}{c} - \frac{\nu h}{\gamma r} \right] (Af_2' - Bf_1') \; F_1 \cos\theta$$

for Q_θ. Simplifying this gives

$$Q_\theta = \frac{1-3\nu}{2} \frac{\rho}{\gamma} (Af_2' - Bf_1') \; F_1 \cos\theta$$

The maximum value of this expression is found to be $0.5(1-3\nu) \rho F_1 \cos\theta$, which is small enough to be neglected, so that

$$Q_\theta = 0 \tag{e}$$

The expression for the lateral shear forces, $N_{\phi\theta} = N_{\theta\phi}$ can be obtained in a similar manner by substituting the known expressions for N_θ and Q_θ in the second of the equilibrium Eqs. (3.19). This expression, for small values of ρ, is

$$N_{\phi\theta} = N_{\theta\phi} = \tan\alpha \, (Af_1 + Bf_2) \; F_1 \cos\theta \tag{f}$$

Grouping expressions (d), (e), and (f), we have

$$\left. \begin{aligned} N_{\phi\theta} &= N_{\theta\phi} = \tan\alpha \, (Af_1 + Bf_2) \; F_1 \cos\theta \\[2mm] M_{\phi\theta} &= - M_{\theta\phi} = \frac{(1-\nu) t \tan\alpha}{2\sqrt{3(1-\nu^2)}} (Af_2 - Bf_1) \; F_1 \cos\theta \\[2mm] Q_\theta &= 0 \end{aligned} \right\} \tag{3.23}$$

The displacement u can now be obtained from the third of the stress-displacement relationships (3.20), by using the expression for v as given by Eq. (3.22) and the above expression for $N_{\phi\theta}$. This gives

$$\tan\alpha\,(Af_1 + Bf_2)\,F_1\,\cos\Theta \approx \frac{Et}{2(1+\nu)}\left(\frac{\gamma}{c}\frac{\partial u}{\partial \eta} + \frac{\rho\gamma}{Et\,\sin\alpha}F_1\cos\Theta - \frac{u}{c}\rho\right)$$

The last two terms are small in comparison with the first, and can therefore be neglected, giving for u the expression

$$u = -\frac{2(1+\nu)}{Et}\frac{ch}{b\gamma}\,(Af_2' - Bf_1')\,F_1\,\cos\Theta \qquad (3.24)$$

The ratio of u to $\frac{\partial w}{\partial \Theta}$ is found to be

$$\frac{u}{\partial w/\partial \Theta} = \left[-\frac{2(1+\nu)}{\sqrt{3(1-\nu^2)}}\frac{(Af_2' - Bf_1')}{(Af_1' + Bf_2')}\right]\frac{t}{r}$$

The ratio t/r is generally very small, so that the assumption made earlier that u is small relative to $\frac{\partial w}{\partial \Theta}$ is correct. It can be checked that the solution represented by Eqs. (3.21) through (3.24) satisfies both the equilibrium equations (3.19) as well as the stress-displacements relationships (3.20) for small values of ρ. This is thus the correct solution for the pure bending of a pipe with V-shaped corrugations as long as the ratio ρ is small.

Calculations show that the unit shear stresses due to the torsional moments and lateral shear forces given by Eqs. (3.23) are small relative to the direct stresses caused by the bending moments and direct forces. Hence only the latter need be considered in calculating the maximum stresses in the pipe.

The meridional stress, σ_φ, is

$$\sigma_\phi = \frac{N_\phi}{t} \pm \frac{6M_\phi}{t^2}$$

The stress in a **plain** pipe due to a moment of $\pi r^2 F_1$ is

$$\sigma = \frac{F_1}{t} \sin \theta$$

For any given angle θ, σ_ϕ is maximum (or minimum) at the crest of the corrugations, and its absolute value is given by

$$\left| \sigma_\phi \right|_{max} = \frac{F_1 \cos\alpha \sin\theta}{t} + \frac{3h}{\gamma t^2} F_1 \sin\theta \frac{\sinh\gamma + \sin\gamma}{\cosh\gamma + \cos\gamma}$$

Defining the meridional stress factor K_ϕ as the ratio of $\left| \sigma_\phi \right|_{max}$ to σ, we find that

$$K_\phi = \cos\alpha + \frac{3h}{\gamma t} \frac{\sinh\gamma + \sin\gamma}{\cosh\gamma + \cos\gamma}$$

For reasons given in Art. 3.2, the term $\cos\alpha$ can be replaced by unity so that

$$K_\phi = 1 + \frac{3h}{t} \frac{\sinh\gamma + \sin\gamma}{\cosh\gamma + \cos\gamma}$$

This expression is exactly the same as the expression given by (3.16) for a pipe under an axial load. Similarly, it can be shown that the circumferential stress factor K_θ for the case of bending is the same as that for axial load as given by (3.17).

It can also be shown that the "reduced" modulus of elasticity to be used for calculating the bending deflections of the pipe is the same as that used in calculating

the axial deflections. To show this we need to calculate the relative deflection Δ between the edges AB and CD [see Fig. 3.3(d)]. From the figure it is seen that

$$\frac{1}{2}\Delta = [v \cos\alpha + w \sin\alpha]_{y=1/2}$$

The angle of rotation $\Delta d\psi$ between the edges AB and CD is

$$\Delta d\psi = \frac{\Delta}{r \sin\theta} = 2 [v \cos\alpha + w \sin\alpha]_{y=1/2}$$

$$= \left[\frac{b \cos\alpha F_1}{Etr} + \frac{6(1-\nu^2)}{\gamma^3} \frac{ch^2 F_1}{Et^3 r} \left(\frac{\sinh\gamma - \sin\gamma}{\cosh\gamma + \cos\gamma}\right)\right]$$

The corresponding angle of rotation for a plain pipe is

$$\Delta d\psi_0 = \frac{F_1 b}{Etr}$$

The bending deflections are proportional to these rotations, so that if N is defined as the ratio of the bending deflection for a corrugated pipe to the corresponding deflection for a plain pipe of the same major dimensions, we have

$$N = \cos\alpha + \frac{6(1-\nu^2)}{\gamma^3} \frac{ch^2}{bt^2} \left(\frac{\sinh\gamma - \sin\gamma}{\cosh\gamma + \cos\gamma}\right)$$

which is also seen to be the same as that given by (3.18). N can as well be thought of as the modular ratio, i.e. the ratio between the actual modulus of elasticity of the pipe material and the "reduced" modulus. The bending deflections of a corrugated pipe can then be easily computed by considering the pipe to be plain but having this reduced modulus as its modulus of elasticity.

It has been shown above that the stress factors K_ϕ and K_Θ and the modular ratio N for a pipe with V-shaped corrugations are the same for bending as for axial compression (or extension) of the pipe. There is no simple way of showing that this is so for pipes with cusped and undulating circular corrugations. It will be assumed that this is true also for these types of corrugations since the only difference between these and V-shaped corrugations is that of geometry.

3.4. <u>Corrugated Pipe Under Bending Moment and Transverse Shear Forces</u>. We have seen that a corrugated pipe under a bending moment or an axial force is more flexible than a plain pipe. This is so because the longitudinal forces due to an axial force and moment are perpendicular to the cross sections of the pipe and thus create bending of the corrugations. However, transverse shear forces being in the plane of the cross sections do not create such bending of the corrugations, so that one would expect that the effect of transverse shear forces is small for corrugated pipes. It can be shown that this is actually so.

For this purpose we shall investigate the effect of shear forces on a pipe with V-shaped corrugations, although the discussion is equally applicable to pipes with cusped and alternating circular corrugations. One of the conical shells forming the pipe is shown in Fig. 3.4. The length

b of this shell can be assumed to be small enough so that
it can be considered to be an elemental length. Transverse
shear forces S are shown acting on the edges AB and CD.
The bending moment on the edge AB is M and this, due to the
shear forces S, increases to M + dM on CD. From equilib-
rium, we have

$$dM = bS \qquad \text{(a)}$$

We shall obtain the distribution of the shearing
stresses over the pipe cross section by a method similar to
that used for ordinary beams. It was shown in the previous
article that the longitudinal forces vary linearly over any
cross section as shown in Fig. 3.4. On the edge AB, they
are given by

$$F = \frac{M \sin\Theta}{\pi r_o^2} \qquad \text{(b)}$$

while on the edge CD we have

$$F + dF = \frac{(M + dM)\sin\Theta}{\pi(r_o + dr_o)^2} \qquad \text{(c)}$$

Consider the equilibrium of the element mAnqCp. On
the side mAn the total force acting in the direction of the
pipe axis is

$$\int_{\Theta}^{\pi-\Theta} F r_o \, d\Theta$$

which, by making use of (b), becomes
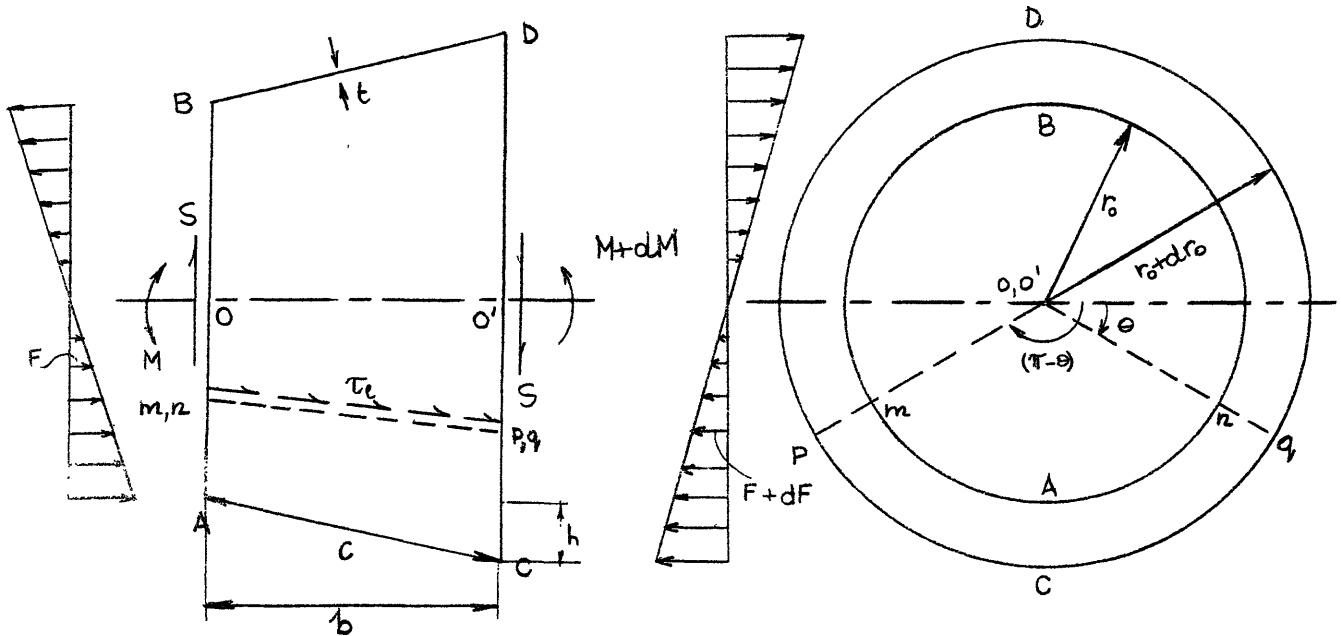
Fig. 3.4. Shear Forces and Bending Moments on an Element of Pipe
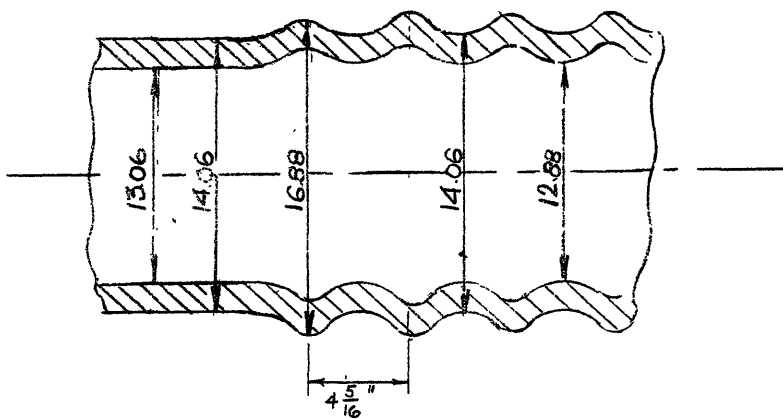
Fig. 3.5. Corrugated Pipe Tested by Cope and Wert

$$\frac{2M\cos\Theta}{\pi r_o} \qquad\qquad (d)$$

Similarly, the total force acting on the side pCq in the direction of the pipe axis is

$$\frac{2(M+dM)\cos\Theta}{\pi (r_o+dr_o)} \qquad\qquad (e)$$

On each of the two planes mp and nq, the force due to unit shearing stresses τ_λ is

$$\tau_\lambda tc$$

The component of this force in the direction of the pipe axis is

$$\tau_\lambda tc \cos\alpha = \tau_\lambda tb$$

Then the total force in the direction of the pipe axis due to the unit shearing stresses τ_λ on planes mp and nq is

$$2\tau_\lambda tb \qquad\qquad (f)$$

The forces given in (d), (e), and (f) must be in equilibrium:

$$2\tau_\lambda tb = \frac{2(M+dM)\cos\Theta}{\pi(r_o+dr_o)} - \frac{2M\cos\Theta}{\pi r_o}$$

If the depth h of the corrugation is small relative to the radius of the pipe, then

$$r_o + dr_o \approx r_o \approx r$$

so that the unit longitudinal shear stress is

$$\tau_\ell = \frac{dM \cos \Theta}{\pi\, rbt}$$

Substituting expression (a) for dM and noting that the shear stresses on any two perpendicular planes are equal, we have for the unit shear stress τ on the cross section the expression

$$\tau = \frac{S \cos \Theta}{\pi\, rt} \tag{3.25}$$

It is seen that this is the same expression as that for a plain pipe.

It can be shown quite simply that the distribution of the shear stresses as given by expression (3.25) makes the internal strain energy of shear a minimum. To show this, let us assume that the distribution is given by the Fourier cosine series

$$\tau = \frac{S}{\pi\, rt} \left[a_1 \cos \Theta + a_3 \cos 3\Theta + \dots + a_{2n+1} \cos(2n+1)\Theta + \dots \right] \tag{g}$$

where a_1, a_3, ... are arbitrary coefficients. Only odd terms are considered, since, because of symmetry, $\tau = 0$ at $\Theta = \pm \pi/2$. The series (g) can be made to represent any distribution by appropriately choosing the values of the coefficients.

By statics, the resultant of the shear stresses τ must equal the external shear force S :

$$\int_{\theta=0}^{2\pi} \tau rtd\theta \cos\theta = S$$

Using for τ the expression (g) and noting that

$$\int_{0}^{2\pi} \cos(2n+1)\theta\cos\theta d\theta$$ is zero for $n \neq 0$, we find that $a_1 = 1$.

Then (g) becomes

$$\tau = \frac{S}{\pi rt}[\cos\theta + a_3\cos 3\theta + \ldots + a_{2n+1}\cos(2n+1)\theta] \qquad (h)$$

The strain energy of shear stored in the element ABCD is

$$dW_s = \int_{\theta=0}^{2\pi} \frac{1}{2}\frac{\tau^2}{G} rtd\theta \cdot c \qquad (i)$$

where G is the modulus of elasticity in shear, and τ is given by (h). For this strain energy to be a minimum, the partial derivative of (i) with respect to the coefficients a_{2n+1} (n=1,2, ...) must be zero:

$$\frac{\partial}{\partial a_{2n+1}}(dW_s) = 0 = \frac{S^2 \sec\alpha dx}{\pi rtG} a_{2n+1} \qquad (n=1,2, \ldots)$$

This can only be satisfied if a_{2n+1} is zero. Then the distribution of the shear stress as given by (h) reduces to the expression given by (3.25).

In a similar way it can be shown that the distribution of the longitudinal forces F as given by (b) makes the strain energy of bending a minimum. The total strain energy, which is the sum of the two, is then also a minimum,

PAGES (S) MISSING FROM ORIGINAL

will be called the shear modular ratio and will be denoted
by the symbol N':

$$N' = \frac{c}{b} \qquad (3.26)$$

A similar analysis shows that the shear modular
ratios for pipes with cusped and undulating circular corru-
gations are also given by Eq. (3.26). The dimensions b and
and c for these two cases are defined in Fig. 3.1(b) and
(c).

It was shown in the previous article that the de-
flection of a corrugated pipe is N times that for a plain
pipe. Thus, the total deflection of a corrugated pipe,
subjected to both bending moment and transverse shear
forces, is

$$\delta = N\delta_{bo} \left(1 + \frac{N'}{N} \frac{\delta_{so}}{\delta_{bo}} \right) \qquad (3.27)$$

where δ_{bo} and δ_{so} are the bending and shearing components
of the deflection of a plain pipe.

The second term in the parentheses represents the
effect of deflection due to shear compared with that due to
bending moment. The ratio N'/N is unity for a plain pipe
and less than one for a corrugated pipe. It is thus seen
that the effect of a shearing component of the deflection
on the total deflection is always less for corrugated pipes
than for plain pipes, if both are of the same major

dimensions and are loaded identically. It is known that
the deflection due to shearing deformation for plain pipes
is only a small percentage of the total deflection, if the
length of the pipe is large in comparison with its radius.
Hence, it can be stated that in calculating the deflection
of corrugated pipes, the effect of shearing deformation
can be neglected whenever it can be done for plain pipes.

3.5. Verification of Theoretical Results with Experimental Results.

Only a few tests on corrugated pipes have been
reported in the literature, and these have only attempted
to find the modular ratio N. Donnell[3] has tested a corru-
gated pipe under both an axial load and under pure moment.
In his paper, Donnell does not specifically mention the
shape of the corrugations. According to Hetenyi[4], the
pipe had undulating circular corrugations. The dimensions
of the pipe were $r = 5.33$ in.; $t = 0.065$ in.; $b = 1.34$ in.;
$h = 0.470$ in.; $c = 1.47$ in. The modular ratio N was found
to be 19.9 for axial load and 20.7 for the pipe under pure
bending. The theoretical value of N for this pipe can be
found by the use of Eq. (3.3) and Fig. A.9. The values of
the angle α and the pipe characteristic β as obtained from
the dimensions of the pipe are 0.337 radians and 2.38,
respectively, for which the value of n for this case is

[3] L. H. Donnell, loc. cited, p. 54.
[4] M. Hetenyi, "Beams on Elastic Foundation," p. 176.

found from Fig. A.9 to be 0.341. Eq. (3.3) then gives the value of 20.5 for the modular ratio N. This is seen to be in very good agreement with the experimental results. The experimental results also show that the value of the modular ratio for the corrugated pipe under bending is, within experimental limitations, the same as that for an axial load, as was assumed in Art. 3.4.

Cope and Wert[5] have tested the corrugated pipe shown in Fig. 3.5. In addition to testing this pipe under an axial load and under a pure moment, they also tested it as a cantilever loaded by a concentrated force applied at the free end. The modular ratios N for these three types of loading were found to be 6.5, 5.1, and 5.2, respectively.[6] However, in obtaining these values, Cope and Wert compared the corrugated pipe with the plain pipe from which it was made. This plain pipe had a wall thickness of 0.5 in. and a mean radius of 6.75 in., whereas these were actually 0.59 in. and 7.44 in., respectively, for the corrugated pipe (see Fig. 3.5). If the corrugated pipe is compared with a plain pipe of thickness 0.59 in. and radius of 7.44 in., then the values of N for the three types of loading mentioned above are 8.4, 7.3, and 7.4, respectively.

---

[5] E. T. Cope and E. A. Wert, "Load-Deflection Relations for Large Plain, Corrugated and Creased Pipe Bends," Trans. Am.Soc.Mech.Eng., FSP-54-12-115, 1932.

[6] The result for the case of axial load was obtained from the Discussion of Donnell's paper (loc.cit., p. 54).

The corrugations of this pipe can be approximated as cusped circular corrugations. The dimensions of the corrugations are r = 7.44 in.; t = 0.59 in.; b = 2.15 in.; h = 1.41 in. From these dimensions it is found that c = 2.73 in., α = 0.579 radians; and β = 1.16. The value of n given by Fig. A.6 is 0.84, which when substituted in Eq. (3.3) gives a value of 6.9 for the modular ratio. The discrepancy between theoretical and experimental results for this pipe is due perhaps to the fact that the thickness of the pipe is not small compared to the radius of curvature of the corrugations as assumed in the theoretical consideration. The radius of curvature r_1 is

$$r_1 = \frac{b}{\sin 2\alpha} = 2.36$$

which gives for the ratio t/r_1 the value of 0.25. This is seen to be fairly large.

CHAPTER 4

CORRUGATED SHELLS

4.1. <u>Introduction</u>. Corrugated shells[1] which are straight
in the axial direction will be considered in this chapter;
the effect of curvature will be taken up in the following
chapter. The behaviour of shells such as the one shown in
Fig. 4.1 under snow and dead loads is very similar to that
of long barrel shells. It is known that the longitudinal
behaviour of long barrel shells is almost identical with the
behaviour of beams with curved cross section, so that the
longitudinal stresses can be determined under the assump-
tion of a straight-line distribution of stress. The
transverse stresses can then be obtained by considering
the equilibrium of an element between two cross sections
an elemental length apart. This method of obtaining
stresses in a barrel shell is sometimes known as the "beam
method."[2] It can be shown that the stresses obtained by
the "beam method" are sufficiently accurate if the

---

[1] For the first time we encounter a structural member
which has corrugations in two directions. The shell
shown in Fig. 4.1 has major corrugations in the longi-
tudinal direction; in addition to these corrugations,
there are secondary transverse corrugations as shown in
Fig. 4.1(a), which are similar to the corrugations in
pipes considered in the previous chapter. In our fur-
ther discussion the term corrugations will refer to the
secondary transverse corrugations; in case of ambiguity,
the main corrugations will be referred to as the major
corrugations.

[2] H. Lundgren, "Cylindrical Shells," Vol. I.
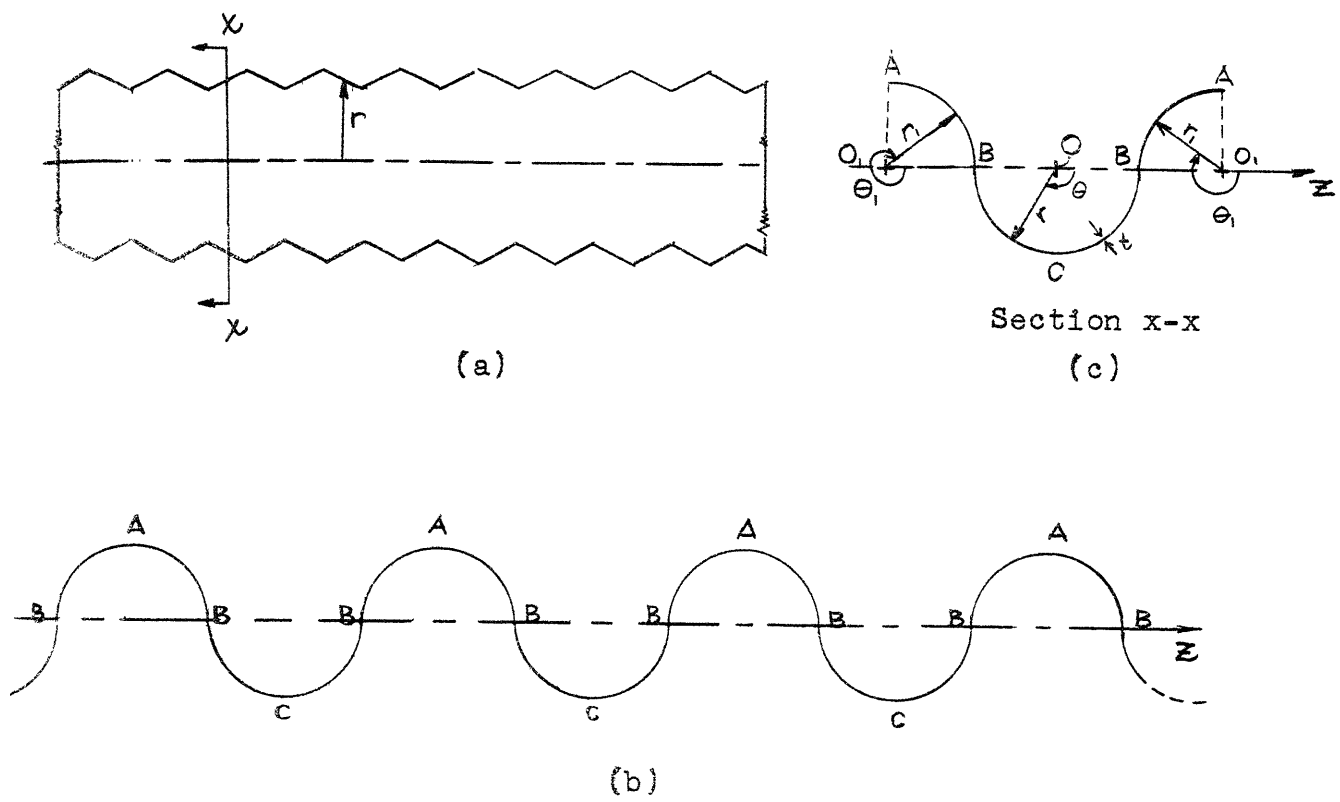
(a)

Section x-x

(c)

(b)

Fig. 4.1. Corrugated Shells

transverse stresses are small relative to the longitudinal stresses.[3] This is generally so for long barrel shells

The major corrugations shown in Fig. 4.1(b) will be assumed to extend over a considerable length in the z-direction. The complete structure is somewhat like a multiple barrel shell. With identical loads on all shells, each shell behaves in like manner, so that only one barrel need be investigated. The condition of continuity in the transversal direction is fulfilled by preventing the longitudinal edges A from moving horizontally and rotating. These restraints at the edges make the distortion of the cross section due to the transverse moments less than that for a single shell. The results obtained by the "beam method" are in error chiefly due to this type of distortion. Hence, it can be said that the "beam method" gives better results for a multiple barrel shell than for a single shell.

The corrugations in the shell further help to increase the transverse stiffness of the shell while at the same time decreasing the longitudinal stiffness. This dual effect makes the transverse moments smaller and the longitudinal stresses larger than those occurring in a plain shell. So the "beam method" when applied to corrugated

[3] Ibid.

shells will give results closer to the true values than for plain shells.

The length of the shells shown in Fig. 4.1 will be assumed to be very large in comparison with the radius r, so that, for reasons mentioned above, it can be assumed that the "beam method" gives satisfactory results.

The solutions for the corrugated shell under axial tension and pure bending will first be obtained from the corresponding solutions for a corrugated pipe. These solutions will then be used to obtain the stresses and deflections for the shell under snow and dead loads.

4.2. Corrugated Shell Under Axial Tension. A shell having V-shaped corrugations is shown in Fig. 4.1. The cross section ABCBA is seen to be composed of four 90° arcs each of radius r. In the diagram the radii of the arcs AB and BC are designated as r_1 and r, respectively, as it makes it convenient to refer to these arcs; it should be kept in mind that r_1 is actually equal to r. In general, the subscript $_1$ will be used to refer to arc AB. The thickness t will be assumed to be constant throughout the shell, and will be assumed to be small relative to the radius r. The dimensions of the corrugations will also be assumed to be small in comparison with r.

The shape of the cross section suggests that the shell under an axial force of $2\pi rF$ behaves like a pipe of

radius r and having the same corrugations, so that the stresses and displacement are given by Eqs. (3.13) and (3.14). However, when these equations are used, the stresses N_Θ are found to be incompatible along the longitudinal sections through B. To see this, let us examine the behaviour of the shell in the vicinity of B. An enlarged view of this portion of the shell is shown in Fig. 4.2. If the element HJMN is considered as part of a pipe, then the circumferential stress N_Θ on the longitudinal section through B is given by the third of Eqs. (3.13), i.e.

$$N_\Theta = - \frac{\sqrt{3(1-\nu^2)}}{\gamma} \frac{Fh}{t} [Af_1'(\eta) + Bf_2'(\eta)] \qquad (a)$$

where

$$\eta = \gamma y$$

By considering the element HJKL as part of another pipe, N_Θ on the longitudinal section through B is

$$N_{\Theta 1} = - \frac{\sqrt{3(1-\nu^2)}}{\gamma} \frac{Fh}{t} [Af_1'(\eta_1) + Bf_2'(\eta_1)] \qquad (b)$$

where

$$\eta_1 = \gamma y_1$$

From Fig. 4.2(b) it is seen that $y_1 = -y$, so that $\eta_1 = -\eta$. Using this relationship in (b) and noting that f_1' and f_2' as given by (3.12) are odd functions of η, we have
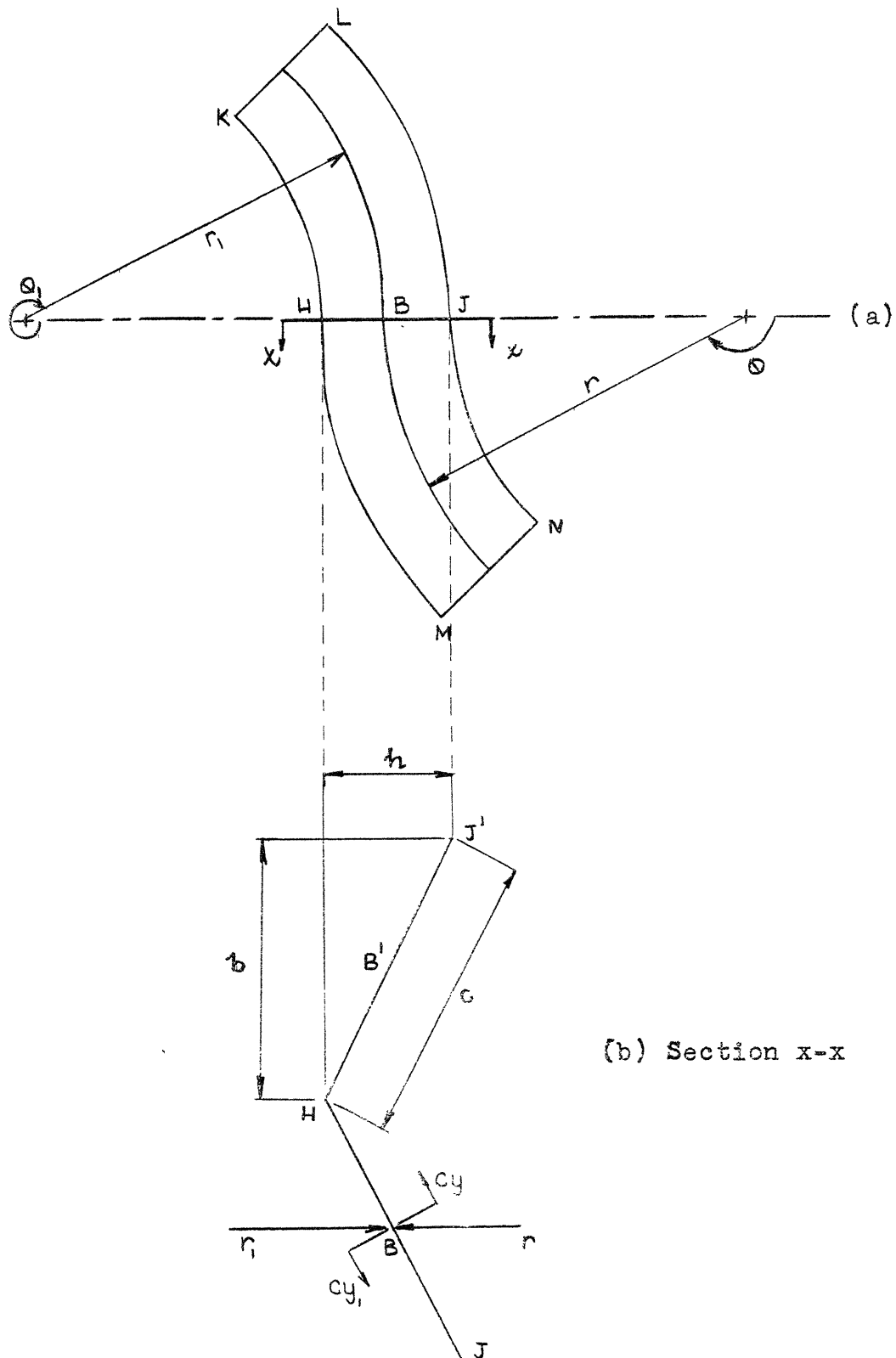
Fig. 4.2. Enlarged View of Cross Section of Shell

$$N_{\theta_1} = \frac{\sqrt{3(1-\gamma^2)}}{\gamma} \frac{Fh}{t} \ [Af_1'(\eta) + Bf_2'(\eta)] \qquad (c)$$

Examination of Eqs. (a) and (c) shows that the circumferential stresses at any point on longitudinal section through B as given by these equations, though of equal magnitude, are of opposite signs. This cannot actually occur, and so the circumferential stress along the entire longitudinal section through B must be zero. The distribution of the circumferential stresses along a longitudinal section through B, as given by either (a) or (c), is also statically equivalent to zero. By Saint-Venant's principle, the stress distribution as given by Eq. (3.13) will be sensibly changed only in the neighbourhood of the longitudinal section through B; the stresses at a distance of h. from this section will be changed by a few per cent only. If the depth of the corrugations h is small relative to the radius r (or r_1) then the displacement Δ for this shell is also given by Eq. (3.14), as the disturbance is spread over only a very small portion of the shell cross section. Hence, in the deflection calculations the reduced modulus, equal to E/N, should be used, where N is given by Eq. (3.18).

The stresses along the longitudinal section through B may be larger than those at a distance from it, but it is difficult to determine their exact values. However, we

shall mainly be concerned with the bending of the shell
shown in Fig. 4.1, for which, as will be shown in the fol-
lowing article, the solution is given exactly by Eqs.
(3.21) and (3.23). When axial forces are present, as in
the case of the shell as a two-hinged arch (Chapter 6),
they are always accompanied by bending moments. As will be
shown in Chapter 6, the effect of the axial forces on the
stresses and deflections can nearly always be neglected
for the types of arches generally used. So in a practical
case, it is not necessary to determine the stress distribu-
tion along the longitudinal section through B due to an
axial force.

4.3. **Corrugated Shell Under Pure Bending Moment.** When the
pipe solution as given by Eqs. (3.21) and (3.23) is used
for the bending of the shell of Fig. 4.1 by couples $\pi r^2 F_1$
at its ends, it is found that there is complete compatibil-
ity along the longitudinal section through B. The only
stresses that occur along this section are the lateral
shear forces and torsional moments, the expressions for
which are given by Eqs. (3.23). These are found to have
the same value for $\pm \eta$, and hence it can be shown that they
are compatible along the longitudinal section through B.
The displacement expressions (3.22) are also found to give
distortion of the cross section which is compatible along
this section.

Thus for the case of bending of the corrugated shell, the stresses and deflections can be obtained by considering it to be a pipe of radius r and thickness t, and having the same corrugations.

4.4. <u>Corrugated Shell Under Distributed Loading</u>. It was shown qualitatively in Article 4.1 that the longitudinal behaviour of a corrugated shell can be approximated quite well by considering it to be a beam of curved cross section if its length is large in comparison with the radius r. From strain energy considerations it will be shown that this is so.

Consider the shell of length ℓ shown in Fig. 4.3. The shell is simply supported at its ends and is under a snow load of q_L per unit area of horizontal projection. By statics the external moment and shear at any cross section is given by

$$M = 2q_L r \ell^2 \frac{x}{\ell} (1 - \frac{x}{\ell}) \tag{4.1}$$

$$S = 2q_L r \ell (1 - \frac{2x}{\ell}) \tag{4.2}$$

In the previous article it was shown that the stress distribution in a shell due to a moment of $\pi r^2 F_1$ is given by Eqs. (3.21) and (3.23). So if

$$F_1 = \frac{2q_L \ell^2}{\pi r} \frac{x}{\ell} (1 - \frac{x}{\ell}) \tag{4.3}$$

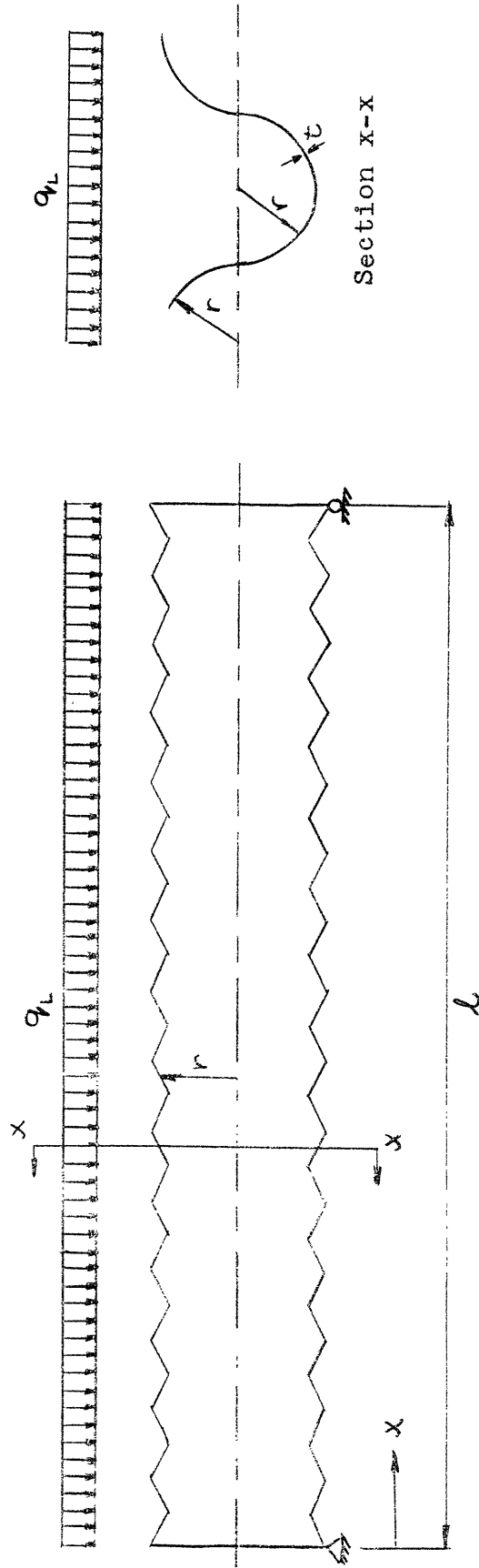then the stress distribution due to the bending moment M

Fig. 4.3. Simply Supported Shell Under Snow Load

is also given by Eqs. (3.21) and (3.23). (When using these equations for the shell, it should be remembered that Θ should be replaced by Θ_1 for the arcs AB.) This solution was obtained by assuming that plane sections remain plane, which is the fundamental assumption of the beam method.

The stresses at the crests of the corrugations can be obtained by multiplying the stress in a plane shell by the stress factors K_ϕ and K_Θ given by Eqs. (3.16) and (3.17). The stress at any point in a plain shell is

$$\sigma_x = \frac{2q_L \ell^2}{\pi r t} \frac{x}{\ell} \left(1 - \frac{x}{\ell}\right) \sin\Theta$$

The maximum meridional and circumferential stresses in a corrugated shell at any given Θ are

$$\left.\begin{aligned}
\left|\sigma_\phi\right| &= K_\phi \frac{2q_L \ell^2}{\pi r t} \frac{x}{\ell} \left(1 - \frac{x}{\ell}\right) \sin\Theta \\
\left|\sigma_\Theta\right| &= K_\Theta \frac{2q_L \ell^2}{\pi r t} \frac{x}{\ell} \left(1 - \frac{x}{\ell}\right) \sin\Theta
\end{aligned}\right\} \tag{4.4}$$

The "beam" deflections of the shell are found to be N times those for a plain shell, where N is given by Eq. (3.18). This can be taken into account by using for the deflection computations a reduced modulus of elasticity which is equal to $\frac{1}{N}$ times the E of the material.

The unit shear stress τ on a cross section due to the shear force S can be found by the method similar to that used for a pipe (Article 3.4). The expression for τ is found to be

$$\mathcal{T} = \frac{S\cos\theta}{\pi\, rt} = \frac{2q_L \ell}{\pi\, t} \left(1 - \frac{2x}{\ell}\right)\cos\theta \qquad\qquad (4.5)$$

As in the case of pipes, the reduced modulus of shear G' must be used in calculating the deflection due to shearing deformation. This is given by

$$G' = \frac{b}{c}\, G \qquad\qquad (4.6)$$

where b and c are the width and length of a corrugation as defined in Fig. 4.2(b). When the ℓ/r ratio is large, the effect of shear on the total deflection is so small that it can safely be neglected.

The transverse stresses can be obtained by considering an element between two cross sections an elemental length dx apart. The load acting on such an element is equal to $2q_L r\, dx$, and this is balanced by the difference in the shear forces acting on the two faces of the element. The transverse moments and axial forces per unit length can be obtained by a method similar to that used for a multiple barrel shell.[4] The expressions for these are given by

---

[4] H. Lundgren. loc.cited, p. 83.

$$M_t = q_L r^2 (\frac{1}{4} - \frac{8}{\pi^2} + \frac{2}{\pi} \sin\theta + \cos\theta - \frac{2}{\pi}\theta\cos\theta - \cos^2\frac{\theta}{2})$$

$$M_{t_1} = q_L r_1^2 (\frac{1}{4} - \frac{8}{\pi^2} - \frac{2}{\pi} \sin\theta_1 - 3\cos\theta_1 + \frac{2}{\pi}\theta_1\cos\theta_1 - \cos^2\frac{\theta_1}{2}) \qquad (4.7)$$

$$N_t = q_L r (\frac{2}{\pi}\sin\theta - \cos\theta + \frac{2}{\pi}\theta\cos\theta + \cos^2\theta)$$

$$N_{t_1} = q_L r (\frac{2}{\pi}\sin\theta_1 - 3\cos\theta_1 + \frac{2}{\pi}\theta_1\cos\theta_1 - \cos^2\theta_1) \qquad (4.8)$$

The boundary conditions used to obtain these expressions were that the longitudinal edges at A are prevented from moving horizontally and rotating because of the restraint provided by the adjacent shells. The moments are considered positive when causing compression on the outside fibre (see Fig. 4.3), and the axial force is positive when tensile.

The absolute maximum value of the transverse moment is found to occur at $\theta = \frac{\pi}{2}$ and at $\theta_1 = \frac{3\pi}{2}$, where it is

$$\left| M_t \right|_{max} = \left| M_{t_1} \right|_{max} = (\frac{1}{4} - \frac{8}{\pi^2} + \frac{2}{\pi}) = 0.07605 \; q_L r^2 \qquad (4.9)$$

The transverse forces have an absolute value of

$$\left| N_t \right|_{max} = \left| N_{t_1} \right|_{max} = \frac{2}{\pi} q_L r = 0.6366 \; q_L r \qquad (4.10)$$

A comparison of Eqs. (4.7) and (4.8) with the stresses due to the bending moment M as given by Eq. 4.4 shows that the transverse moments are small relative to these stresses if the ratio $\frac{l}{r}$ is fairly large. This then makes the beam

method valid for the shell of Fig. 4.3 subjected to a snow load.

The unit stresses due to the transverse moments and thrusts can be found by using the sectional properties of the corrugation given in Fig. 4.4. The maximum stress is given by

$$|\sigma_t|_{max} = q_L \frac{r}{t} \left[0.6366 \frac{b}{c} + 0.4563 \frac{r}{t} \frac{\frac{c}{b} + \frac{h}{t}}{(\frac{c}{b})^3 + \frac{ch^2}{bt^2}} \right] \qquad (4.11)$$

Let us consider a particular case of a shell whose dimensions are as follows: $l = 120"$, $r = 4"$, $t = 0.05"$. The corrugations of this shell will be assumed to be V-shaped with $b = 0.500$, $h = 0.100$, and $c = 0.510$. With these values, the maximum transverse stress is found from Eq. (4.11) to be

$$|\sigma_t|_{max} = 1,767 \ q_L \qquad (a)$$

For the dimensions given above, the value of the characteristic β is 1.13 for which the stress factors given by either Eqs. (3.16) and (3.17) or by the curves of Figs. A.1 and A.2 are

$$K_\phi = 6.30 \quad \text{and} \quad K_\theta = 2.56$$

The maximum meridional and circumferential stresses at mid span are, from Eqs. (4.4),
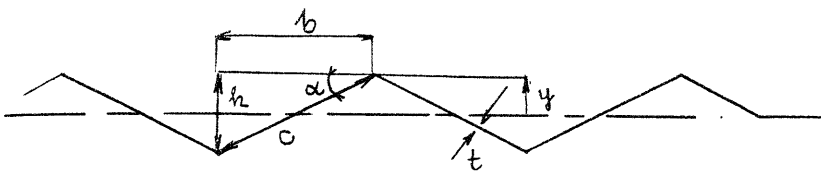
V-Shaped
Corrugations

$$\bar{y} \approx \frac{1}{2}(t + h)$$

$$A_t = \frac{ct}{b}$$

$$I_t = \frac{1}{12}\left[\left(\frac{ct}{b}\right)^3 + \frac{ch^2 t}{b}\right]$$
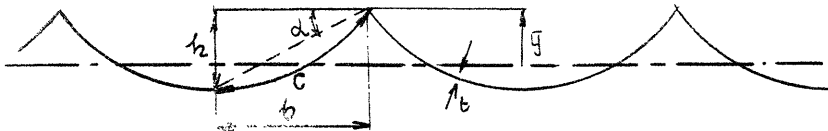
Cusped
Corrugations

$$\bar{y} \approx \frac{1}{2}\left[t + h\,\frac{\sin 2\alpha - 2\alpha\cos 2\alpha}{\alpha(1 - \cos 2\alpha)}\right]$$

$$A_t = \frac{ct}{b}$$

$$I_t = \frac{t^3}{12}\left(\frac{4\alpha + \sin 4\alpha}{4\sin 2\alpha}\right) + \frac{ch^2 t}{b}\left[\frac{4\alpha^2 + \alpha^2\sin 4\alpha - 2\sin^2 2\alpha}{8\alpha^2(1 - \cos 2\alpha)^2}\right]$$
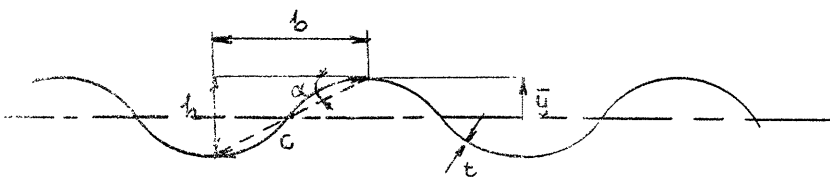
Undulating
Corrugations

$$\bar{y} = \frac{1}{2}(t + h)$$

$$A_t = \frac{ct}{b}$$

$$I_t = \frac{t^3}{12}\left(\frac{4\alpha + \sin 4\alpha}{4\sin 2\alpha}\right) + \frac{ch^2 t}{b}\left[\frac{4\alpha + 8\alpha\cos^2 2\alpha - 3\sin 4\alpha}{32(1 - \cos 2\alpha)^2}\right]$$

Fig. 4.4. Average Area and Moment of Inertia per
Unit Length of Corrugation

$$\sigma_\phi = 72,200 \; q_L \quad \text{and} \quad \sigma_\theta = 29,400 \; q_L \tag{b}$$

These are seen to be much larger than the transverse stresses σ_t given by (a). In a practical case the $\frac{\ell}{r}$ ratio will be much larger than the one used in the above example, so that one would not need to consider the transverse moments M_t.

Dead Load: The stresses and deflections of the shell under the influence of its own weight can be found by the same method used for the case of snow load. However, because of the distribution of the load, there are no transverse moments; the transverse forces are found to be

$$N_\theta = q_D r \sin\theta$$

$$\tag{4.12}$$

$$N_{\theta_1} = q_D r \sin\theta_1$$

where q_D is the weight per unit area of the shell.

It is evident that the stress due to these forces will be very small in comparison with the longitudinal stresses, so that for this case the beam method will give very good results.

4.5. <u>Shells with Circular Corrugations</u>. In the preceding articles the shells were considered to have V-shaped corrugations. However, the discussion is equally applicable to the cusped and undulating circular corrugations. The

stress factors and modular ratios needed to obtain the stresses and deflections of shells having these types of corrugations can be found from the curves of Figs. A.4 through A.9 of Appendix A. The sectional properties of these corrugations, which are needed to obtain the transverse stresses, are given in Fig. 4.4.

CHAPTER 5

BENDING OF CURVED SHELLS

5.1. <u>Introduction</u>. It is well known that a curved tube with a comparatively thin wall is much more flexible during bending than a straight tube of the same cross section due to distortion of the cross section to an ellipse-like shape.[1] A similar phenomenon would also occur in the curved shell of Fig. 5.1.

Consider an element between two adjacent cross sections of the shell which is bent by couples in the direction indicated. Due to the curvature of the shell both the compressive forces at the convex side and the tensile forces at the concave side have resultants away from the neutral axis, so that the originally circular cross sections distort to a shape shown approximately by the dotted line in Fig. 5.1(b). This distortion of the cross section affects the strain of the longitudinal fibres of the shell. Let R be the radius of the centre line of the undeformed shell, $d\psi$ the angle between the two cross sections, ds the length of the outermost fibre, and r the radius of the circular arcs forming the cross section. Let $R + \Delta R$, $d\psi - \Delta d\psi$,

---

[1] This phenomenon for a pipe of circular section was first explained by Th. v. Karman, V.D.I., Vol. 55, 1911, p. 1189. This problem was later investigated by others, among whom is L. Beskin, Trans. A.S.M.E., Vol. 67, 1945, p. A-1. The case of a tube with rectangular cross section was considered by S. Timoshenko, Trans. A.S.M.E., Vol. 45, 1923, p. 135.

(a)
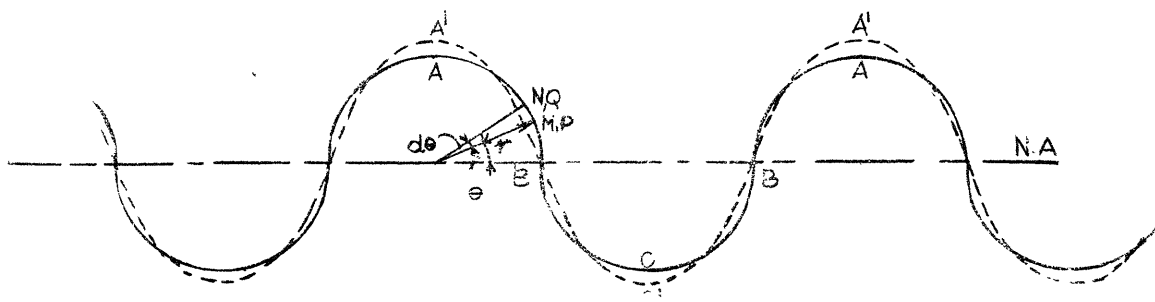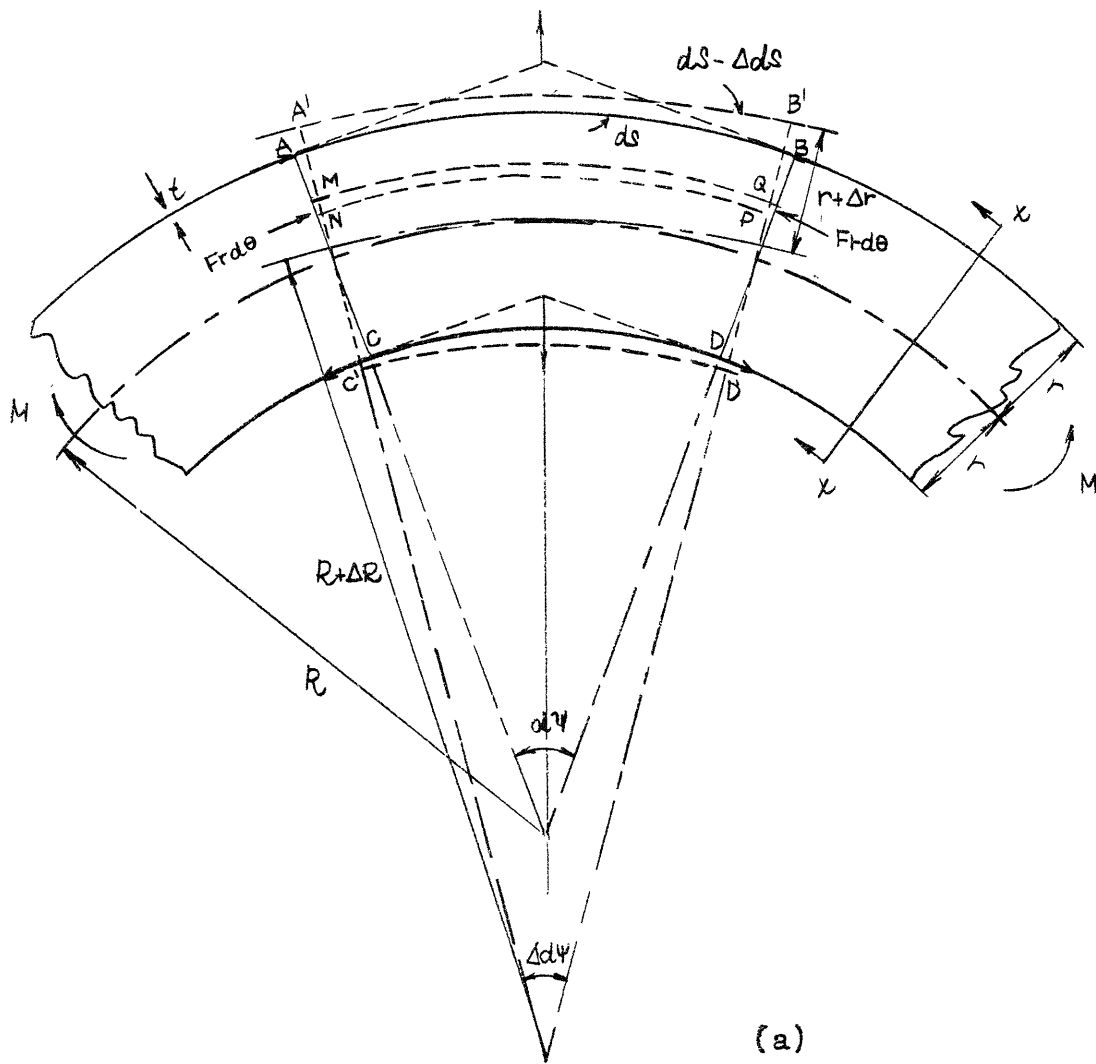
(b) Section x-x

Fig. 5.1. Bending of Curved Shell

$ds - \Delta ds$, and $r + \Delta r$ be the corresponding quantities for the deformed shell. The length of the fibre AB is

$$ds = (R + r)\, d\psi$$

After deformation its length becomes

$$ds - \Delta ds = [(R + \Delta R) + (r + \Delta r)](d\psi - \Delta d\psi)$$

The compressive strain $\Delta ds/ds$ in the outermost fibre is then

$$\frac{\Delta ds}{ds} = \frac{\Delta d\psi}{d\psi} - \frac{\Delta R + \Delta r}{R + r} \tag{a}$$

Since the centre line remains unchanged in length we have the relation

$$(R + \Delta R)(d\psi - \Delta d\psi) = R\, d\psi$$

Neglecting products of small quantities, we have

$$\frac{\Delta d\psi}{d\psi} = \frac{\Delta R}{R}$$

Using this relation in (a) then gives

$$\frac{\Delta ds}{ds} = \frac{r}{R + r}\left(\frac{\Delta R}{R} - \frac{\Delta r}{r}\right) \tag{b}$$

as the expression for the compressive strain in the outermost fibre. The ordinary theory for bending of curved bars assumes that the shape of the cross section remains unchanged, so that the corresponding expression for the strain given by this theory is

$$\frac{\Delta ds}{ds} = \frac{r}{R + r}\frac{\Delta R}{R} \tag{c}$$

Comparison of expressions (b) and (c) shows that
the effect of the distortion of the cross sections reduces
the strain in the outermost fibres; the effect is appreci-
able as soon as the ratio $\Delta r/r$ is of the same magnitude as
$\Delta a/a$. A change in the direction of the bending moment
causes a change of sign of the longitudinal forces, and as
a result the cross section distorts to a shape indicated by
the dotted line in Fig. 5.3(b). From the same reasoning
as above it may be shown that here again the distortion of
the cross section reduces the strain in the most remote
fibres. Consequently, a smaller bending moment is required
to produce a given change of curvature in the curved shell.
Defining the rigidity of the shell as the ratio of bending
moment to change of curvature it follows that the distor-
tion of the cross sections reduces the rigidity of the
shell.

Detailed analysis shows that the initial curvature
of the centre line of the shell not only increases the
flexibility but has other effects as well. Marked devia-
tions may occur from the linear distribution of stresses
over the cross section which holds for a shell with
straight axis, and secondary wall bending stresses arise
which may be as large or larger than the primary fibre
stresses parallel to the centre line.

In the following article the case of bending of the curved shell without longitudinal corrugations is solved by the principle of least work. Use is made of an infinite trigonometric series which converges very rapidly and gives an exact solution of the problem. This analysis is theoretically valid only in the case when the ratio of the radius of curvature of the centre line of the shell to the radius r of the cross section is large, so that the neutral axis can be taken as passing through the centroid of the cross section. This assumption means the same for the present problem as disregarding the difference between hyperbolic and linear bending stress distributions means for solid beams with curved axis. The analysis applies only to shells of uniform thickness, with a constant radius r and a constant curvature of the centre line. The method presented is similar to the method used by Beskin for obtaining the solution of curved thin pipes.[2]

The solution obtained for the plain shell can, as shown in Art. 5.3, be used, after a slight modification, for a curved shell corrugated in the transverse direction.[3] It is found that the distortion is less for this case than for a plain shell. This is to be expected since the secondary corrugations help to increase the transverse stiffness of the shell.

---

[2] L. Beskin, loc. cit. p. 100.

[3] See footnote 1 on p. 83.

In a general case of loading there will be axial and shear forces on a cross section in addition to a bending moment. This occurs, for example, when the shell acts as a two-hinged arch and is subjected to a snow load. In such cases it will be assumed that the stresses due to these forces will be distributed in the same manner as in a straight shell. This is permissible since the stresses produced by these forces are small in comparison with those produced by the bending moment for arches whose span length is large relative to the cross sectional dimensions as is usually the case. (See Arts. 6.2 and 6.3.)

5.2. <u>Pure Bending of Curved Shell</u>. Let us examine the forces acting on an element MNPQ of the shell (Fig. 5.1). The total force acting on each of the two faces MN and PQ is $Frd\theta$, where F is the longitudinal force per unit length. These forces act in a plane parallel to the neutral surface of the shell. The resultant of these forces is directed away and normal to the neutral surface, and has a magnitude of

$$\text{Resultant} = Frd\theta d\psi \qquad\qquad \text{(a)}$$

The arc length MP of the element is

$$\overset{\frown}{MP} = (R + r\sin\phi)d\psi = R(1 + \tfrac{r}{R}\sin\theta)d\psi$$

The arc length $\overset{\frown}{MP}$ is approximately equal to $Rd\psi$ if $R \gg r$.

Taking the arc length $\overset{\frown}{MP}$ equal to unity the resultant force given by (a) can be written as $\frac{Frd\theta}{R}$. The resultant force per unit area of the shell is then

$$p = \frac{F}{R} \qquad\qquad (5.1)$$

The distortion of the cross section is due to these p-forces, as stated in the previous article.

Fig. 5.2 shows the forces and moments acting on the element MNPQ. The horizontal force is denoted by H, the vertical force by P, and the moment by m. In addition to these, there is the distributed vertical force p on the element. The horizontal force H must be constant since no horizontal forces are applied to the surface of the element MNPQ.

The equilibrium of forces in the vertical direction gives

$$dP + prd\theta = 0 \qquad\qquad (b)$$

Using the expression (5.1) for p gives

$$P = -\frac{r}{R} \int Fd\theta + \frac{M}{2\pi rR} C_1 \qquad\qquad (5.2)$$

in which the last term is a constant of integration. Equilibrium with respect to moments gives

$$dm + Hrcos\theta d\theta - Prsin\theta d\theta = 0 \qquad\qquad (c)$$

if products of small quantities are neglected. Upon
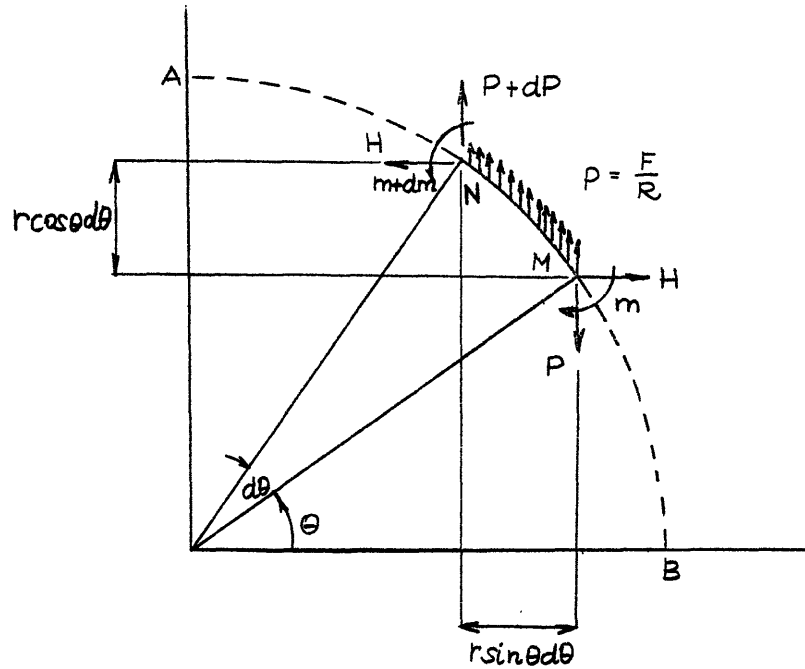
Fig. 5.2. Stresses Acting on an Element of Curved Shell
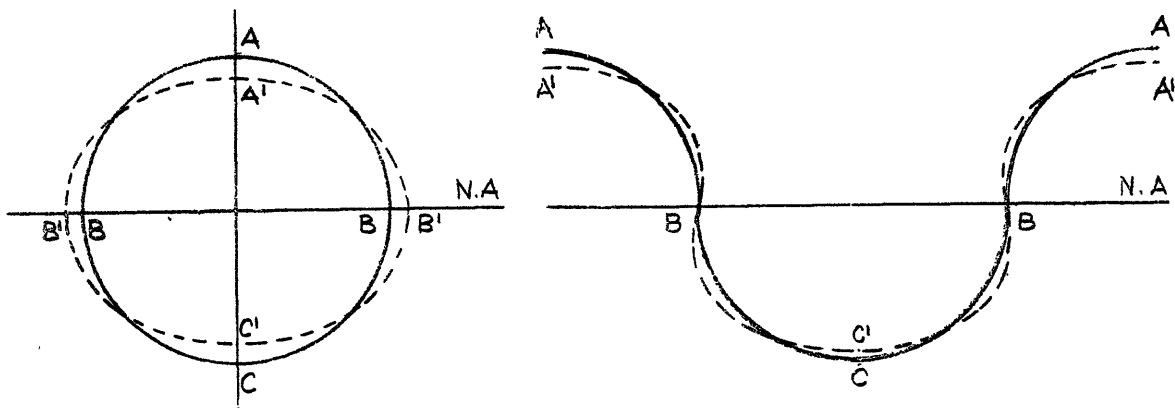

Fig. 5.3. Distortions of the Cross Sections
of a Pipe and a Shell

subsitution of expression (5.2) in (c), it is found that

$$\frac{dm}{d\theta} = - \left[Hr\cos\theta + \frac{r^2}{R} \sin\theta \int F d\theta - \frac{M}{2\pi R} C_1 \right] \qquad (5.3)$$

The distortion of the cross section is shown by the dotted line of Fig. 5.1(b). It is seen that the distortion is symmetrical about points A and C and anti-symmetrical about points B. Because of this only one quadrant AB need be considered. The vertical force P must be zero at **A**, while the bending moment m must vanish at B. Furthermore, the relative horizontal displacement between the points **A** and B must be zero. Thus, the boundary conditions for the quadrant AB are:

$$[P]_{\theta=\pi/2} = 0 \; ; \; [m]_{\theta=0} = 0; \quad \int_0^{\pi/2} m \, r\sin\theta \, \frac{rd\theta}{EI_t} = 0 \qquad (d)$$

where θ is the angle shown in Fig. 3.2 and I_t is the moment of inertia of a transverse section of the shell given by

$$I_t = \frac{1}{12} t^3 \qquad (5.4)$$

The last of the expressions (d) was obtained by the principle of virtual work considering only bending distortions.

By statics the external bending moment on the shell must be equal to the moment of the longitudinal forces F. If the moment on each shell ABCBA is M, then

$$\int_0^{\pi/2} Fr d\theta \cdot r\sin\theta = \frac{M}{4} \qquad (e)$$

It is convenient to introduce the dimensionless parameters

$$X = \frac{2\pi r^2 F}{M} \quad ; \quad Y = \frac{2\pi R m}{M} \tag{5.5}$$

and

$$C_2 = \frac{2\pi r R H}{M} \tag{f}$$

Substitution of these relationships in Eq. (5.3) gives

$$\frac{dY}{d\Theta} = - [C_2 \cos\Theta + \sin\Theta \int X d\Theta + C_1] \tag{5.6}$$

The first of the boundary conditions (d) when used in (5.2) gives

$$\left[\int f d\Theta\right]_{\Theta = \pi/2} = \frac{M}{2\pi r^2} C_1$$

Substituting the first of the relationships (5.5) in the above equation gives

$$\left[\int X d\Theta\right]_{\Theta = \pi/2} = C_1 \tag{5.7}$$

as one of the boundary conditions. Substitution of the second of the relationships (5.5) in the two remaining boundary conditions (d) results in

$$[Y]_{\Theta = 0} = 0 \tag{5.8}$$

and

$$\int_0^{\pi/2} Y \sin\Theta d\Theta = 0 \tag{5.9}$$

Similarly, the relationship between the external and internal moments given by (e) becomes

$$\int_0^{\pi/2} X \sin\theta \, d\theta = \pi/2 \qquad (5.10)$$

Let us assume that the function X is represented by the Fourier sine series

$$X = 2\sin\theta + 6b_3 \sin 3\theta + 10 \, b_5 \sin 5\theta + \ldots \qquad (g)$$

in which the first coefficient 2 is defined by Eq. (5.10). Only odd terms are considered since

$$\frac{dF}{d\theta} = \frac{dX}{d\theta} = 0 \qquad \text{at } \theta = \pi/2$$

in order to satisfy the condition of symmetry at A. The series (g) can be written in the compact form

$$X = 2 \sum_{n=0}^{\infty} (2n+1) \, b_{2n+1} \sin(2n+1)\theta \quad (b_1 \equiv 1) \qquad (5.11)$$

with the convention that $b_1 \equiv 1$.

Substituting this into the boundary condition (5.7) gives $C_1 = 0$. Setting $C_1 = 0$ in Eq. (5.6) and integrating it leads to

$$Y = - C_2 \sin\theta - \int \sin\theta \left[\int X d\theta \right] d\theta + C$$

where C is another constant of integration. Carrying out the integration by using for X its series representation (5.11) and introducing the boundary condition (5.8) gives

$$Y = \sum_{n=1}^{\infty} \frac{\sin^2 n\theta}{n} (b_{2n-1} + b_{2n+1}) - C_2 \sin\theta \qquad (h)$$

The constant C_2 is found to be

$$C_2 = \frac{8}{\pi} \sum_{n=1}^{\infty} \frac{n}{4n^2-1} (b_{2n-1} - b_{2n+1})$$

by introducing the boundary condition (5.9) in (h) so that
we finally obtain for Y the expression

$$Y = \sum_{n=1}^{\infty} (b_{2n-1} - b_{2n+1})[\frac{\sin^2 n\theta}{n} - \frac{8n}{\pi(4n^2-1)} \sin\theta] \quad (5.12)$$

The coefficients b_3, b_5 ... appearing in Eqs. (5.11)
must be such as to make the total strain energy in the
shell a minimum. Considering only the distortion due to
the longitudinal forces F and the transverse bending
moments m, the expression for the strain energy per unit
length along the centre line is

$$dW_s = 4 \left[\frac{1}{2} \int_0^{\pi/2} \frac{F^2 rd\theta}{Et} + \frac{1}{2} \int_0^{\pi/2} \frac{m^2 rd\theta}{D_1} \right] \quad (5.13)$$

in which

$$D_1 = \frac{Et^3}{12(1-\nu^2)} \quad (5.14)$$

Upon using the expressions (5.5) the above expression for
the strain energy becomes

$$dW_s = \frac{M^2}{2\pi^2 r^3 Et} \left[\int_0^{\pi/2} X^2 d\theta + \frac{1}{\beta_1^2} \int_0^{\pi/2} Y^2 d\theta \right] \quad (5.15)$$

in which the parameter β_1 is defined by

$$\beta_1 = \frac{R}{r^2}\sqrt{\frac{D_1}{Et}} = \frac{1}{\sqrt{12(1-\nu^2)}}\frac{Rt}{r^2} \tag{5.16}$$

The strain energy is a minimum if

$$\frac{\partial(dW_s)}{\partial b_{2a+1}} = 0 \qquad (a = 1,2,3,\ldots,n,\ldots)$$

Using these conditions in Eq. (5.15) gives

$$\int_0^{\pi/2} X\frac{\partial X}{\partial b_{2a+1}}d\theta + \frac{1}{\beta_1^2}\int_0^{\pi/2} Y\frac{\partial Y}{\partial b_{2a+1}}d\theta = 0$$

$$(a=1,2,3,\ldots,n,\ldots) \tag{5.17}$$

Substituting expressions (5.5) into this and integrating it gives

$$
\left.\begin{aligned}
&\sum_{\substack{n=1,2,\ldots,a-1,\\ a+2,a+3,\ldots}}^{\infty}(b_{2n-1}-b_{2n+1})\left[\frac{16n}{\pi^2(4n^2-1)(2a-1)(2a+3)} - \frac{1}{8na(a+1)}\right]\\
&\quad - b_{2a-1}\left[\frac{a+3}{16a^2(a+1)} - \frac{16a}{\pi^2(2a-1)(4a^2-1)(2a+3)}\right]\\
&\quad + b_{2a+1}\left[\beta_1^2(2a+1)^3 + \frac{2a^2+2a+3}{16a^2(a+1)^2} - \frac{16}{\pi^2(2a-1)^2(2a+3)^2}\right]\\
&\quad - b_{2a+3}\left[\frac{a-2}{16a(a+1)^2} + \frac{16(a+1)}{(4a^2-1)(2a+3)^2}\right] = 0\\
&\qquad (a=1,2,\ldots,n,\ldots);\ b_1 \equiv 1
\end{aligned}\right\} \tag{5.18}
$$

The above expression will yield a set of infinite linear simultaneous equations. However, an approximate solution of the problem can be obtained by retaining only

a finite number of terms in Eq. (5.11). If only (n+1) terms are retained in Eq. (5.11), then we shall have n simultaneous equations involving the n unknown b's $(b_3, b_5, \ldots, b_{2n+1})$. The approximate solution so obtained will be referred to as the approximation of the nth order. The number of terms, (n+1), to be retained in Eq. (5.11) in order to give a desired accuracy depends on the value of the parameter β_1; as β_1 decreases, the number of terms to be retained increases. As will be shown later, the solution obtained with n=1 gives a very good approximation for values of β_1 as small as 0.04.

Having obtained the coefficients $b_3, b_5, \ldots, b_{2n+1}$, the stresses and the change in curvature can easily be computed. The unit longitudinal stress, σ_ϕ, is equal to F/t. In terms of the parameter X defined by (5.5), the absolute maximum value of this stress is

$$\left| \sigma_\phi \right|_{max} = \frac{M}{2\pi r^2 t} \left| X \right|_{max}$$

The corresponding stress in a plain shell having a straight axis is

$$\sigma_o = \frac{M}{\pi r^2 t}$$

so that

$$\left| \sigma_\phi \right|_{max} = \sigma_o \left[\frac{\left| X \right|_{max}}{2} \right] \equiv \sigma_o \cdot K_{\phi 1} \qquad (5.19)$$

Similarly, the absolute value maximum transverse stress due to the moment m is

$$\left|\sigma_\theta\right|_{max} = \frac{6m}{t^2} = \frac{6M}{2\pi R t^2} \left|Y\right|_{max}$$

or

$$\left|\sigma_\theta\right|_{max} = \frac{3\sigma_o r^2}{Rt} \left|Y\right|_{max} = \frac{\sigma_o \left|Y\right|_{max}}{\beta_1} \sqrt{\frac{0.75}{(1-\gamma^2)}}$$

in which the parameter β_1 is defined by (5.16). For $\gamma = 0.3$, the above expression becomes

$$\left|\sigma_\theta\right|_{max} = \sigma_o \left[\frac{\left|Y\right|_{max}}{1.102\beta_1}\right] \equiv \sigma_o K_{\theta 1} \qquad (5.20)$$

To this the stress due to the direct force in the transverse direction should be added. This is found to be so small relative to the stress given by expression (5.20) that it can safely be neglected.

Based on the fact that the internal strain energy is equal to the work done by the external moment M, we have

$$dW_s = \frac{1}{2} M \frac{\Delta d\psi}{R d\psi} \qquad (1)$$

in which $\Delta d\psi$ is the change in angle between two adjacent cross sections a distance $Rd\psi$ apart along the centre line [see Fig. 5.1(a)] and dW_s is the strain energy per unit length along the centre line. Substituting (5.15) in this gives

$$\frac{\Delta d\psi}{Rd\psi} = \frac{M}{\pi r^3 tE} \left[\frac{1}{\pi} \int_0^{\pi/2} X^2 d\theta + \frac{1}{\pi \beta_1^2} \int_0^{\pi/2} Y^2 d\theta \right] \qquad (j)$$

The quantity $\frac{\Delta d\psi}{Rd\psi}$ represents the change in curvature of the shell due to the moment M. The corresponding change in curvature for a plain shell is

$$\left[\frac{\Delta d\psi}{Rd\psi} \right]_0 = \frac{M}{\pi r^3 tE}$$

so that

$$\frac{\Delta d\psi}{Rd\psi} = N_1 \left[\frac{\Delta d\psi}{Rd\psi} \right]_0 \qquad (5.21)$$

where N_1 represents the parentheses on the right hand side of Eq. (j). Upon substitution of expressions (5.5) into these parentheses, it is found that

$$N_1 = \sum_{n=0}^{\infty} (2n+1)^2 b_{2n+1}^2 + \frac{1}{\beta_1^2} \left\{ \frac{3}{16} \sum_{n=1}^{\infty} \frac{1}{n^2}(b_{2n-1}-b_{2n+1})^2 \right.$$

$$+ \frac{1}{4} \sum_{k=1}^{\infty} \frac{1}{k}(b_{2k-1}-b_{2k+1}) \sum_{n=k+1}^{\infty} \frac{1}{n}(b_{2n-1}-b_{2n+1})$$

$$\left. - \frac{16}{\pi^2} \left[\sum_{n=1}^{\infty} \frac{n}{4n^2-1}(b_{2n-1}-b_{2n+1}) \right]^2 \right\} \qquad (5.22)$$

The first two approximations to the factors K_{ϕ_1}, K_{θ_1}, and N_1 were obtained as functions of the parameter β_1, and are shown graphically in Appendix B. Comparison

of the two approximations shows that the first approximation gives very good results for values of β_1 as small as 0.04. The curved shells used for roofs are of such dimensions that the values of β_1 are generally larger than 0.1, so that for our purposes, it is not necessary to calculate approximation of an order higher than the second.

Upon comparison of the results shown in Appendix B with the results for a curved pipe given in the paper by Beskin[4], it was found that for a given value of the parameter β_1 the value of N_1 was less for the shell than for a pipe. For example, for $\beta_1 = 0.04$, $N_1 = 2.55$ for the shell, whereas for a pipe $N_1 = 12.50$. This difference can be explained by a consideration of the distortion of the cross sections. It is known that the cross section of a curved pipe distorts to an ellipse-like shape, as shown in Fig. 5.3(a); the distorted shape of the cross section of the shell is shown in Fig. 5.3(b). It is seen that the points B of the pipe lying on the neutral axis move towards the centre O, whereas the corresponding points of the shell have no displacement due to the antisymmetry of the deformations. Thus, the distortion of the cross sections of a shell will be less than that of the cross sections of a pipe and this makes the shell less flexible than the pipe.

[4] L. Beskin, loc.cit., p. 100.

5.3. **Pure Bending of Curved Corrugated Shell.** The equations relating the longitudinal forces F and the transverse forces and moments in a corrugated shell will be the same as those for a plain shell [Eqs. (5.1) through (5.3)] since these were derived solely by a consideration of equilibrium. Thus, Eqs. (5.11) and (5.12) will also apply for a corrugated shell. In order to satisfy compatibility, the strain energy in the shell must be a minimum. The strain energy per unit length due to the transverse moment m is

$$4\left[\frac{1}{2}\int_0^{\pi/2}\frac{m^2 r d\theta}{D_2}\right] = \frac{rM^2}{2\pi^2 R^2 D_2}\int_0^{\pi/2} Y^2 d\theta \qquad (a)$$

where D_2 is the transverse flexural rigidity of the shell and Y the parameter defined by (5.5). The strain energy due to the longitudinal forces F is approximately

$$4\left[\frac{1}{2}\int_0^{\pi/2}\frac{Nf^2 r d\theta}{Et}\right] = \frac{M^2 N}{2\pi^2 r^3 Et}\int_0^{\pi/2} X^2 d\theta \qquad (b)$$

where X is the parameter defined by (5.5) and N is the modular ratio given by Eq. (3.3). This expression for the strain energy is strictly correct only when all of the undetermined coefficients b in the Fourier series representation of X [Eq. (5.11)] are zero. It will be shown later that the distortion of the cross section is negligible so that these coefficients are very small in comparison

with the coefficient 2 of the first term in Eq. (5.11).
Hence, it is permissible to use (b) as the expression for
the strain energy due to the longitudinal forces. The
total strain energy per unit length is the sum of (a) and
(b), or

$$dW_s = \frac{M^2 N}{2\pi^2 r^3 Et}\left[\int_0^{\pi/2} X^2 d\theta + \frac{1}{\beta_2^2}\int_0^{\pi/2} Y^2 d\theta\right] \qquad (c)$$

in which the parameter β_2 is defined by

$$\beta_2 = \frac{R}{r^2}\sqrt{\frac{D_2 N}{Et}} = \beta_1\sqrt{\frac{D_2 N}{D_1}} \qquad (5.23)$$

In order that the strain energy be a minimum, the partial
derivative of (c) with respect to each of the coefficients
b_3, b_5, ... must be zero, or

$$\int_0^{\pi/2} X\frac{\partial X}{\partial b_{2a+1}} d\theta + \frac{1}{\beta_2^2}\int_0^{\pi/2} Y\frac{\partial Y}{\partial b_{2a+1}} = 0$$

$$(a=1,2,3, ... n, ...) \qquad (d)$$

This system of equations is the same as that represented
by (5.17) except that β_1 is replaced by β_2. Thus, the
coefficients b for the corrugated shell can be determined
from Eqs. (5.18) if β_1 in these equations is replaced by
β_2.

It can be shown that the expression for N_1 as given
by Eq. (5.22) can also be used for a corrugated shell if

β_1 is replaced by β_2. In this case N_1 should be taken as
the ratio of the change in curvature for a curved corru-
gated shell to the change in curvature for a corresponding
corrugated shell with a straight axis.

The factor $\sqrt{D_2 N/D_1}$ appearing in (5.23) is always
greater than unity for a corrugated shell, so that $\beta_2 > \beta_1$.
It can be deduced from the curves in Appendix B that the
distortion of the cross sections increases with decreasing
values of β_1. Therefore it can be said that the distor-
tion of the cross sections is less in a curved corrugated
shell than in a plain shell of the same major dimensions.

The depth h of the corrugations of the shells manu-
factured by the Wonder Building Corporation is greater
for a shell with a smaller radius of curwature R than that
with a larger R due to the fabrication process involved in
the manufacture of these shells. Consequently, the value
of $\sqrt{D_2 N/D_1}$ increases with a decrease in R. This has
the effect of keeping the value of the parameter β_2, as
defined by (5.23), large for the shells. As an example,
consider a plain curved shell having a cross section shown
in Fig. 5.1(b). If the radius r of the cross section is
4 in., the thickness t is 0.05 in., and the radius of
curvature R is 180 in., then the value of β_1 is found from
expression (5.16) to be 0.170, for which $N_1 = 1.24$ (see
Fig. B.1). Even though this is an extreme case, the

flexibility is increased by only 24%. With the presence of corrugations the factor N_1 is considerably reduced. Assuming V-shaped corrugations with h = 0.10 in., b = 0.50 in., and c = 0.51 in., it is found that for ν = 0.3.

$$\frac{D_2}{D_1} = (\frac{c}{b})^3 + \frac{ch^2}{bt^2} (1-\nu^2) = 4.77$$

and $\qquad N = \frac{b}{c} + \frac{ch^2}{bt^2} n = 4.45$ (See Fig. A.3)

Eq. (5.23) then gives β_2 = 0.783 for which N_1 as given by Fig. B.1 is 1.02. This means that the flexibility of the curved corrugated shell is only 2% larger than that of a straight corrugated shell. Thus, the distortion of the cross section of a corrugated shell can be neglected and the longitudinal forces can be assumed to be linearly distributed over the cross section.

CHAPTER 6

SHELL AS TWO-HINGED ARCH

6.1. <u>Arch Under a General Case of Loading</u>. Having obtained the effects of both the corrugations and the curvature in the previous two chapters, it is now possible to analyse the shell as a two-hinged arch under various types of loading. This arch is statically indeterminate to the first degree, and we shall take the horizontal reaction H at the right support as the redundant [Fig. 6.1(a)]. The value of this redundant for the various types of loading will be determined by the superposition method. The value of the redundant H is given by the equation

$$\Delta_{bo} + H\delta_{bb} = 0 \tag{6.1}$$

where

Δ_{bo} = horizontal deflection of the point B due to the applied load with H = 0, plus when in the direction of H;

δ_{bb} = horizontal deflection of the point B due to zero applied load and H = 1.

Eq. (6.1) merely states that the deflection of B is zero. The value of the deflections Δ_{bo} and δ_{bb} will be found by the method of virtual work.

If a unit virtual load is applied at B in the direction of H, then the external virtual work done by this load

(a)
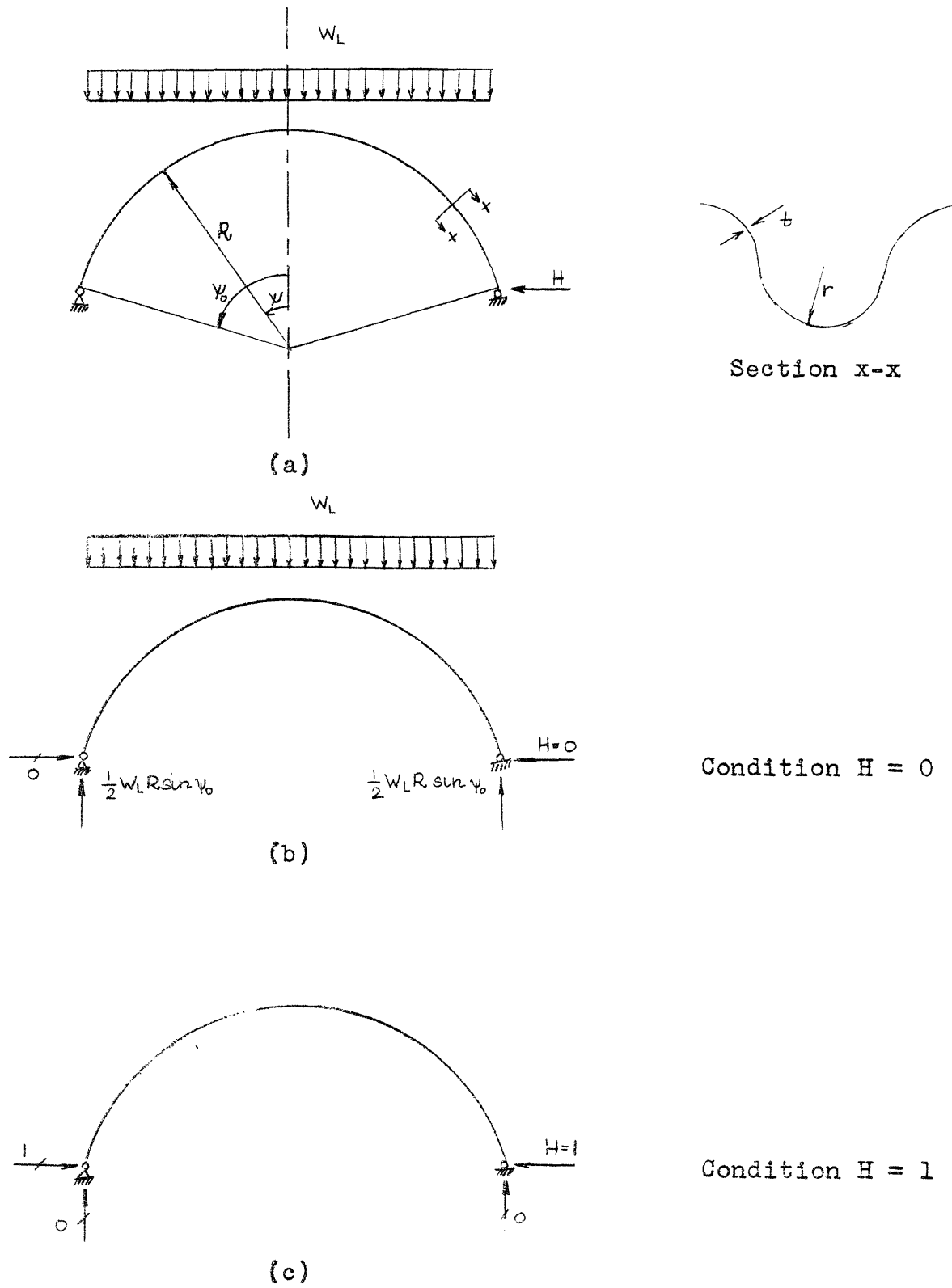
Section x-x

(b)

Condition H = 0

(c)

Condition H = 1

Fig. 6.1. Analysis of Two-Hinged Arch

as the point deflects by an amount Δ_{bo} must be equal to the virtual internal work done by the stresses due to this load as the structure deflects. The internal work due to bending distortion is

$$2 \int_{0}^{\psi_o} NN_1 \frac{M_o M_1 Rd\psi}{EI} \qquad \text{(a)}$$

where M_o = moment due to the applied load with H = 0,

plus when causing compression on the convex side;

M_1 = moment due to a unit horizontal load at B in the direction of H, plus when causing compression on the concave side;

I = moment of inertia of the cross section about its neutral axis ($\pi r^3 t$);

R = radius of curvature of the centre line of the arch;

ψ = angle between the mid-span cross section and that at any other point on the arch [Fig. 6.1(a)];

and ψ_o = angle between the mid-span cross section and that at the support.

Expression (a) is the same as the corresponding expression for an arch of solid cross section except for the factors N and N_1. It was shown in Art. 4.2 that the corrugated

shell is N times as flexible as a plain shell, while in Art. 5.3 it was shown that due to the curvature, the deflection of a curved corrugated shell is N_1 times that of a corrugated shell with a straight axis. This is the reason for the inclusion of the factors N and N_1 in expression (a).

Similarly, the internal work due to axial deformation is

$$2\int_0^{\psi_0} N\frac{T_0 T_1 R d\psi}{AE} \tag{b}$$

where T_0 = axial force due to the applied load with

H = 0, plus when tensile;

T_1 = axial force due to a unit horizontal load at

B in the direction of H, plus when tensile;

and   A = area of the cross section.

Again here N is the factor taking into account the effect of the corrugations.

In a curved bar an axial force T_0 produces tensile or compressive forces uniformly distributed over the cross section and equal to T_0/A. Due to these stresses the centre line undergoes extension or contraction and the angle $d\psi$ between two adjacent cross sections increases by the amount

$$\Delta d\psi = \frac{T_0 R d\psi}{AE} \cdot \frac{1}{R}$$

For a corrugated shell, this expression should be multiplied

by the factor N. The internal work done by the virtual moment M_1 is

$$- 2 \int_0^{\psi_0} N \; \frac{T_0 M_1 d\psi}{AE} \tag{c}$$

where the minus sign is used since the moment M_1 is considered positive when it tends to increase the angle $d\psi$ between two adjacent cross sections.

Finally, the internal work due to shearing deformations is

$$2 \int_0^{\psi_0} N' \; \frac{S_0 S_1 R d\psi}{AG} \tag{d}$$

where S_0 = shear force due to the applied load with

$H = 0$, plus when it tends to displace the
right side downward relative to the left
side;

S_1 = shear force due to a unit horizontal load
at B in the direction of H, plus when it
tends to displace the right side downward
relative to the left side.

Again here the factor N' as given by Eq. (3.26) takes into account the effect of the corrugations on the shearing deformations. In obtaining expressions (b), (c), and (d) it was assumed that the curvature of the arch does not alter the distribution of the stresses over a cross section due to axial and shear forces, i.e., the distribution

is the same as in a straight shell.

The external work done by the unit virtual load is $1 \cdot \Delta_{bo}$ which must be equal to the total internal virtual work as represented by expressions (a) through (d). Thus, the deflection Δ_{bo} is

$$\Delta_{bo} = 2\left[\int_0^{\psi_0} NN_1 \frac{M_o M_1 Rd\psi}{EI} + \int_0^{\psi_0} N \frac{T_o T_1 Rd\psi}{AE} + \int_0^{\psi_0} N \frac{T_o M_1 d\psi}{AE}\right.$$
$$\left. + \int_0^{\psi_0} N' \frac{S_o S_1 Rd\psi}{AG}\right] \quad (6.2)$$

In a similar manner the deflection δ_{bb} is found to be

$$\delta_{bb} = 2\left[\int_0^{\psi_0} NN_1 \frac{M_1^2 Rd\psi}{EI} + \int_0^{\psi_0} N \frac{T_1^2 Rd\psi}{AE} + \int_0^{\psi_0} N \frac{T_1 M_1 d\psi}{AE}\right.$$
$$\left. + \int_0^{\psi_0} N' \frac{S_1^2 Rd\psi}{AG}\right] \quad (6.3)$$

The value of the redundant H can then be found by substituting the above expressions into Eq. (6.1). Rewriting Eq. (6.1) gives

$$H = -\frac{\Delta_{bo}}{\delta_{bb}} \quad (6.4)$$

The moment M, the axial force T, and the shear S in the actual structure can easily be obtained from the following expressions

$$M = M_o + HM_1 \qquad (6.5)$$

$$T = T_o + HT_1 \qquad (6.6)$$

$$S = S_o + HS_1 \qquad (6.7)$$

These are obtained by superposing the stresses due to the applied load $(H = 0)$ with those due to the redundant force H.

6.2. **Arch Under a Uniformly Distributed Snow Load.** An arch under a uniformly distributed snow load of W_L lbs. per horizontal foot is shown in Fig. 6.1(a). The expressions for the external moments and forces will be found by making use of the general equations (6.2) through (6.6).

The case of $H = 0$ is shown in Fig. 6.1(b). The expressions for the moment, axial force, and shear force for this case are

$$M_o = \frac{W_L R^2}{2} (\sin^2\psi_o - \sin^2\psi) \qquad (6.8)$$

$$T_o = - W_L R \sin^2\psi \qquad (6.9)$$

$$S_o = W_L R \sin\psi\cos\psi \qquad (6.10)$$

The corresponding expressions for the case of $H = 1$ can be obtained by reference to Fig. 6.1(c). These are found to be

$$M_1 = - R (\cos\psi - \cos\chi_o) \qquad (6.11)$$

$$T_1 = -\cos\psi \tag{6.12}$$

$$S_1 = -\sin\psi \tag{6.13}$$

Substitution of the above expressions into Eqs. (6.2) and (6.3) and integrating results in the following expressions for the displacements Δ_{bo} and δ_{bb}:

$$\Delta_{bo} = -\frac{W_L R^4}{EI} N\left[N_1\left(\frac{2}{3}\sin^3\psi_o + \frac{1}{2}\psi_o\cos\psi_o\cos2\psi_o - \frac{1}{4}\cos\psi_o\sin2\psi_o\right)\right.$$

$$+ \frac{I}{2AR^2}(\cos\psi_o\sin2\psi_o - 2\psi_o\cos\psi_o)$$

$$\left. + \frac{2EI}{AGR^2}\frac{N'}{N}\left(\frac{2}{3}\sin^3\psi_o\right)\right] \tag{d}$$

$$\delta_{bb} = \frac{2R^2}{EI} N\left[N_1\left(\frac{1}{2}\psi_o + \psi_o\cos^2\psi_o - \frac{3}{4}\sin2\psi_o\right) + \frac{I}{2AR^2}(\sin2\psi_o)\right.$$

$$\left. + \frac{2EI}{AGR^2}\frac{N'}{N}\left(\frac{1}{2}\psi_o - \frac{1}{4}\sin2\psi_o\right)\right] \tag{e}$$

It can be shown that the effects of axial and shear distortions on Δ_{bo} are negligible if the radius r of the cross section is very small in comparison with the radius of curvature R [Fig. 6.1(a)]. We shall assume that this is so, so that

$$\Delta_{bo} = -\frac{W_L R^4 N N_1}{6EI}(4\sin^3\psi_o + 3\psi_o\cos\psi_o\cos2\psi_o - 3\sin\psi_o\cos^2\psi_o) \tag{f}$$

The effects of axial and shear distortions on δ_{bb} are also negligible when the ratio r/R is small, provided the angle

ψ_o is not very small. For a flat arch, however, the effect of axial distortion on δ_{bb} is not negligible. Thus, if only the effect of shear distortion is neglected, then

$$\delta_{bb} = \frac{R^3}{EI} N \left[N_1(\psi_o + 2\psi_o\cos^2\psi_o - 3\sin\psi_o\cos\psi_o) + \frac{I}{2AR^2}(\sin\psi_o\cos\psi_o) \right] \quad (g)$$

Substitution of expressions (f) and (g) into Eq. (6.4) gives

$$H = \frac{W_L R}{6} \left[\frac{4\sin^3\psi_o + 3\psi_o\cos\psi_o\cos2\psi_o - 3\sin\psi_o\cos^2\psi_o}{(\psi_o + 2\psi_o\cos^2\psi_o - 3\sin\psi_o\cos\psi_o + \frac{I}{2N_1 AR^2}(\sin\psi_o\cos\psi_o))} \right]$$

The second term in the denominator, which represents the effect of axial distortion, is of significance only when the angle ψ_o is small. For small values of ψ_o the radius R is large, so that the factor N_1, which represents the effect of the distortion of the cross section due to the curvature of the arch, is approximately equal to unity. Taking $N_1 = 1$, we have

$$H = \frac{W_L R}{6} \left[\frac{4\sin^3\psi_o + 3\psi_o\cos\psi_o\cos2\psi_o - 3\sin\psi_o\cos^2\psi_o}{(\psi_o + 2\psi_o\cos^2\psi_o - 3\sin\psi_o\cos\psi_o + \frac{I}{2AR^2}(\sin\psi_o\cos\psi_o))} \right] \quad (6.14)$$

This expression is the same as that for an arch of solid cross section. The values of the moment, axial and shear forces on any cross section can now be found from Eqs. (6.5) through (6.7). Expressions for the redundant H for various other types of loading, such as partial snow loads, dead load, and wind loads, can be found by a similar

method. In each case the analysis reduces to that for a corresponding load on an arch of solid cross section.

6.3. <u>Unit Stresses in the Arch</u>. The values of the bending moment, the axial force and the shear force on any cross section of the arch can be found, as shown in the previous article, by considering the arch to be of solid cross section. It was shown in Chapter 4 that the stresses in a corrugated shell due to a moment and axial and shear forces are the same as in a corrugated pipe of radius r and under the same loading. Thus, the maximum stress in the meridional and circumferential directions due to a moment M and axial force T are (if the distortion of the cross section due to curvature is neglected)

$$\sigma_{\phi max} = \left[\frac{M}{\pi r^2 t} \pm \frac{T}{2\pi r t}\right] K_\phi = \frac{M}{\pi r^2 t}\left[1 \pm \frac{Tr}{M}\right] K_\phi \qquad (6.12)$$

$$\sigma_{\theta max} = \left[\frac{M}{\pi r^2 t} \pm \frac{T}{2\pi r t}\right] K_\theta = \frac{M}{\pi r^2 t}\left[1 \pm \frac{Tr}{M}\right] K_\theta \qquad (6.13)$$

where K_ϕ and K_θ are the stress factors given by Eqs. (3.1) and (3.2). In Art. 5.3 it was shown that the distortion of the cross section due to curvature is very small in a corrugated shell, so that it will not be considered here. The term Tr/M in Eqs. (6.12) and (6.13) is found to be proportional to r/R. Generally, the ratio r/R is very small so that the effect of axial force on the stresses σ_ϕ and σ_θ can be neglected.

The unit shear stresses due to the shear force S on a cross section of the corrugated shell are the same as in a plain shell, and these two are found to be very small for small values of the ratio r/R.

The deflection calculations for the arch can be made by considering the shell to be plain but having a reduced modulus of elasticity equal to E divided by the modular ratio n (Eq. 3.3). The effects of shearing distortion and the distortion of the cross sections due to curvature can be neglected in the deflection computations.

CHAPTER 7

THE WONDER BUILDING ARCH

7.1. <u>Introduction</u>. The cross section of the actual
Wonder Building arch (Fig. 7.1) is much different than the
idealized cross section of Fig. 5.1(a). The shape of the
cross section is such that it cannot be represented by any
simple geometrical figure. The problem is further compli-
cated due to the fact that the shell is corrugated in the
bottom portion only. For this reason only an approximate
solution is given in this chapter.

The corrugated portion of the shell consists of a
circular arc and two tangents as shown in Fig. 7.1(a). A
longitudinal section through the corrugated portion is
shown in Fig. 7.1(b). From this it is seen that the actual
corrugations can be approximated as V-shaped corrugations.
We shall assume that the corrugations are V-shaped for
which the dimensions, b, c, and h are shown in Fig. 7.1(b).

In obtaining the solution for the corrugated shell
having the idealized cross section of Fig. 4.1(b) it was
shown that each one of the quadrants behaved as if they
were parts of a complete pipe. On this basis it will be
assumed that the circular corrugated arc CDC is a part of
a pipe of radius 9.125 in., and that each of the two tan-
gents BC is a part of a pipe whose radius is equal to in-
finity. The modular ratio N for the arc CDC will be

(a)
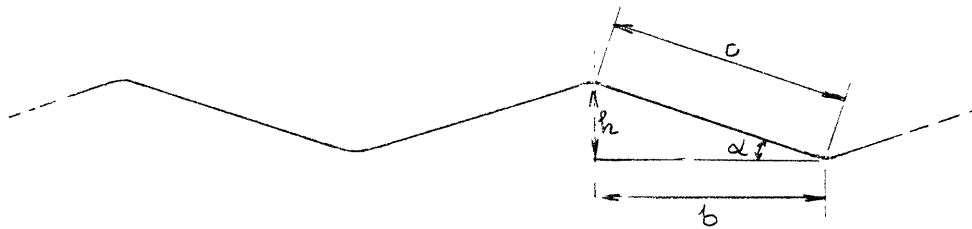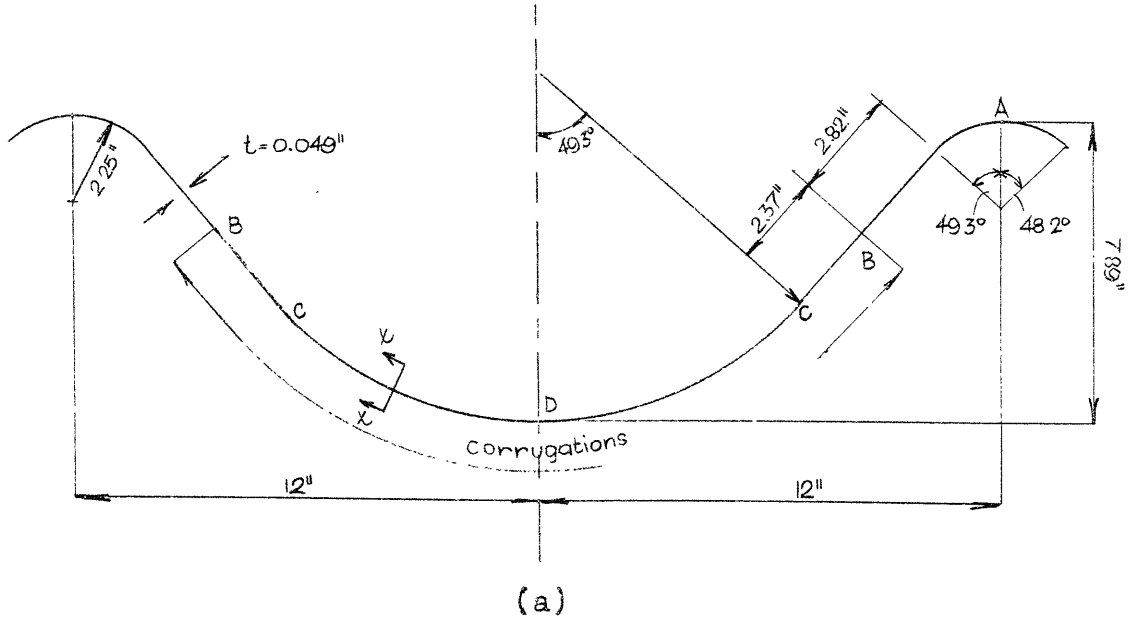
Section x-x
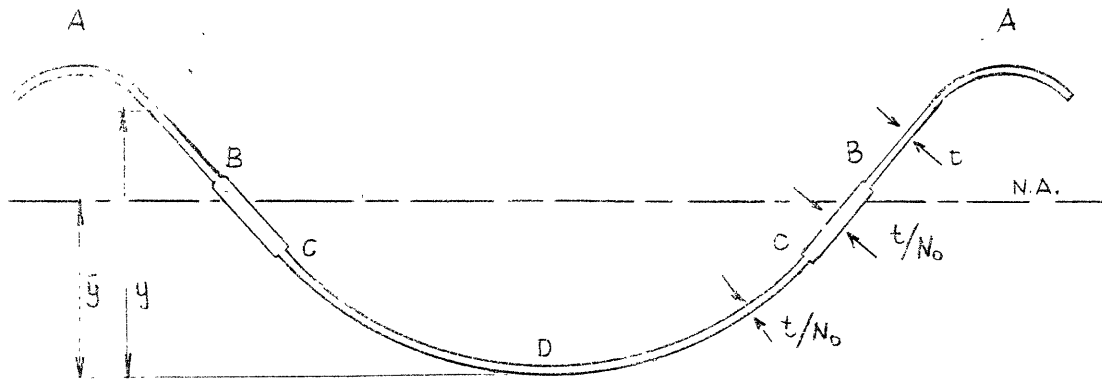
(b)

Fig. 7.1. Cross Section of Wonder Building Arch

Fig. 7.2. Transformed Cross Section

different from that for the tangents BC as they have different radii of curvature. Thus, the reduced modulus of elasticity which is equal to E divided by the modular ratio will be different for these parts of the cross section. The remainder of the cross section has no corrugations, so that its modular ratio is unity. The cross section can be considered as being formed of three different materials having different moduli of elasticity. For an ordinary beam of composite sections it is assumed that plane sections remain plane after bending. This will also be assumed in our case. Furthermore, it will be assumed that the effect of the distortion of the cross section due to curvature on the stresses and deflections is negligible. This seems reasonable since it was shown in Art. 5.3 that this is true for a curved corrugated shell having the idealized cross section of Fig. 5.1(b). Also, on the basis of the results obtained in the previous chapter, it will be assumed that the effect of the shear force on stresses and deflections is negligible. Even though so many assumptions have been made, the approximate solution so obtained gives results which are in very good agreement with the available test results.

7.2. <u>Calculation of Stresses and Deflections</u>. The stresses and deflections can be obtained by a method very similar to that used for beams of composite sections. The

modular ratio for the tangents BC [Fig. 7.1(a)] will be
denoted by the symbol N_a, while that for the arc CDC will
be denoted by N_b; by definition, the modular ratio for the
remainder of the section is unity. The transformed sec-
tion is obtained by dividing the thickness t of BC by N_a
and that of CDC by N_b (Fig. 7.2). The centroidal axis of
the transformed section is located a distance $\bar{y}$ above the
point D, where $\bar{y}$ is given by

$$\bar{y} = 6.94 \left[\frac{0.1848\ N_a + 0.2085\ N_b + N_a N_b}{1.176\ N_a + 0.358\ N_b + N_a N_b} \right] \text{ in.} \qquad (7.1)$$

The area A_T of the transformed section is

$$A_T = \left[0.652 + \frac{0.232}{N_a} + \frac{0.769}{N_b} \right] \text{ in.}^2 \qquad (7.2)$$

and the moment of inertia I_T about the centroidal axis is

$$I_T = \left[0.652(\bar{y}^2 - 13.89\bar{y} + 49.0) + \frac{0.232}{N_a}\ (\bar{y}^2 - 8.12\bar{y} + 16.75) \right.$$
$$\left. + \frac{0.769}{N_b}\ (\bar{y}^2 - 2.115\bar{y} + 2.055) \right] \qquad (7.3)$$

In obtaining the above expressions, the length of the cor-
rugated tangent BC was taken to be 2.37 in., in accordance
with the measurements made by Tabush on samples of the
Wonder Building Shell.[1]

---

[1] J. Tabush, "An Experimental Study of a Thin Steel Arch
Panel," S.M. Thesis, Massachusetts Institute of Tech-
nology, August 1958.

In the deflection computations, the expressions
(7.2) and (7.3) must be used for the area and moment of
inertia, while the modulus of elasticity should be the
same as that of the material. For example, in obtaining
the redundant H for the Wonder Building arch under a uni-
formly distributed snow load, A_T and I_T of the transformed
section must be used in Eq. (6.14) instead of the area A
and moment of inertia I of the actual cross section.

The longitudinal strain ϵ_x at any point of the
cross section due to an axial force T and a moment M can
be obtained from the formula

$$\epsilon_x = \frac{T}{A_T E} + \frac{M(\bar{y} - y)}{I_T E} \tag{7.4}$$

where y is the distance as defined in Fig. 7.2. This ex-
pression for the strain is obtained by assuming that plane
sections remain plane. The stress at any point can be ob-
tained by multiplying the strain, as given by Eq. (7.4), by
the corresponding reduced modulus of elasticity. Thus, for
a point on the circular arc CDC, the stress is obtained by
multiplying the strain by E/N_b; for a point on the tangent
BC the strain is to be multiplied by E/N_a; and for any
other point outside of these corrugated portions, the
stress is equal to $\epsilon_x E$. There will be discontinuity along
the longitudinal sections through C since there is an
abrupt change of curvature, similar to that occurring in

the shell of the idealized cross section under an axial load, which was discussed in Art. 4.2. In Fig. 7.1 it is shown that the corrugations end abruptly at B, so that there would also be a discontinuity here. However, this is not actually so as the depth of the corrugations gradually reduce from h to zero over a length of about an inch. The location of B was taken as the midpoint of this length of one inch. In any case we shall be interested in the stresses at A and D since the stresses are maximum here, as will be shown in the next article. The longitudinal stresses at these two points are

$$\sigma_{Ax} = \frac{T}{A_T} + \frac{M(\overline{y} - 7.875)}{I_T} \qquad (a)$$

$$\sigma_{Dx} = \frac{1}{N_b} \left[\frac{T}{A_T} + \frac{M\overline{y}}{I_T} \right] \qquad (b)$$

The stress σ_{Dx} given by (b) should be multiplied by the stress factors $K_{\phi b}$ and $K_{\theta b}$ [given by Eqs. (3.1) and (3.2)] in order to obtain the absolute maximum value of the meridional and circumferential stresses at the crest of the corrugations. The factor K_ϕ is always larger than K_θ, so that we shall consider only the meridional stress, $\sigma_{Dx}K_\phi$. Since we are considering only the meridional stress, we shall drop the subscript x. The maximum absolute values of the stresses at A and D are then

$$\sigma_A = \left| \frac{T}{A_T} + \frac{M(\bar{y} - 7.875)}{I_T} \right| \qquad (7.5)$$

$$\sigma_D = \frac{K_\phi b}{N_b} \left[\left| \frac{T}{A_T} \right| + \left| \frac{M\bar{y}}{I_T} \right| \right] \qquad (7.6)$$

It will be shown in the next article that these stresses depend primarily upon the depth of the corrugations h. Particular cases are worked out to show the effect of h on the stresses.

7.3. <u>Effect of the Depth of the Corrugations on the</u> <u>Stresses</u>. The arches constructed by the Wonder Building Corporation of America have the same cross sections even though their span lengths vary; only the depth h of the corrugations varies. The manufacturing process is such that h increases with an increase in curvature of the arch. In order to study the effect of the depth of the corrugations on the stresses, we shall consider two extreme cases of arches as constructed by the Wonder Building Corporation, which will be referred to as X-P and M arches, in accordance with the designation used by the manufacturer. The dimensions of the arches and the corrugations for these two arches are:

X-P Arch: $\quad R = 15$ ft.; $\psi_o = 86°$; $b = 0.50$ in.; $h = 0.200$ in.

M Arch: $\qquad R = 33$ ft.; $\psi_o = 67°$; $b = 0.50$ in.; $h = 0.092$ in.

in which the dimensions R and ψ_o are defined in Fig. 6.1(a).

The values of N_a, N_b, $K_{\phi b}$ can be obtained from Eqs. (3.1) and (3.3) and Figs. A.1 and A.3; the properties of the transformed section can then be found from Eqs. (7.1) through (7.3). These are found to be

	N_a	N_b	$K_{\phi b}$	$\bar{y}$(in.)	A_T(in.^{2})	I_T(in.^{4})
X-P Arch:	17.2	16.7	12.9	6.51	0.712	2.09
M Arch:	4.24	4.14	6.48	5.55	0.892	5.82

With this information the stress at any point on the cross section due to a moment M and axial force T can be determined. From Eq. (7.5) it is found that the stresses σ_A and σ_D are

$$
\left.
\begin{array}{l}
\text{X-P Arch:} \quad \sigma_A = \left|1.40T - 0.653M\right| \text{psi}; \quad \sigma_D = \left[\left|1.08T\right| + \left|2.40M\right|\right] \text{psi} \\[2mm]
\text{M Arch:} \quad \sigma_A = \left|1.12T - 0.400M\right| \text{psi}; \quad \sigma_D = \left[\left|1.76T\right| + \left|1.49M\right|\right] \text{psi}
\end{array}
\right\} (7.7)
$$

where M is expressed in lb.in. and T is expressed in lb. It will be shown later that the stress due to T is small in comparison with that due to the moment M, so that in both the cases the stress is maximum at D. The stresses at the points B and C are found to be less than σ_D for these two arches.

The bending moment and axial force on any cross section due to any loading can be calculated by the method indicated in Chapter 6. We shall consider only a uniformly distributed snow load of W_L lbs. per horizontal inch

over the entire arch. The maximum negative moment and the
axial force at the section where the negative moment is
maximum are

X-P Arch: M = - 2520 W_L lb.in.; T = - 180 W_L lb.

M Arch: M = - 5330 W_L lb.in.; T = - 396 W_L lb.

When these are substituted into expressions (7.7) it is
found that

X-P Arch: σ_D = (194 + 6050)W_L = 6240 W_L psi

M Arch: σ_D = (697 + 7930)W_L = 8630 W_L psi

The effect of the axial force on the stresses is found to
be very small. It is seen that even though the span of the
M arch is approximately twice that of the X-P arch, the max-
imem stress in the M arch is only 1.4 times that in the
X-P arch. This is due chiefly because the depth h in-
creases with the curvature. As h increases N_a, N_b, and
$K_{\phi b}$ increase as can be seen by examining Eqs. (3.1) and
(3.3). The factors n and k_ϕ appearing in these equations
are functions of the characteristic β defined by Eq. (3.5)
For the tangent part BC [Fig. 7.1(a)], β_a = 0, so that
n_a = 0.91. The ratio c/b is generally very near unity, so
that N_a is seen to depend primarily on h (the thickness t
is the same for all arches). The characteristic β_b for
the circular arc CDC is found to be approximately 0.72 for
both the arches, and for this value, n and k_ϕ are

approximately the same as those for $\beta = 0$. So N_b and $K_{\phi b}$ are also mainly dependent on h. Thus, when h increases, the factors N_a, N_b, and $K_{\phi b}$ all increase so that for a given moment M, the stresses increase with the depth h (or increase with an increase in curvature of the arch). However, when the curvature is large the span length of the arch is small, so that the moments are also smaller. This then makes it possible to use the same cross section over a wide range of span lengths.

7.4. <u>Comparison of Test Results with Theoretical Results</u>. Tests were performed by Tabush[2] at M.I.T. on three samples of shells provided by the Wonder Building Corporation of America. These were components of the M arch discussed in the last article. The chord lengths of these shells were 111 in. and the mid span rise was 4 in. Each shell was simply supported at its ends and loaded by two equal loads placed symmetrically about the mid span, so that the region between the loads was in pure bending. The deflection at mid span was measured relative to two symmetrically located points within the region of pure bending. Using a value of 29.3×10^6 psi for the modulus of elasticity, it was found from the deflection measurements that the transformed moment of inertia I_T of the cross section ranged from

---

[2] J. Tabush, loc.cit. p. 135.

4.53 in.^{4} to 5.20 in.^{4}, with a mean of 4.89 in.^{4}. This
compares favourably with the theoretical value of 5.82 in.^{4}
computed in the previous article for the M arch. The dis-
crepancy between the theoretical and experimental values is
perhaps due to the fact that the cross-sectional shape was
observed to differ from the standard shape to which the
shells were supposed to have been rolled. It was shown
in the last chapter that the maximum stress occurred at
the lowermost point of the section, and is given by Eq.
(7.7). From this equation the moment at which this stress
is equal to the yield stress of the material can be ob-
tained. Tabush performed tensile tests on specimens of
the shells and found that the yield stress had an average
value of $38,500$ psi. Using this value in Eq. (7.7), it is
found that the moment at which yielding first occurs is
2.15 k.ft. It was difficult to ascertain from the experi-
mental load versus deflection curves as to at what point
the curve became nonlinear, since the deviation from a
straight line in the inelastic range is very small.
Approximately, the yield point moment ranged from 1.9 to
3.0 k.ft.

Another series of tests on three similar shells
was performed by Chipman at U.C.L.A.[3] In these tests the

[3] R. D. Chipman, "Bending Test Conducted on M.P.H. Building
Sheets," Report No. C54-59, Dept. of Engineering, Uni-
versity of California, Los Angeles, July 1954.

samples were simply supported on pipes and subjected to a
concentrated load at mid span. Mid span deflections were
measured relative to the testing machine platform which
did not move with reference to the laboratory floor. A
plot of the experimentally determined deflections versus
the bending moment at mid span is shown in Fig. 7.3(a).
The deflection readings were measured to the nearest
thirty second of an inch, which makes the error in the de-
flection reading large when the loads are small. Further-
more, the pipes on which the shells were supported were
found to deflect under the load when plain shells (i.e.
without corrugations) were tested. The deflection of the
pipes for a moment of 4.75 k.ft. was found to be 1/32 of an
inch in one case and 2/32 of an inch in another case.
Since the tests were run primarily to determine the ulti-
mate load for the corrugated shells, no attempt was made
to measure the pipe deflections during the bending tests of
these shells. However, in the elastic range the deflec-
tions are very small, and thus the deflection readings for
low loads are not very accurate. For comparison, the
theoretical mid span deflection was calculated from the
formula

$$\delta = \frac{PL^3}{48EI_T} = \frac{ML^2}{12EI_T} \tag{7.8}$$

in which M is the mid span moment and L is the distance

(a)

Midspan Deflection in 32nds of an Inch

(b)

Strain ($\mu^{in}/^{in}$)

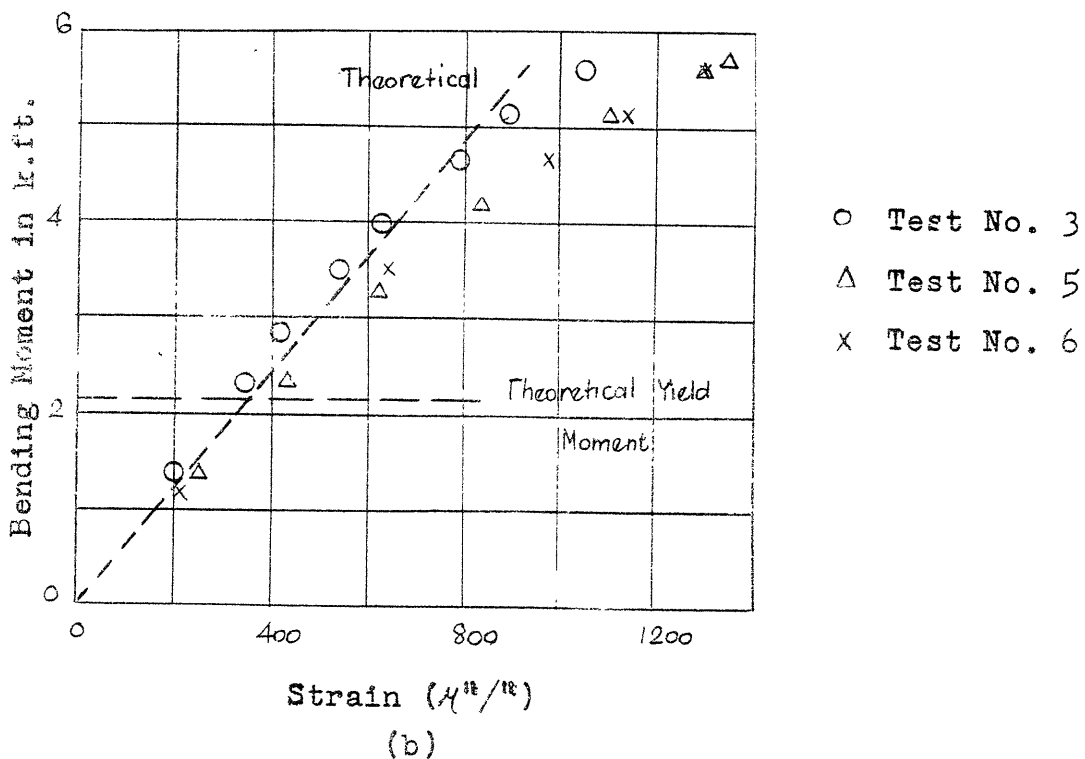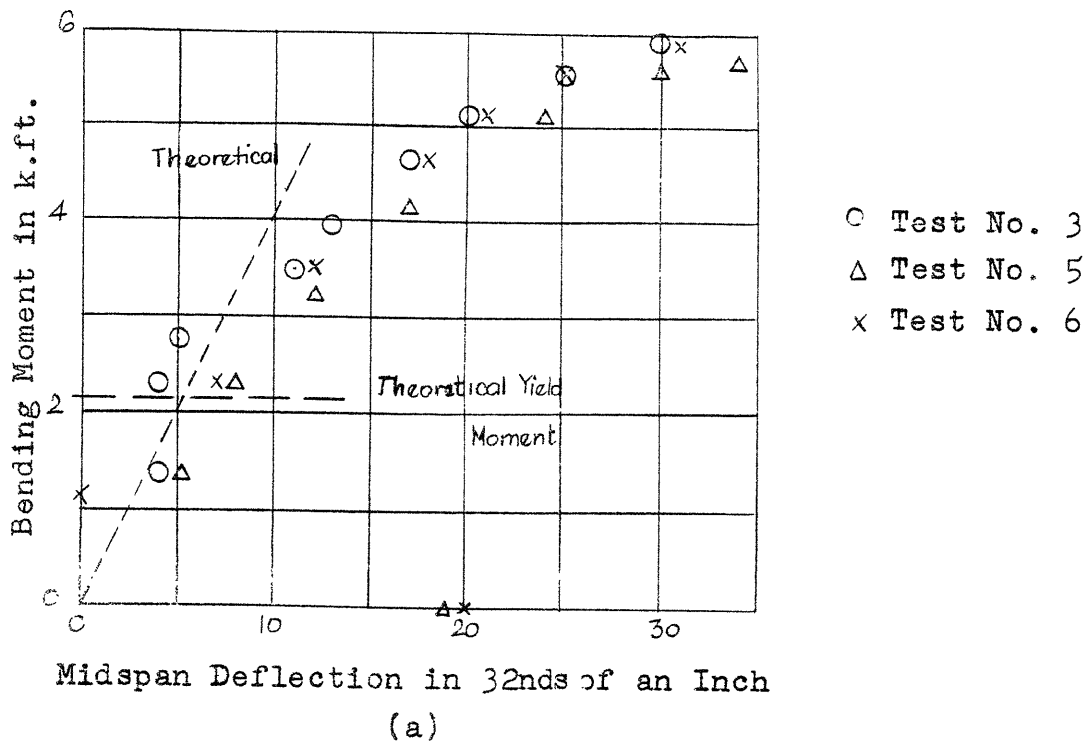Fig. 7.3. Deflection and Strain Measurements
in Wonder Building Shell

between the supports. The values of E and I_T were taken to be 29.3 x 10^6 psi and 5.82 in.^{4}, respectively. The curve for δ versus M is shown in Fig. 7.3(a). This curve is valid only in the elastic range; based on a yield stress of 38,500 psi, the moment at which yield first occurs is 2.15 k.ft., as was shown earlier.

Strain measurements were also made at the point A [Fig. 7.1(a)] at mid span. These are shown in Fig. 7.3(b) together with the theoretical strain calculated from Eq. (7.4). Here the deflections of the pipe supports do not affect the strain measurements. It is seen that the agreement between the experimental and theoretical results is very good when the moment is within the elastic range.

The shells tested at M.I.T. and at U.C.L.A. all failed in the inelastic range due to local buckling of the upper flange at mid span. The ultimate moment at mid span ranged from 5.2 k.ft. to 6.0 k.ft. The theory developed earlier in this chapter is applicable only for elastic behaviour, and does not consider the question of instability, so that no conclusion can be made with reference to the mode of failure.

The experiments that were made at M.I.T. and at U.C.L.A. were performed on shells which behaved as simply supported beams. Actually they are components of the actual arch so that experiments should be conducted by

loading the shells as two-hinged arches, and preferably having a larger span. Strain and deflection measurements should be made at more frequent load intervals than was done in the U.C.L.A. tests, so that a better value of the yield moment may be found. The strains in the corrugated portion are very difficult to measure since the corrugations are very small and the bending moment in them varies rapidly. However, the elongation between two successive crests can easily be measured with Huggenberger tensometers, and the elongation could then be compared with the theoretical results. On the basis of these tests the theoretical results could be modified by empirical constants if serious discrepancy exists between theoretical and experimental results. Until this is done, the theory should be used in designing the Wonder Building Arches using an adequate factor of safety.

BIBLIOGRAPHY

Beskin, L., "Bending of Curved Thin Tubes," Transactions of the American Society of Mechanical Engineers, Vol. 67, 1945, p. A-1.

Chipman, R. D., "Bending Test Conducted on M.P.H. Building Sheets," Report No. C54-59, Department of Engineering, University of California, Los Angeles, July 1954.

Cope, E. T. and Wert, E. A., "Load-Deflection Relations for Large Plain Corrugated and Creased Pipe Bends," Transactions of the American Society of Mechanical Engineers, FSP-54-12-115, 1932.

Donnell, L. H., "The Flexibility of Corrugated Pipes Under Longitudinal Forces and Bending," Transactions of the American Society of Mechanical Engineers, A.P.M.-54-7-69, 1932.

Hetenyi, M., "Beams on Elastic Foundation," The University of Michigan Press, Ann Arbor, 1946.

Hildebrand, F. B., Advanced Calculus for Engineers, Prentice-Hall, Inc., New York, 1949.

Karman, Th. v., "Über die Formanderung dünnwandiger Röhre," Zeitschr., Vereines Deutscher Ingeniure, Band 55, 1911, p. 1889.

Love, A. E. H., A Treatise on the Mathematical Theory of Elasticity, Dover Publications, New York, 1944.

Lundgren, H., Cylindrical Shells, Vol. 1, The Danish Technical Press, Copenhagen, 1949.

Meissner, E., "The Elasticity Problem for Thin Shells of Toroidal, Spherical or Conical Shape," David W. Taylor Model Basin Translation 238 (Translated by William A. Nash) from "Das Elastizitäts problem für düne Schalen von Ringflächen-, Kugel-oder Kegelform," Physikalische Zeitschrift, Vol. 14, 1913.

Reissner, H., Müller-Breslau-Festschrift, Leipzig, 1912.

Tabush, J., "An Experimental Study of a Thin Shell Arch Panel," S.M. Thesis, Massachusetts Institute of Technology, August 1958.

Timoshenko, S., "Bending Stresses in Curved Tubes of Rectangular Cross Section," Transactions of the American Society of Mechanical Engineers, Vol. 45, 1923, p. 135.

Timoshenko, S., Theory of Plates and Shells, McGraw-Hill Book Company, Inc., New York, 1940.

Wissler, M, "Festigkeifsherechung Von Ringflachenschalen," Doctoral Thesis, Eidgenössischen Technischen Hochschule, Zurich, 1916.

APPENDIX A

CURVES FOR THE DETERMINATION OF STRESS FACTORS AND
MODULAR RATIO OF CORRUGATED PIPES

Explanation of Symbols:

a) V-shaped Corrugations

b) Cusped Corrugations

c) Undulating Corrugations
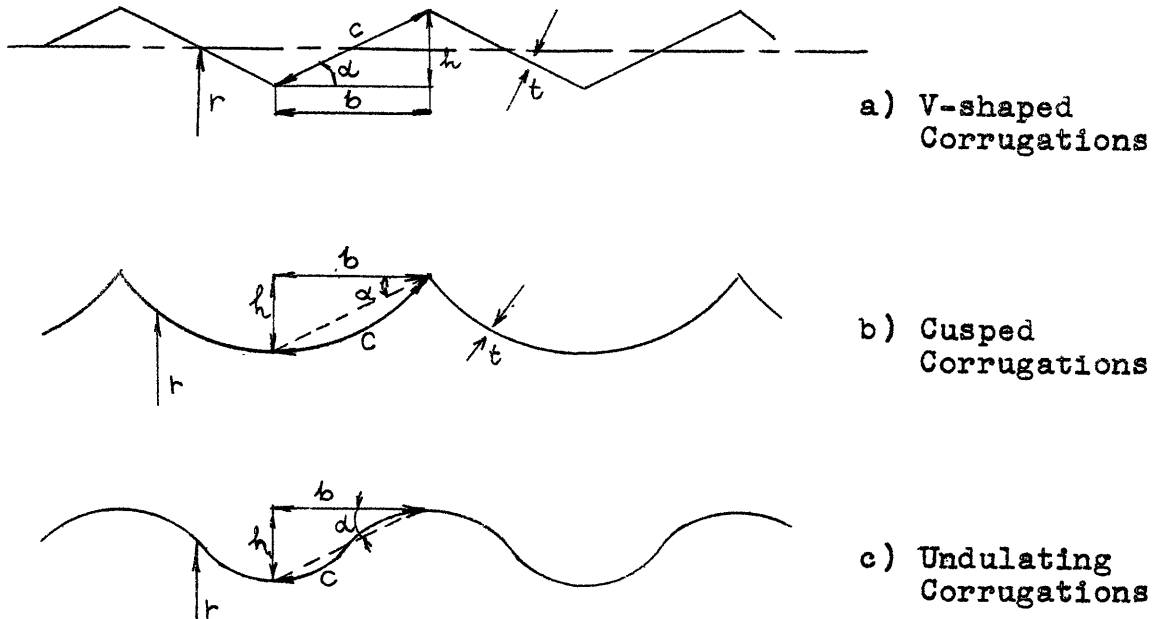
Meridional Stress Factor: $\qquad K_\phi = 1 + \frac{h}{t} k_\phi \qquad$ (3.1)

Circumferential Stress Factor: $\quad K_\theta = \frac{h}{t} k_\theta \qquad$ (3.2)

Modular Ratio: $\qquad\qquad\qquad N = \cos\alpha + \frac{ch^2}{bt^2} n \qquad$ (3.3)

The quantities k_ϕ, k_θ, and n can be determined from the curves on the following pages. These curves are plotted as functions of α and β, where
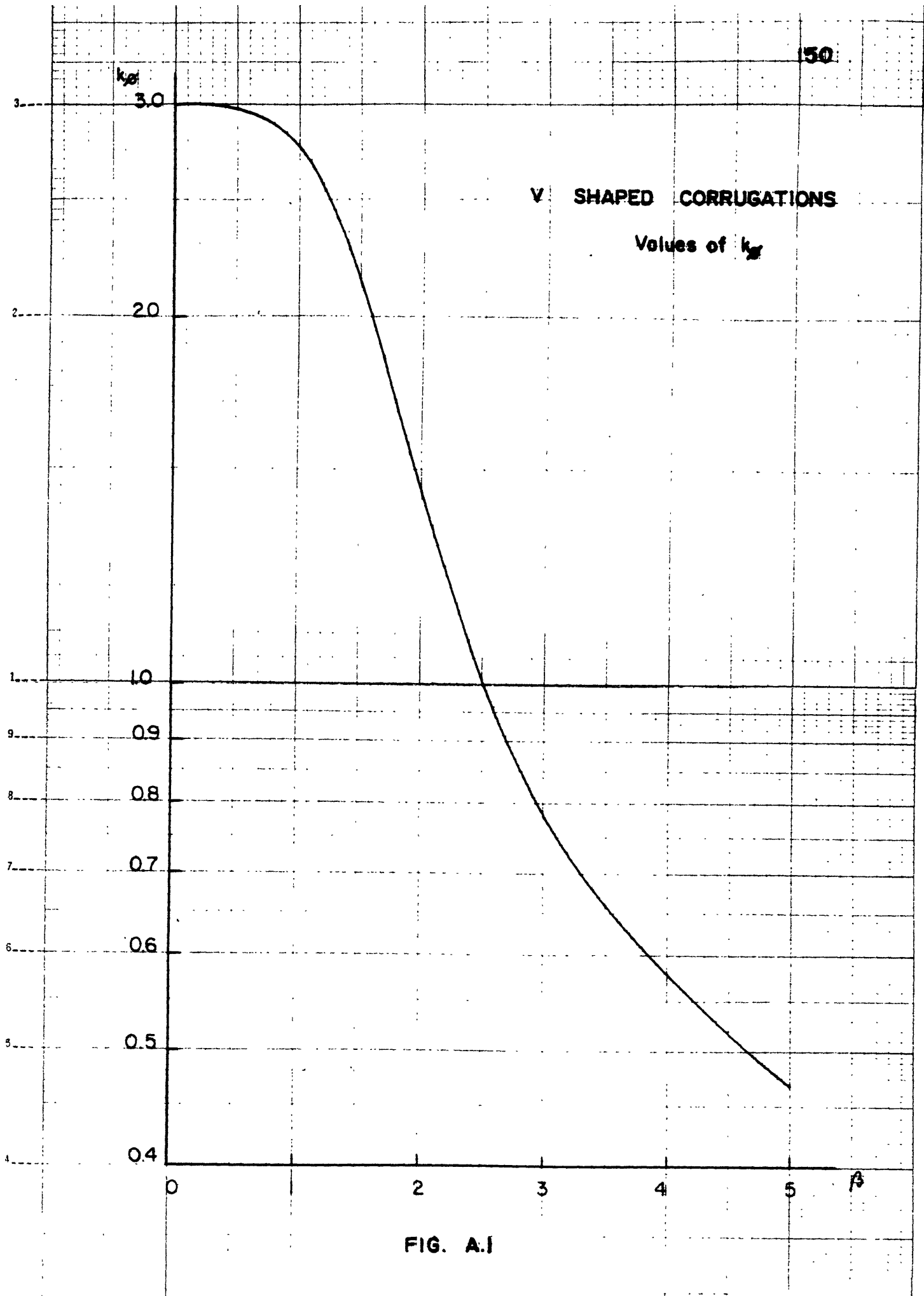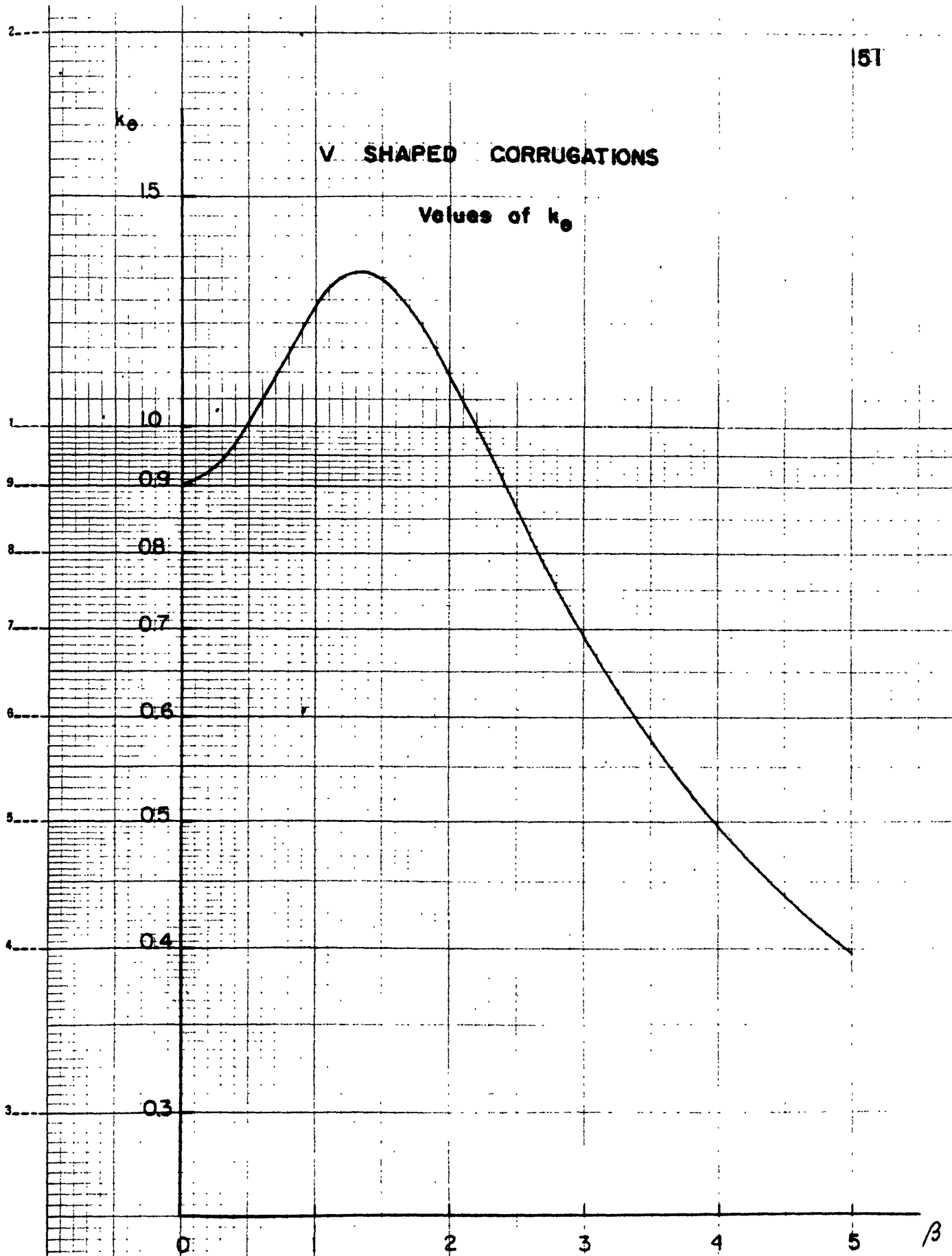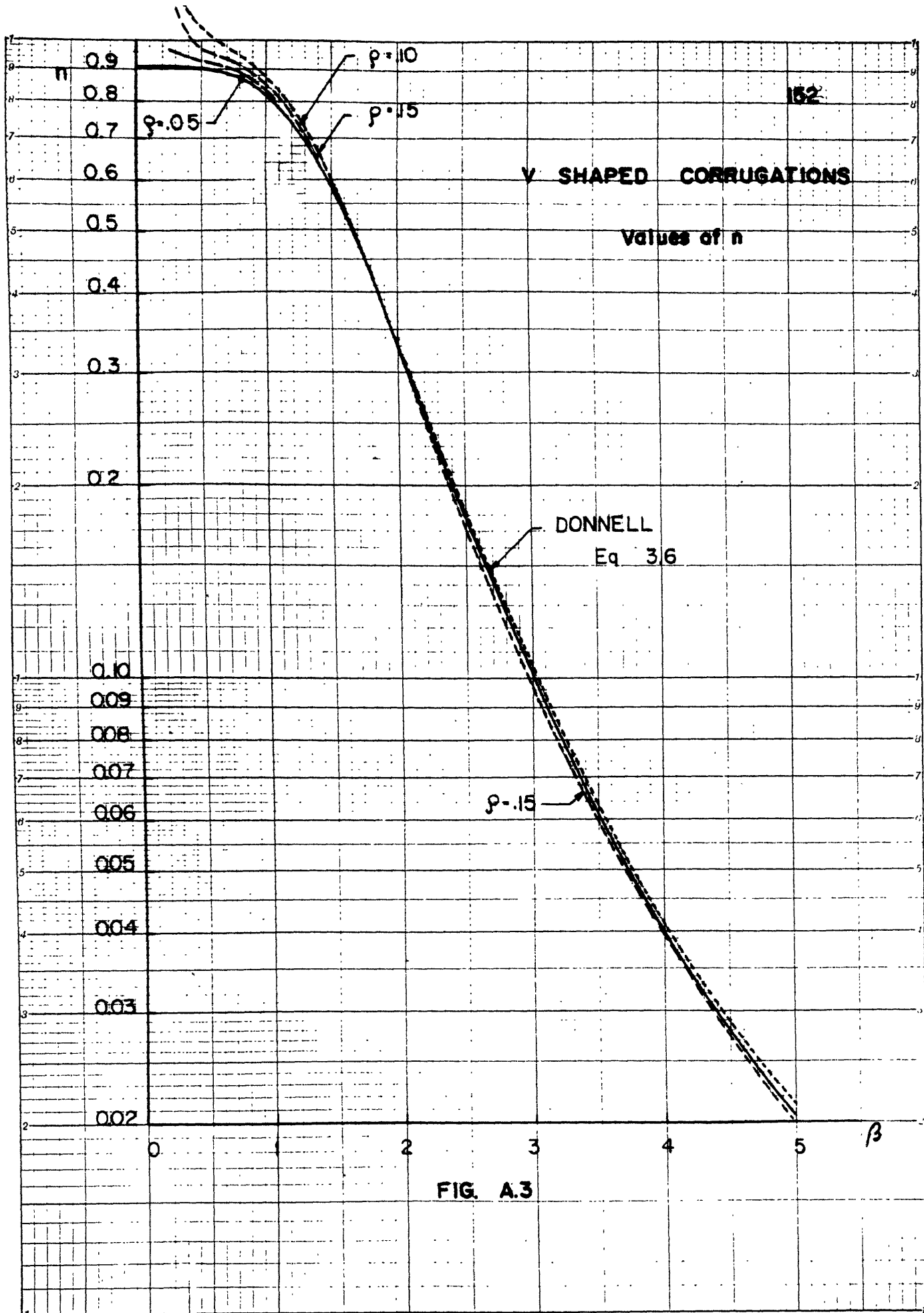
$$\alpha = \tan^{-1} h/b \qquad (3.4)$$

$$\beta = \sqrt{\frac{bc}{rt}}$$

V SHAPED CORRUGATIONS

Values of k_ϕ

FIG. A.I

V SHAPED CORRUGATIONS

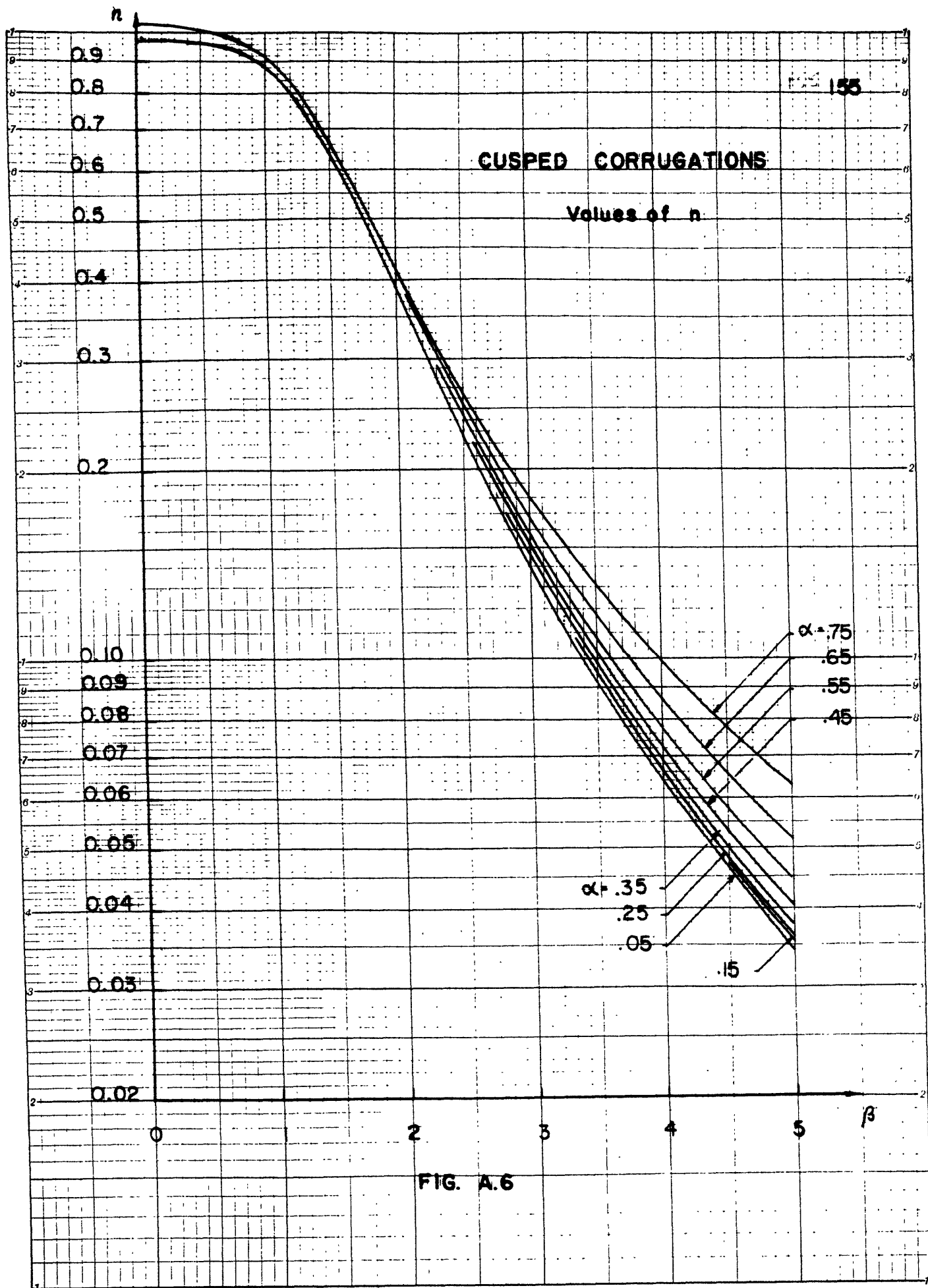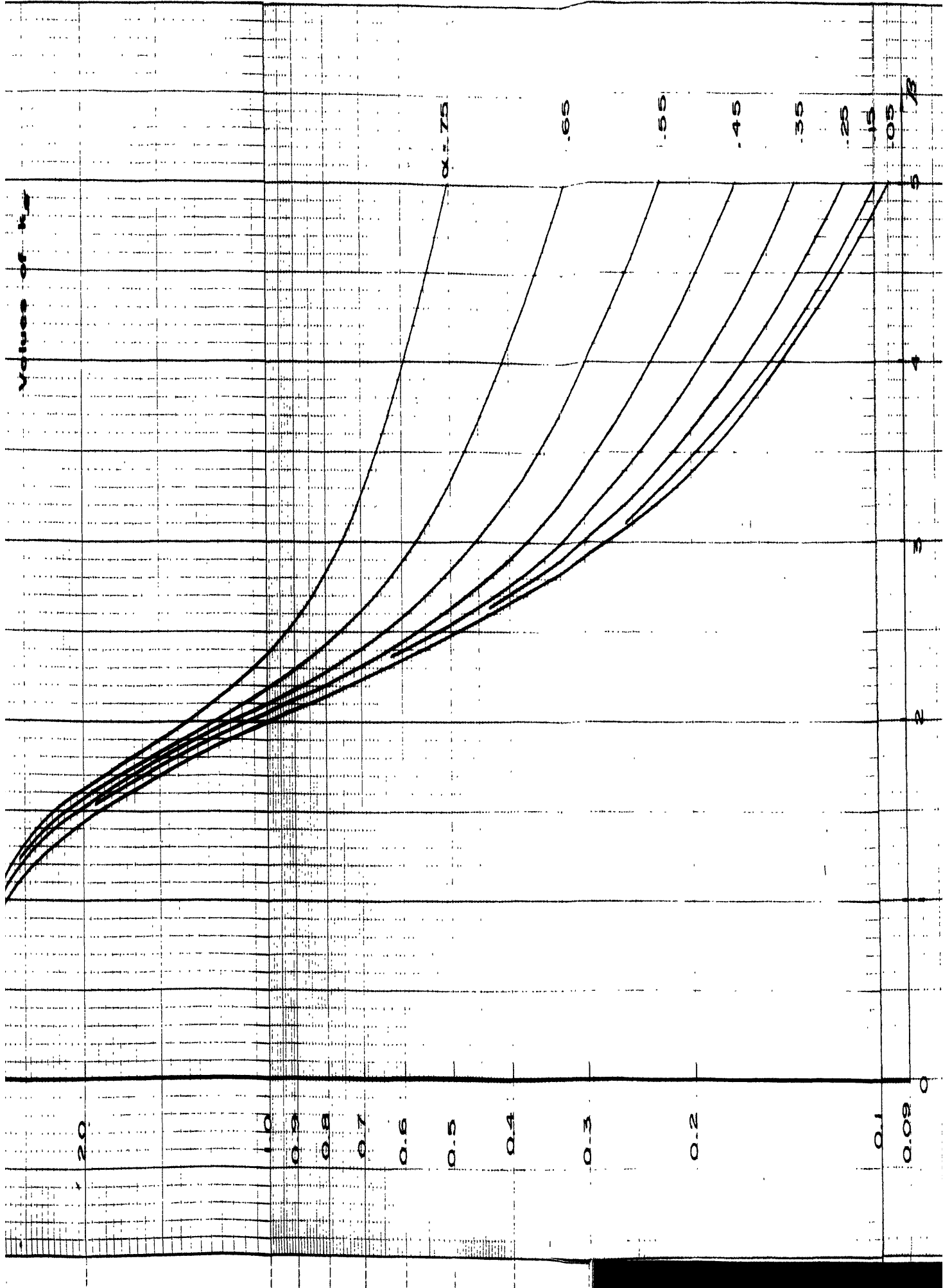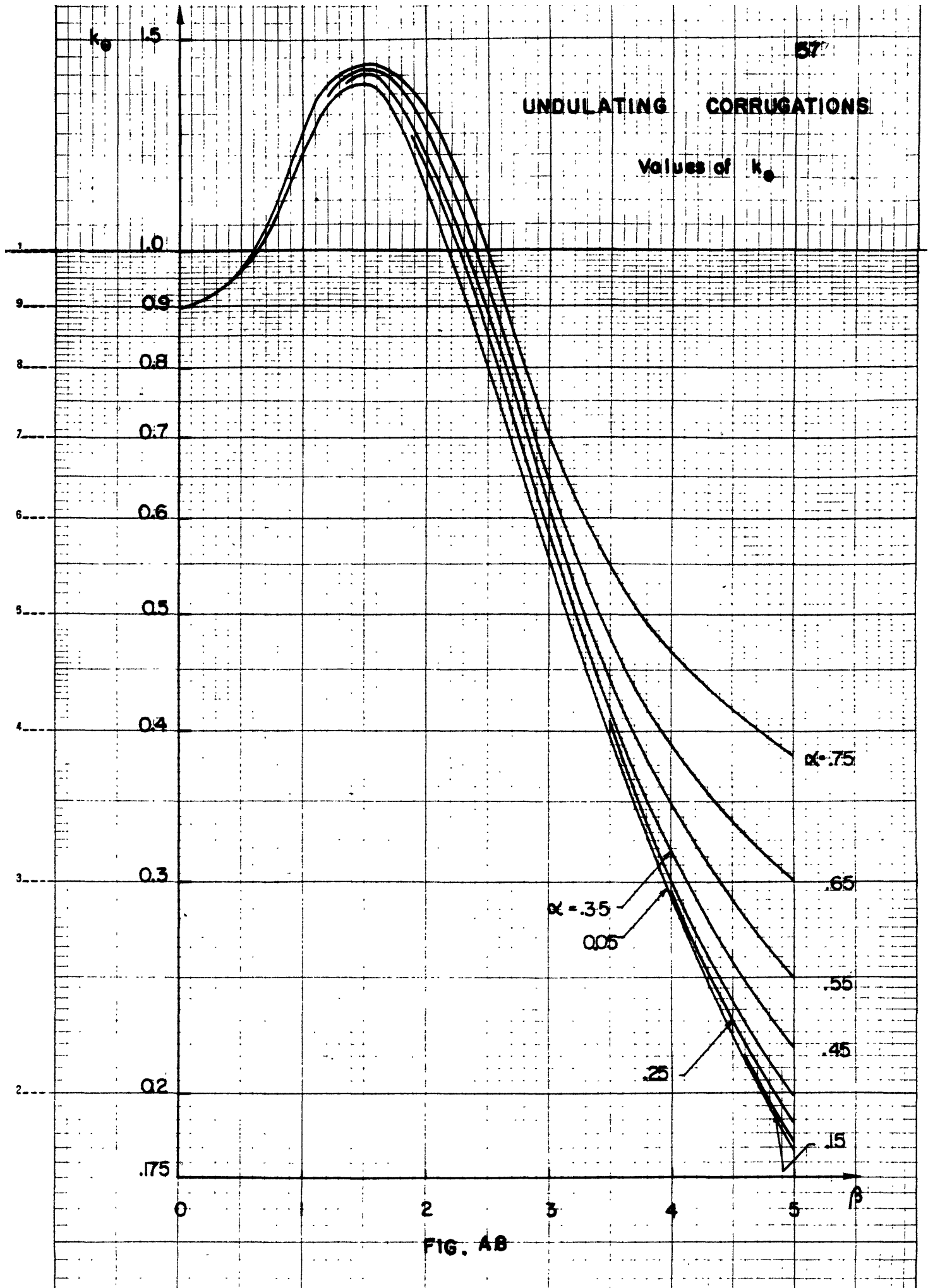Values of k_θ

FIG. A2

FIG. A.3

CUSPED CORRUGATIONS

Values of k_ϕ

FIG. A.4

CUSPED CORRUGATIONS

Values of k_θ

FIG. A5

CUSPED CORRUGATIONS

Values of n

FIG. A.6

Values of k_w

UNDULATING CORRUGATIONS

Values of k_θ

$\alpha = .75$

$\alpha = .35$

0.05

.65

.55

.45

.25

.15

.15

FIG. A8
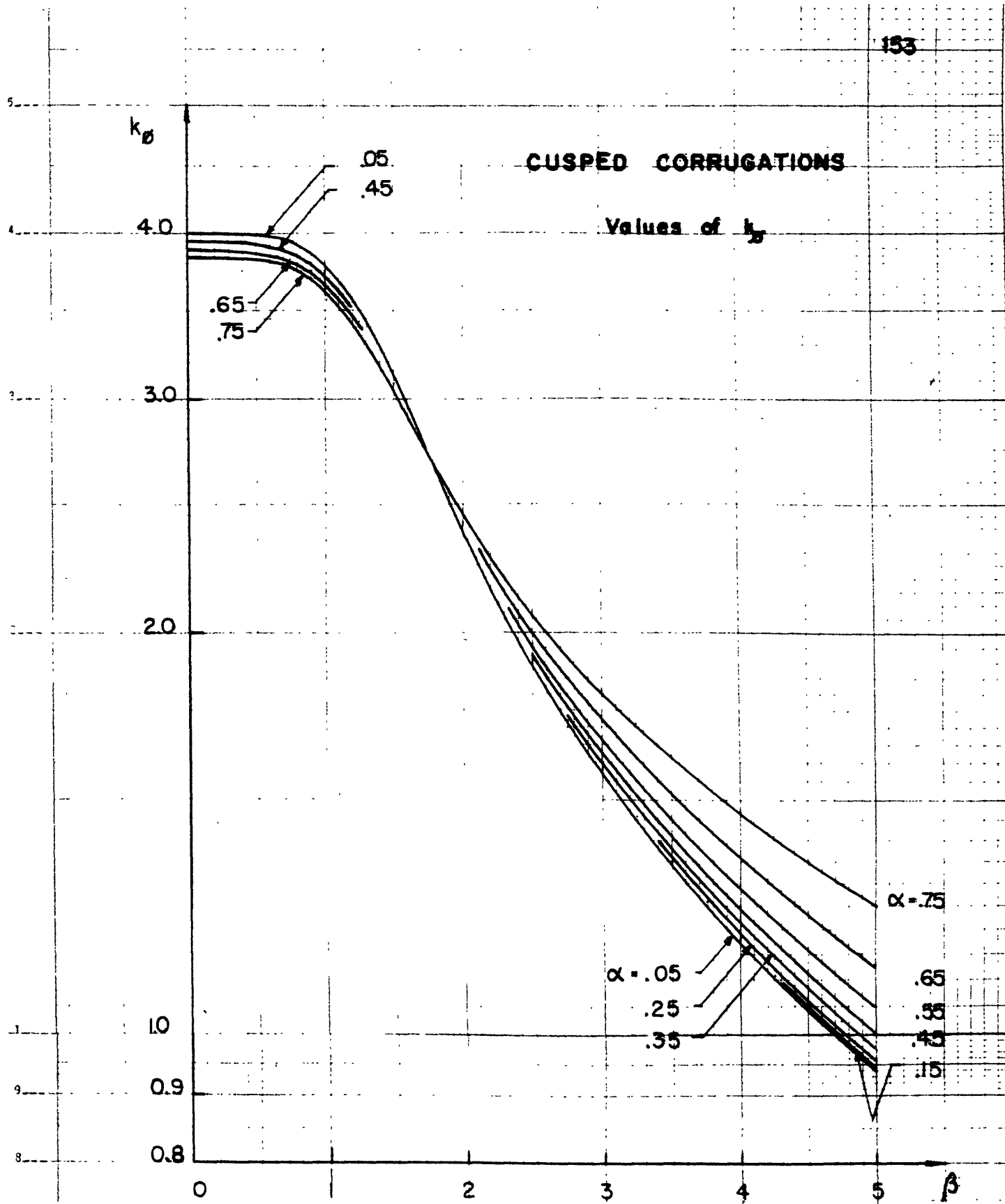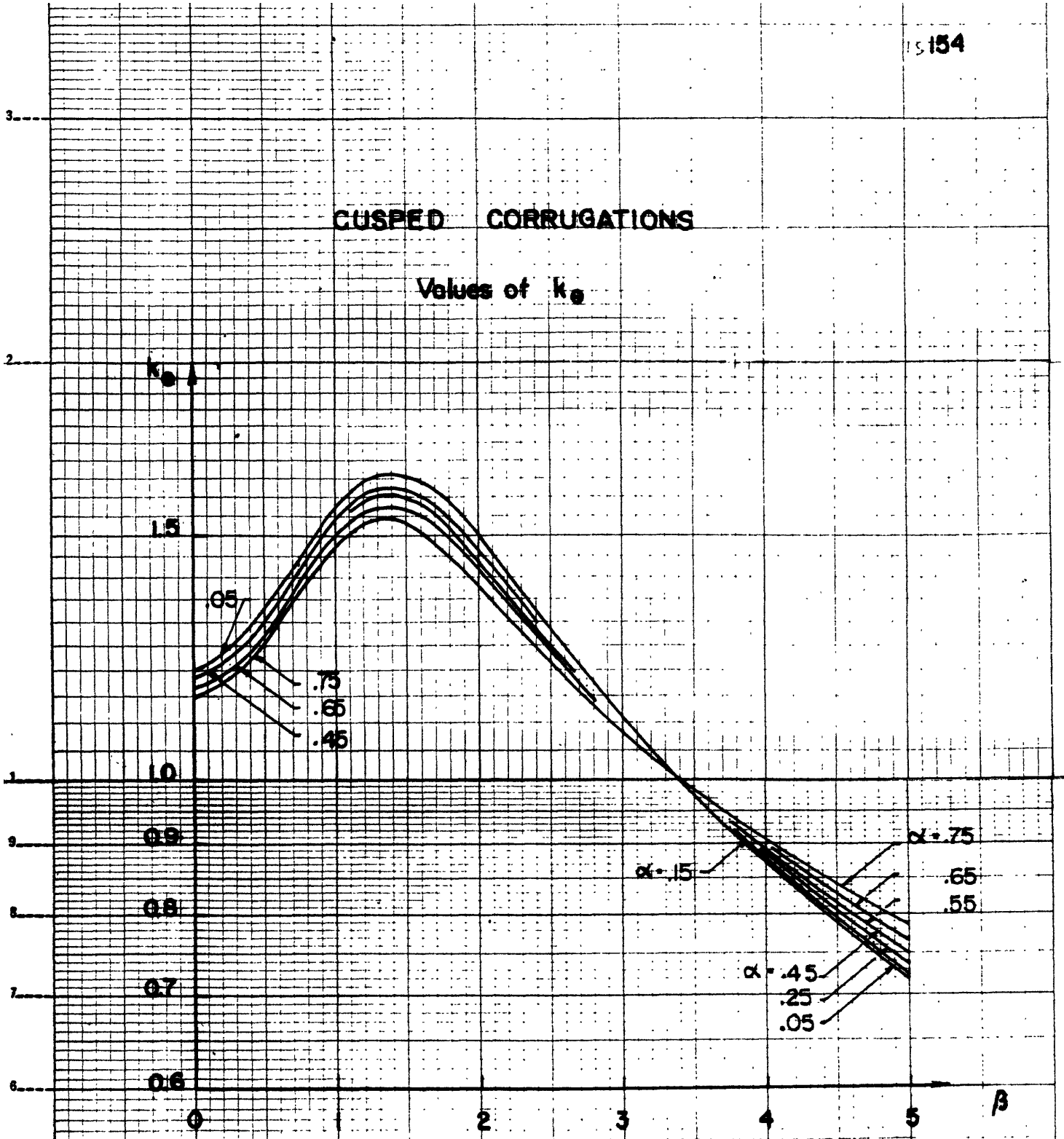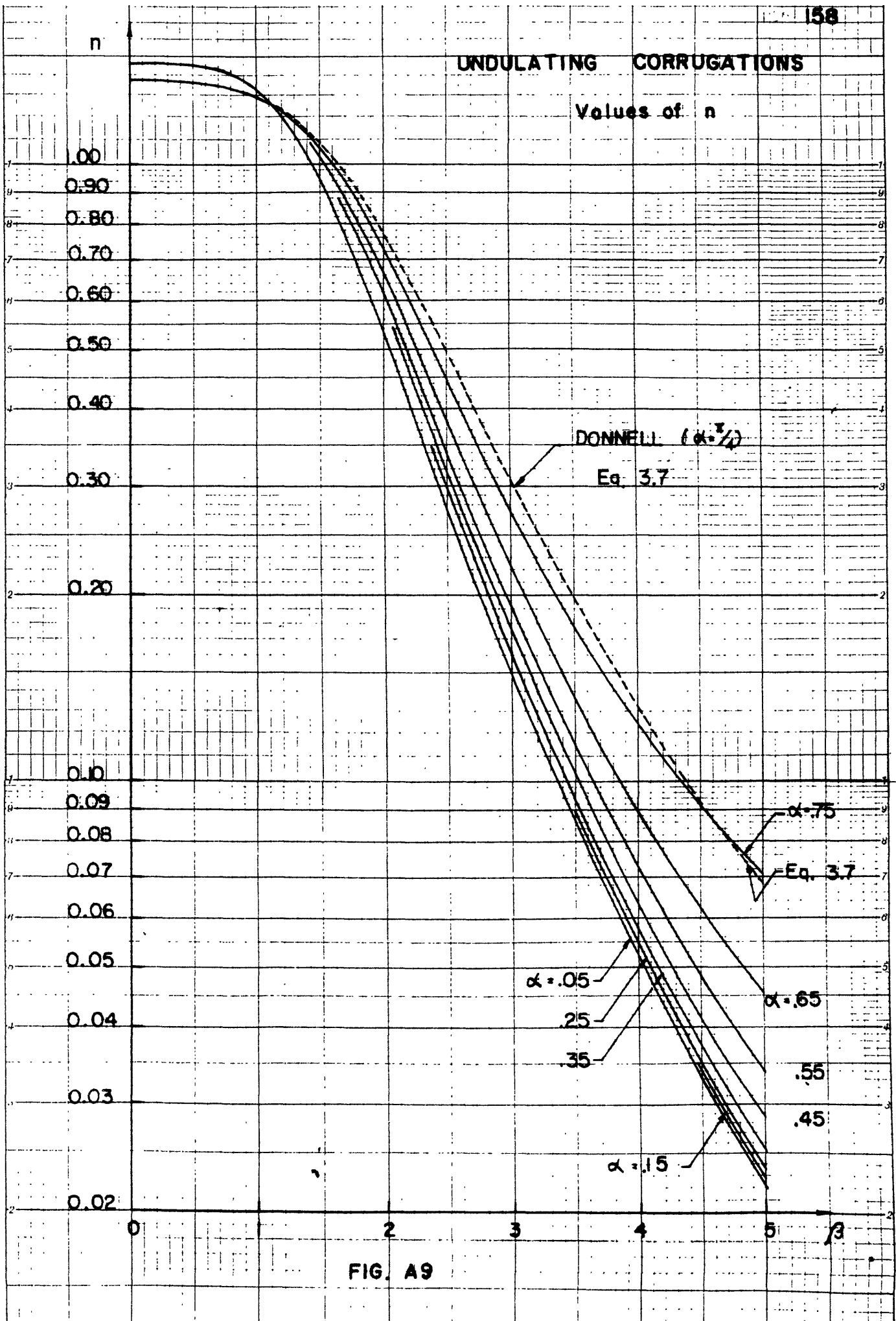
UNDULATING CORRUGATIONS

Values of n

FIG. A9

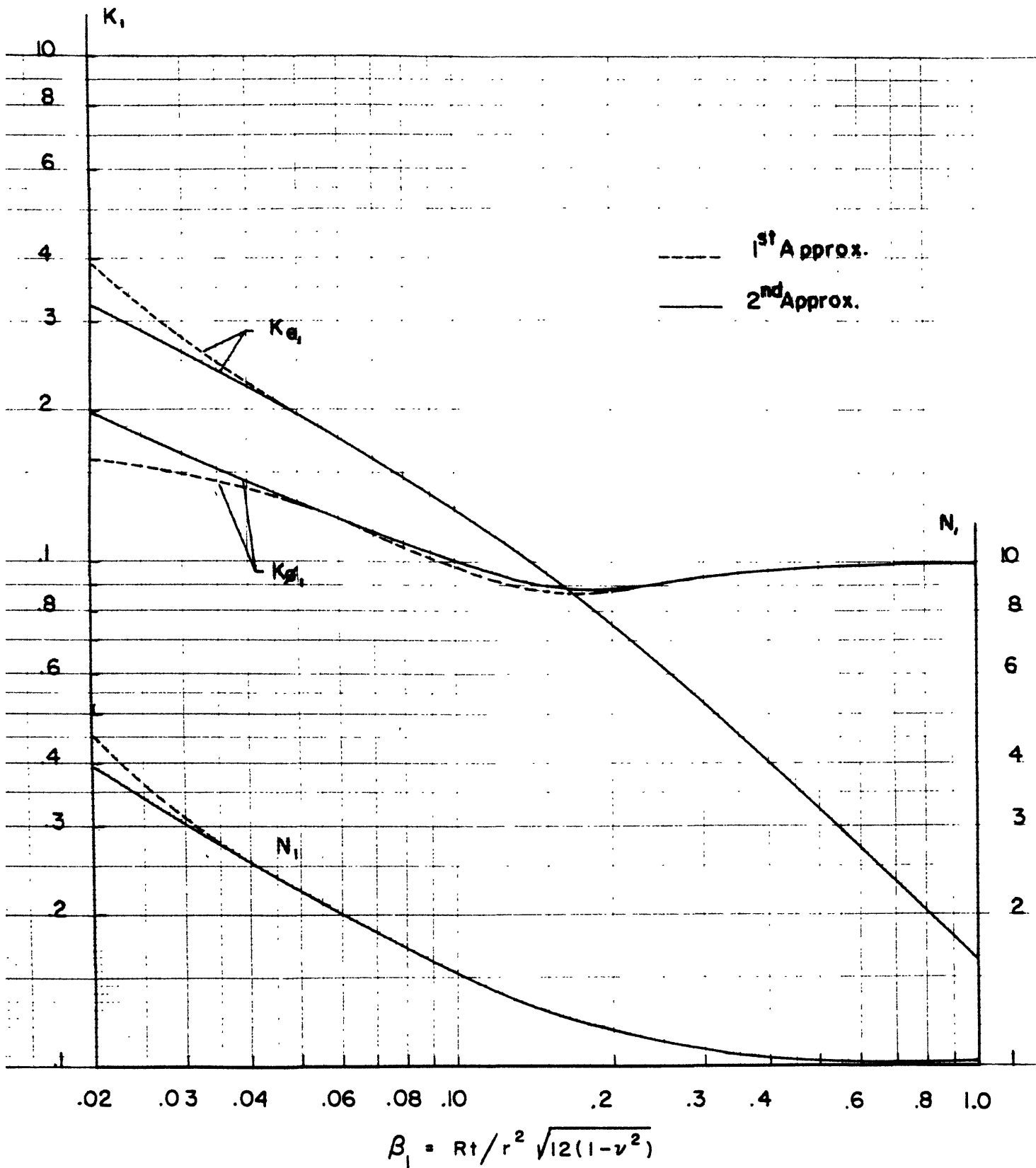# APPENDIX B

CURVES FOR N_1, $K_{\phi 1}$, $K_{\Theta 1}$

FIG. B.1

BIOGRAPHY

The author was born in Bombay, India on March 14, 1934. From 1942 to 1950 he received his primary and secondary education at the Cathedral and John Connon High School in Bombay, India.

In September 1951 he entered the Massachusetts Institute of Technology and received the degree of Bachelor of Science in Civil Engineering in June 1955.

He entered the M.I.T. Graduate School in September 1955 as a student in the Department of Civil and Sanitary Engineering.